DEVELOPMENT OF A UNIFIED METHOD FOR THE DETECTION AND ANALYSIS OF LATE POTENTIALS AS NON-INVASIVE PREDICTORS TO VENTRICULAR TACHYCARDIA IN ELECTROCARDIOGRAPHY

AYAD ADAM MOUSA

Hacettepe Üniversitesi
Fen Bilimleri Enstitüsü Yönetmeliğinin
Elektrik ve Elektronik Mühendisliği Anabilim Dalı İçin Öngördüğü

DOKTORA TEZİ
olarak hazırlanmıştır

2005

Fen Bilimleri Enstitüsü Müdürlüğü'ne,

Bu çalışma jürimiz tarafından **ELEKTRİK ve ELEKTRONİK MÜHENDİSLİĞİ ANABİLİM DALI 'nda DOKTORA TEZİ** olarak kabul edilmiştir.

Başkan	…..... Prof. Dr. Selçuk Geçim
Üye	…..... Prof. Dr. Murat Eyüboğlu
Üye	…..... Prof. Dr. A. Salim Kayhan
Üye (Danışman)	…..... Yrd. Doç. Dr. Atila Yılmaz
Üye	…..... Yrd. Doç. Dr. Mücahit Üner

ONAY

Bu tez ...../...../..... tarihinde Enstitü Yönetim Kurulunca belirlenen yukarıdaki jüri üyeleri tarafından kabul edilmiştir.

...../...../.....

Prof.Dr. Ahmet R. ÖZDURAL
FEN BİLİMLERİ ENSTİTÜSÜ MÜDÜRÜ

I would like to dedicate this work to Adam and Hawa, my late parents whom I wished to be with me to share this moment.

ELEKTROKARDİYOGRAFİDE VENTRİKÜL TAŞİKARDİSİNİN NON-İNVAZİF PREDİKTÖRLERİ OLARAK GEÇ POTANSİYELLERİN TESPİTİ VE ANALİZİ İÇİN BİRÖRNEK YÖNTEM GELİŞTİRİLMESİ

Ayad Adam Mousa

Hacettepe Üniversitesi, Elektrik ve Elektronik Mühendisliği Bölümü

ÖZ

Ventriküler geç potansiyeller (VLPs), ventrikül taşikardisi (VT) geliştirmeye yatkın olan myokard enfarktüslü hastaların non-invazif markerleri olarak değerlendirilmektedir. Geç potansiyellerin tabiatı ve gerçek nedeni tam olarak anlaşılmamıştır ve bu nedenle iyi tanımlanmamıştır ve sinyal genlikleri genel olarak gürültüden ayırt etmek için çok fazla düşüktür.

Bir VT hastasını standart yöntemlerle sınıflamak yanıltıcı olabilir ve başka şekilde önlenebilecek ölüme bile yol açabilen ağır sonuçları bulunmaktadır. VT'nin non-invazif göstergesi olarak VLP'nin analizinde ve tespitinde mevcut yöntemlerin düşük tahmin oranı, elde edilen sinyallerin net olmayan tabiatının yanı sıra, bu yöntemlerle ilgili güçlüklere de bağlı olabilir. Eğer hemen yardım edilirse ve kalp krizi hastasının yaşamını kurtaracak anahtar olan hemen tıbbi bakım sağlanırsa kalp krizi geri döndürülebilir, fakat istatistiklere göre kalp krizi kurbanlarının yüzde 95'i hastaneye ulaşmadan ölmektedir. EKG'lerinde VLP bulunmayan hastaların gösterilmiş VLP bulunanlara göre daha büyük hayatta kalma şansı bulunmaktadır. Aritmik olaylarda ve ani kardiyak ölümde tahmin aracı olarak bunların değeri hala oldukça düşüktür (%10-30), fakat VLP negatifse %95'inde olaysız olduğunu göstererek, iyi seyir tahmininde çok yüksek değer taşımaktadır.

Bu çalışmanın temel amacı, sosyal karakteristikleri açısından VLP'leri meydana getiren şeyi tanımlamak ve analiz bölgesini QRS kompleksinin sonu yerine tüm kardiyak siklusu (döngüyü) kapsayacak şekilde genişletmektir.

Tahmin oranlarını artırmak ve daha iyi alternatifler sunmak amacıyla, mevcut yöntemlerin güçlüklerini de en aza indirmeyi amaçlıyoruz.

İnfarktın fiziksel özelliklerinin dinamiklerine, yani Büyüklük (**S**ize), Konum (**P**osition) ve Oryantasyonun (**O**rientation) yanı sıra Zaman (**T**ime) varyasyonlarına (SPOT) dayanarak geç potansiyelleri meydana getiren şeyin genel tanımını sunduk. Ayrıca günümüzdeki yöntemlerin temel güçlüklerini belirledik ve ayrı zaman ve frekans yöntemlerinin bildirilen başarılarını kullanan birörnek yaklaşımı sunduk. Bu alternatif yollar geç potansiyellerin tespit oranlarını ve analiz doğruluğunu artırmaya yardımcı olabilir ve umarız daha fazla hayat kurtarır.

Bu birörnek yöntem mevcut yöntemlerin güçlüklerinden kaçınırken, bildirilen başarılarının avantajlarını kullanmaktadır. Dalga biçimi dönüşüm yöntemi (wavelet transform method), karmaşık cepstrum, homomorfik filtreleme ve yapay nöral ağlarla destklenen sürecin iskeletini meydana getirdi. Günümüzdeki yöntemlerin bildirilen sonuçları ile kıyaslandığında, bu yöntem artmış bir performans gösterdi.

Anahtar Kelimeler: Ventriküler geç potansiyeller (VLPs), ventrikül taşikardisi (VT), SPOT

Danışman: Yrd. Doç. Dr. Atila YILMAZ, Hacettepe Üniversitesi, Elektrik ve Elektronik Mühendisliği Bölümü

DEVELOPMENT OF A UNIFIED METHOD FOR THE DETECTION AND ANALYSIS OF LATE POTENTIALS AS NON-INVASIVE PREDICTORS TO VENTRICULAR TACHYCARDIA IN ELECTROCARDIOGRAPHY

Ayad Adam Mousa

Hacettepe University, Department of Electrical and Electronics Engineering

ABSTRACT

Ventricular late potentials (VLPs) are considered as non-invasive markers of patients with myocardial infarction, which are prone to the development of ventricular tachycardia (VT). The nature and exact cause of late potentials are not well understood and therefore not well defined and signal amplitudes are usually too low to be differentiated from noise.

Classifying a VT patient by standard methods can be misleading and have grave consequences that may even lead to an otherwise preventable death. The low prediction rate of current methods in the analysis and detection of VLP as a non-invasive indicator of VT may be due to the drawbacks associated with these methods as well as the unclear nature of the sought signal. Heart attack can be reversed if help is given quickly and the key to saving the life of a heart attack patient is immediate medical care but according to statistics, 95 percent of heart attack victims die before reaching the hospital. Patients without VLP in their ECGs have a greater chance of survival than those who have demonstrated VLP. Their value as predictive of arrhythmic events and sudden cardiac death is still relatively low (10-30%), but very high in predicting a good outcome, showing 95% event free if VLP negative.

The main aim of this work is to define what constitutes VLPs in terms of their physical characteristics and to broaden the analysis region to include the entire cardiac cycle rather than just the end of the QRS complex. We also aim

to minimize the drawbacks of current methods in order to increase their predictive rates and present better alternatives.

We have introduced a general definition to what constitutes late potentials based on the dynamics of the physical properties of the infarct; namely **S**ize, **P**osition **O**rientation in addition to their **T**ime variations (SPOT). Also we tackled the major drawbacks of current methods and presented a unified approach that utilizes the reported successes of individual time and frequency methods. These alternative means may help in improving the detection rates and analysis accuracy of late potentials and hopefully save more lives.

This unified method avoids the potential pitfalls of current methods while taking advantage of their reported successes. The wavelet transform method formed the backbone of the process supported by the complex cepstrum, homomorphic filtering and artificial neural networks. The method showed an improved performance as compared to the reported results of current methods.

Keywords: Ventricular late potentials (VLP), Ventricular tachycardia (VT), SPOT.

Advisor: Assist. Prof. Dr. Atila YILMAZ, Hacettepe University, Department of Electrical and Electronics Engineering.

ACKNOWLEDGEMENT

This thesis is the result of many years of work whereby I have been accompanied and supported by many people. It is a pleasant aspect that I have now the opportunity to express my gratitude for all of them.

I feel a deep sense of gratitude for my late father and mother who formed part of my vision and taught me the good things that really matter in life. The happy memory of my parents still provides a persistent inspiration for my journey in this life.

I would like to thank my supervisor Dr. Atila Yilmaz. I have been under his supervision since 1999 when I started my Ph.D. at the Hacettepe University in Ankara. During these years I have known him as a sympathetic and principle-centered person. His enthusiasm and integral view on research and his mission for providing 'only high-quality work and not less', has made a deep impression on me. Besides being an excellent supervisor, Dr. Atila and his wife were as close as relatives and good friends to me, I am really glad that I got to know them in my life.

I want to thank all the people at the Electrical and Electronics department of the Hacettepe University. I am very grateful to all the staff of the cardiology department at the Hacettepe hospital for their help during the data recording stage. I would also like to thank all the members of my PhD committee who monitored my work and took effort in reading and providing me with valuable comments on this thesis.

I would like to give my special thanks to my wife Suad and my children Saif, Hawa, Sanad, Adam and Mohammed for taking this long journey with me whose patience and support enabled me to complete this work. I am grateful for all my brothers and sisters for rendering me the sense and the value of brotherhood. I am glad to be one of them.

This research has been supported and funded by the University of Omar Muktar and Ministry of Education in Libya, I thank them all for their confidence in me. I would like to thank the people at the Libyan Embassy who kept an

eye on the progress of my work and always were available when I needed their help.

I am also grateful for the department of computer science at the Çankaya University for providing me an excellent work environment during the past years.

TABLE OF CONTENTS

DEFINITION OF TERMS AND ABBREVIATIONS

A_C	common gain
A_D	differential gain
ADC	analog to digital converter
AMI	acute myocardial infarction
ANN	artificial neural network
AV node	atrio ventricle node
BBB	bundle branch block
BPM	beats per minute
CCEPS	complex cepstrum
CHD	cardiac heart desease
CMRR	common mode rejection ratio
D4	Daubechies wavelet
DP	delayed potentials
DSP	discrete signal processing
ECG	electrocardiography
EKG	electrokardiography
EMG	electromyography (muscle)
FFT	fast Fourier transform
FQRS	filtered QRS
HAMFS	high amplitude medium frequency signal
HRECG	high resolution ECG
LAHFS	low amplitude high frequency signal
LAS40	low amplitude signal in last 40 ms
LMS	least-mean-square
LP	late potential
MALFS	medium amplitude low frequency signal
MI	myocardial infarction
MLP	multilayer perceptron
MPC	minimum phase correspondanse
P	p-wave in ECG
PR	interval from P to R

QRS	complex including Q, R and S waves
QRSDUR	portion of ECG from Q to S
QT	portion of ECG from Q to T
QTc	corrected QT
RMS	root-mean-square value
RMS40	root-mean-square value of last 40 msec of QRS
RR	portion of signal between two successive R peaks
SA node	sinoatrial node
SAECG	signal avereaged ECG
SCD	sudden cardiac death
SL	signal length
SNR	signal to noise ratio
SPOT	size-position-orientation-type
T wave	the T wave part of ECG signal
VLP	ventricular late potential
VT	ventricular tachycardia
WT	wavelet transform

ACUTE	sudden
MYO	muscle
CARDIA	heart
MYOCARDIUM	heart muscle
INFARCT	artery being clogged

LIST OF TABLES

LIST OF FIGURES

CHAPTER 1

INTRODUCTION

1.1 Introduction

Ventricular late potentials (VLP) or simply late potentials (LP) are fragmented activities originating from electrically unstable regions of myocardium, and are markers of reentry arrhythmia in a period of one year after the myocardial infarction (MI). The medical term for a heart attack is *acute myocardial infarction*. The term acute means sudden, *myo* refers to muscle, and *cardia* refers to heart. M*yocardium* is the medical name for the heart muscle and *infarct* refers to the artery being plugged or clogged up. If an AMI results in the stopping of the heart then this is termed sudden cardiac death (SCD).The delayed activity in the form of fragmented deflections, seen terminal with the ventricular depolarization wave front, is usually found in border zones surrounding the scar tissue of previous myocardial infarctions. The border zone that exists is composed of conducting and non-conducting tissue, which slows and fragments the wave of electrical depolarization as it sweeps through the ventricular myocardium (Breithardt et al. 1991).

Late potentials are obscured in the conventional surface ECG because of their low amplitude and the overlay of noise, but they can be visualized through special processing such as high resolution and signal-averaged ECG. LPs are thought to be a non-invasive marker of potential ventricular tachycardia (VT). This hypothesis has been confirmed by a large number of studies in the last decade. However, LP analysis has not yet become a routine diagnostic tool in clinical cardiology. There are on going studies including this one to show that LP analysis might become an important noninvasive means for LP detection.

The two main problems in detecting ventricular late potentials from surface ECGs are that the inherent additive noise and QRS morphology effectively

mask the time and frequency domain late potential characteristics. Therefore from the surface ECG, the morphology of a complex containing late potential activity is similar to the morphology of one without LP (Cain et al. 1996)(Jane, Rix and Caminal, 1991).

1.2 Studies on analysis methods for VLP

Signal-averaging technique was first applied to the human heart as a tool for enhancing biological signals. In 1875 signal-averaging principles were first used, and in 1947 the technique began to be used to improve detection of electroencephalographic signals. Hon and Lee in 1963 were able to detect fetal heart signals from skin surface electrograms by a so-called “computer of average transient’s” method. Eddlemon described a computer-based modification of the original averaging technique in 1968, essentially the approach used today. Edward Berhari one of the pioneers of this new technique, described signal-averaging in 1973 as a signal processing technique usually done digitally, whereby repeated or periodic waveforms which are contaminated by noise can be enhanced. That is, the signal-to-noise ratio can be improved. By summing successive noisy waveforms the random components (noise), will decrease while the deterministic components, (the desired signal), will be unchanged. During 1973 Berhari’s group and one year later the group of Nancy Flowers published their first success in recording His potentials from the body surface. By the year 1973 it was further observed that electrocardiograms from ischaemic canine myocardium were delayed and fragmented and that electrical activity was detectable, bridging diastole and preceding the onset of ventricular tachyarrhythmia. Guy Fontaine and colleagues in 1977 were the first to describe the detection of ventricular late potentials from the body surface in a patient with ventricular tachycardia: Fontaine had earlier recorded delayed potentials on the endocardium in the same patient. In the years that followed, the relationship between ventricular late potentials detected by the signal-averaging technique and reentrant ventricular tachycardia in patients following myocardial infarction was established by a number of authors. One of the most important contributions leading to widespread acceptance and use of the method came from Michael

Simson, who developed criteria for the detection of LP in 1981. This technique is now widely accepted and since 1991 it has become an international Standard that two out of three Simson-derived criteria constitute a positive LP. In addition to the usual analysis of LP in the time domain, frequency domain analysis using fast Fourier transformation and spectral turbulences during the entire QRS complex have been developed though not yet standardized. Further promising tools for detecting dynamic changes of electrical activity is beat-to-beat, and wavelet transform analysis (Vester, Strauer 1994)(Rompelman, Ros, 1986)(Simson, 1981).

1.3 Commonly applied methods for VLP

A number of different methods have been used to identify Late Potentials and thereby assess the risk of serious ventricular arrhythmias and sudden death. Time domain signal averaging of many complexes is one existing technique, which suppresses the random noise component of periodic data. Simson adopts this method of noise reduction before high pass filtering XYZ lead data and forming the vector magnitude to determine the existence of late potentials. Typically, a large number of complexes are required to reduce the noise to a level below that of the late potential activity.

Frequency domain analysis suffers from several drawbacks: it fails to provide time localization of signal singularities characterized by high-frequency components and hence information on the precise incidence of LP is lost. In an effort to widen the window and thus increase frequency resolution, many investigators have extended the analyzed region toward the end of the ECG signal (T-wave), covering the entire ST-segment.

1.3.1 Time domain analysis

Time domain analysis divides further into:

- High-resolution Low-noise ECG
- Signal averaging
- Beat-by-beat analysis

1.3.1.1 High-resolution low-noise ECG

Non-invasive methods of diagnosis of cardiac disorders involve digital recording of cardiac signals at the body surface (chest) and subsequent computerized analysis. Such methods and instruments provide a vital first step to the diagnosis of the heart without involving surgical procedures. One such non-invasive field is High Resolution ECG (HRECG) described in detail by Zimmermann and co-workers. Three channels are recorded simultaneously and the analog input signal is fed through a preamplifier with a fixed gain of 1000 times. Adjustable high-pass and low-pass filters perform band-pass filtering. In optimal clinical conditions the noise level can be reduced to 1 to 2 μV from peak to peak, a usual value can be as high as the maximum gain of the amplifier used. A high-resolution electrocardiogram detects very low amplitude signals such as LPs. High Resolution Electrocardiography is not being the sole diagnostic tool, but it does provide information on cardiac electrical instability that is not available through other noninvasive tests. A standard electrocardiogram cannot detect these signals. High-resolution electrocardiography enhances the diagnostic capabilities of ECG signals.

1.3.1.2 Signal-averaging

The purpose of signal averaging is to reduce the level of noise, which contaminates the surface ECG, and to detect low-amplitude signals in the terminal QRS complex. The main source of noise is skeletal muscle activity exhibiting amplitudes of 5 to 25 μV. Muscle noise cannot easily be eliminated by filtering, because its frequency content corresponds with that of high-frequency cardiac potentials, but it may be markedly reduced by the signal averaging technique which amplifies repetitive waveforms like the QRS complex and suppresses random non-repeating waveforms like skeletal muscle noise (Jane, Rix and Caminal, 1991).

The most common type of processing is ensemble signal averaging for which a few prerequisites are necessary. Thus the waveform of interest must first be repetitive so that multiple samples can be obtained to form an averaged

waveform. Before averaging, by comparing every new beat against a template of previous beats, ectopic beats can be excluded prior to processing.

Second, waveforms must have a common fiducial point (usually a large or rapidly moving component of the QRS complex) used as a reference time enabling the computer to average similar sampling points of the repeating signal.

A third prerequisite is that the waveform of interest be independent from noise, meaning noise must be random. If there is a repetitive noise artifact arising from electrode motion or other sources, the signal-averaging process will amplify it. Using this method, noise reduction is proportional to the square root of the number of QRS complexes averaged.

1.3.1.3 Beat-by-beat analysis (spatial averaging)

A second form of signal averaging is spatial averaging which allows the analysis of beat-to-beat events, which cannot be detected by the temporal averaging technique. A number of closely spaced independent electrode pairs are summed up to reduce the expected noise, representing a substantial disadvantage compared to temporal averaging. The advantage of this technique, however, is the detection of dynamic changes of VLP in real time. Other methods use adaptive identification to achieve a beat-by-beat fine ECG estimation. Information provided by this method allows for better interpretation of low and very low level signals (Wu, Qiao, Gao and Lin, 2001).

1.3.2 Frequency domain analysis

Spectral or frequency analysis method examines the voltage or power over a spectrum of frequencies within a pre-selected time interval. The generally accepted hypothesis is that VLP or late depolarizations are characterized by higher frequency content than expected from repolarizations. Fast Fourier transformation (FFT) is usually used to estimate the scalar lead spectral of the terminal QRS and ST segment of signal-averaged XYZ. Results may be given as relative contributions of specific frequencies constituting these ECG segments.

Different techniques have been developed to quantify the spectral content of the QRS complex, and account at least in part, for the inconsistency of the results. Area ratios of the energy spectral derived from the FFT were calculated using separate intervals. These started after QRS onset and before QRS finished, extending to the T wave as described by Worley *et al.* This suggests that frequency analysis of signal-averaged ECGs with FFT is an available method for detecting the high-frequency component within the QRS complex in some patients with VT.

As with time domain analysis, accepted standards are not yet established. Nevertheless, frequency analysis offers potential advantages for the identification and characterization of patients prone to ventricular tachycardia (VT). A complex high-pass filtering is not necessary and differentiation of VLP and noise is improved.

1.3.3 Previous results of time domain and frequency domain analysis

The results of clinical studies comparing time domain and frequency analysis give a controversial picture. Engel and co-workers found that spectral analysis was not as reproducible as duration measurements performed in the time domain. Furthermore, the results of spectral analysis were more noise dependent. On the one hand the poor frequency resolution of short data segments and spectral leakage is a known limitation of conventional spectral analysis. On the other, the limitations of the conventional time domain analysis are that high-pass filtering may disturb signals that discrimination between LP and noise may be difficult and that patients with bundle branch block (BBB) are usually excluded from analysis. According to an expert consensus document:

"These findings provide an objective rationale for expansion of the ECG interval analyzed to include more of the cardiac cycle, which should increase the chances of detection of signals generated by myocardium critical to ventricular tachycardia. Indeed, previously undefined magnitude, phase and spatial features over the entire cardiac cycle of sinus beats that distinguish signal-averaged ECGs from patients with from those without sustained ventricular tachycardia have recently been identified." (CAIN et al., 1996)

A number of studies have been performed to compare both methods in different clinical settings. Most of the studies deal with patients presenting sustained ventricular tachycardia. Worley *et al,* found FFT analysis the only significant index to differentiate between patients after myocardial infarction without VT and normal controls, whereas filtered QRS (FQRS) duration in the time domain was the only independent factor to separate patients with or without VT. Machac and Gomesi found frequency domain analysis no improvement over time domain analysis in differentiating patients with ventricular tachycardia from those without. In contrast, Pierce *et. al.*, concluded from their study, which included similar patients that high frequencies in late potentials, but not their duration or reduced voltage, most usefully identify with coronary heart disease prone to VT. Kinoshita published data on patients with ventricular tachycardia of left ventricular origin where area ratios calculated from FFT analysis showed significantly higher values in patients with VT as compared to those without, whereas time domain analysis gave negative results in all cases. Nogamilul suggested, as a conclusion from his analysis of a great number of different time domain and frequency domain parameters, the use of a combination of both approaches to enhance the accuracy of this technique for screening post-myocardial infarction patients prone to VT.

The prevalence of LP after acute myocardial infarction depends on the time of recording, the analyzing technique, the site of myocardial infarction and definition of what constitutes an LP. El-Sherif found more LP at 6 to 30 days than before or later. In general, LP measurement is recommended upon patient discharge. The incidence of LP slowly declines during long-term follow-up, as was shown by Kuchar and co-workers. Frequency domain analysis gave results independent of infarct location, whereas time domain analysis showed lower sensitivity with anterior than with inferior infarction.

1.4 Aim and scope of work

This thesis is concerned with the extraction of small cardiac signals normally concealed by noise in the recorded ECG. These microvolt signals are derived from the cardiac conducting system and from the fragmented activation of

damaged areas of heart muscle as in the case of Ventricular Late Potentials (VLP). VLPs are found in ventricular tachycardia (VT) patients that could be used as an early warning to the development of VT. The detection and delineation of these signals can give early warning of various cardiac disorders. This is challenging since the nature and exact causes of late potentials are not well understood and therefore not well defined and are usually concealed in noise and other portions of the ECG signal. Wrongly classifying a VT patient may have grave consequences that may even lead to an otherwise preventable death. Based on the findings of the analysis of the QRS portion alone, a case with abnormalities at other portions of the conduction path may wrongly be classified as normal and discharged from hospital. This situation deprives the patient from a vital chance to receive immediate medical care and might lead to his death. The low prediction rate of current methods in the analysis and detection of VLP as a non-invasive indicator of VT may be due to the drawbacks associated with these methods as well as the unclear nature of the sought signal. The main aim of this work is to define what constitutes VLPs in terms of their physical characteristics and to broaden the analysis region to include the entire cardiac cycle rather than just the end of the QRS complex. This enables the detection of abnormalities that might occur anywhere in the conduction path of the heart. We also aim to minimize these drawbacks in order to increase the predictive rate and present better alternatives based on our tests.

Digital signal processing techniques such as, wavelet transforms, complex cepstrum and artificial neural network are employed to provide signal enhancement and provide better classification.

In order not to reinvent the wheel, this work starts at where others have left off. This means taking advantage of the reported successes of commonly accepted and applied methods while avoiding their drawbacks and problem causing issues. We begin by providing suitable data for the analysis. This implied the design and implementation of a high-resolution data recording system with controllable gain. Both time-domain and frequency-domain methods are utilized here for their individual performance using the wavelet

transform techniques. In addition to the WT denoising ability, we aim to apply signal averaging to reduce noise in the signal without its associated problems such as offline analysis, alignment errors and averaging of uncorrelated beats. The application of the wavelet transform along with our suggested method of dynamic averaging aim to avoid the drawbacks of signal averaging techniques and allowing real time analysis. Calculating the vector magnitude without the generation of cross terms associated with classical methods is another aim of this study. The final aim is to set up an automatic scheme for the recognition and classification of different signals according to their status abnormality content.

1.5 Outline of thesis

The structure of the remainder of the thesis is as follows:

Chapter 2 describes the electrical behavior of the heart and the origin of the recorded surface ECG. It introduces the concept of the lead systems and discusses the theory, which forms the basis of the ECG techniques. It expands on the details of the lead system used. It also covers the basics of myocardial infarctions and ventricular late potentials both their origin and their diagnostic values.

Chapter 3 Limitations and drawbacks of standard detection methods look at the problems associated with standard methods and in particular the Simson method. The three standard parameters are investigated in order to identify problematic issues. It investigates the problems associated in calculating the vector magnitude based on the classical methods. It suggests a new wavelet transform based method to calculate the vector magnitude. The chapter also covers problems encountered in the VLP detection process.

Chapter 4 covers the different DSP techniques used and is divided as follows:

Section 4.1 covers wavelet transforms theory and its practical sides in a simple and easy to understand way, avoiding the cumbersome and detailed abstract mathematics normally encountered in the study of wavelet transforms. The section concludes with the presentation of the Mallat's

algorithm known as the pyramid algorithm, both forward and inverse operations. A simple example is given for clarifying the basic concepts.

Section 4.2 introduces the notion of the complex cepstrum and the associated mathematical background. The homomorphic theory is covered in this chapter. Other needed topics such as minimum and maximum phase are presented, as well as the concept of signal length.

Section 4.3 gives a brief insight into artificial neural networks. It discusses the feed-forward multi-layer perceptron (MLP) artificial neural network (ANN), which is used as the classifier for the pre-processed data. It includes a discussion of ANN's, learning characteristics and general performance.

Chapter 5 is concerned with the data acquisition system, which was designed and implemented for this thesis at Hacettepe University. The chapter starts with introducing the basic instrumentation amplifier and progresses to the complete system. The chapter discusses the operation of the isolation instrumentation amplifier and other hardware components employed. Here we cover the basic problems encountered in the recording of high-resolution ECG signals and how to minimize their effects. The chapter discusses the various techniques for improving the systems performance. It gives a brief introduction to data acquisition principles and the associated problems involved.

Chapter 6 covers a process that clusters the information contained in long-term ECG records. This clustering process summarizes the entire record and serves as a preprocessing step prior to analysis.

Chapter 7 presents a detailed look at the methods employed in this work. It also covers the entire analysis method carried out. It discusses the different patient categories and introduces the data acquisition techniques employed. The chapter presents the different DSP methods used in an integrated analysis approach. In this chapter the graphics user interface for both acquisition and analysis is introduced.

Chapter 8 presents results and conclusions reached in this study.

CHAPTER 2

VENTRICULAR LATE POTENTIALS

2.1 Introduction

The beating heart generates an electric signal called electrocardiogram (ECG) that can be used as a diagnostic tool for examining some of the functions of the heart. The ECG is a clinical tool to measure the electrical activity of the heart from the exterior of the body non-invasively. With the ECG, important information about the live beating heart can be observed. ECG produces timing information on the electrical activity of the heart, a graph with time on the x-axis and voltage on the y-axis. We collect spatial information by looking at the heart from different directions using the 12-lead or a three orthogonal XYZ lead system. The latter approach is the type used in the data acquisition in this thesis. The electric activity of the heart can be approximately represented as a vector quantity, thus we need to know the location at which signals are detected, as well as the time-dependence of the amplitude of the signals (Malmivuo, Plonsey, 1995).

This chapter introduces the material needed to discuss the subject of ventricular late potentials starting from the different ECG components to the concept of myocardial infarction.

2.2 Components of the Normal Cardiac cycle

The electrocardiogram represents the depolarization and repolarization of the major chambers of the heart as shown in Fig. 2.1. Depolarization is the electrical activation of the myocardium while repolarization **i**s the restoration of the electrical potential of the myocardial cell. Changing charges create the voltage outside the heart and the waves of depolarization produce voltages on the outside. For the entire time that the myocardium is totally depolarized, there is zero voltage on the ECG and after depolarization, myocytes spontaneously repolarize.

Depolarization occurs at the sino-atrial (SA) node where current travels through internodal tracts of the atria to the Atrioventricular (AV) node; then through the Bundle of Hiss, which divides into right and left bundle branches. The left bundle branch divides into left anterior and posterior fascicles.

In a normal heart rhythm, the SA node generates an electrical impulse, which travels through the right and left atrial muscles producing electrical changes, which is represented on the ECG by the P-wave. The electrical impulse then continues to travel through specialized tissue known as the AV node, which conducts electricity at a slower pace. This will create a pause (PR interval) before the ventricles are stimulated. This pause is helpful since it allows blood to be emptied into the ventricles from the atria prior to ventricular contraction to propel blood out into the rest of the body. The ventricular contraction is represented electrically on the ECG by the QRS complex. This is followed by the T wave, which represents the electrical changes in the ventricles, as they are relaxing. The cardiac cycle after a short pause repeats itself, and so on. Therefore, on an ECG in normal sinus rhythm P waves are followed after a brief pause by a QRS complex, then a T wave. Normal sinus rhythm not only indicate that the rhythm is normally generated by the sinus node and traveling in a normal fashion in the heart, but also that the heart rate, i.e. the rate at which the sinus node is generating impulses is within normal limits. There is no one normal heart rate, but this varies by age and other factors. It is normal for a newborn to have a heart rate up to 150 beats per minute, while a child of five years of age may have a heart rate of 100 beats per minute. The adult's heart rate is even slower at about 60-80 beats per minute.

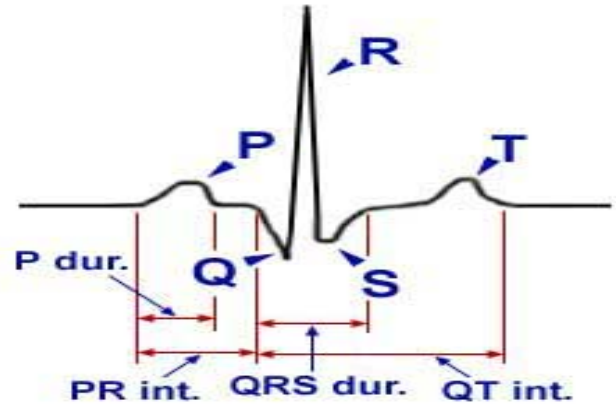

Figure 2.1 ECG signal showing different cardiac components

The P-Wave

Normal SA nodal cells have fastest depolarization, so they are the first to depolarize. However, there is so little SA nodal tissue so that the depolarization of the SA node is not easily detected. The depolarization then passes as a wave through the atria. This wave passes from the SA node inferiorly and leftward to the AV node and left atrium. This produces a positive potential recorded as a positive deflection in the ECG tracing which is defined as the P wave. The P wave is relatively small because the atrial muscle mass is relatively small and ends when all the atria are depolarized. The wave of depolarization is then present inside the AV node. The P wave represents the sequential activation of the left and right atria (atrial depolarization) and lasts from 60 ms to 110 ms.

The PR interval

The PR interval represents the conduction of electricity from the SA node to the AV node and atrial depolarization through the AV node. It is measured from the beginning of the P wave to the beginning of the QRS complex. The AV node contains specialized cells that slow the speed of the depolarization wave. Like the SA node, there is so little AV nodal tissue that no depolarization is detected. The space between the P wave and the QRS complex is called the PR segment. The time from the beginning of the P wave to the beginning of the QRS complex is called the PR interval.

The PR interval is empirically the best measure of the time that it takes for the wave of depolarization to pass through the AV node. A normal PR interval is between 120 and 200 ms.

The QRS Complex

The QRS complex is the result of ventricular depolarization through the Bundle Branches and Purkinje fibers. It is measured from the beginning of the first wave in the QRS to where the last wave in the QRS returns to the baseline. Normal measurements for this interval are 60 ms to 100 ms.

When the wave of depolarization passes into the bundle of Hiss and out into the Purkinje system and ventricle, there is a large positive potential which is the QRS complex. The amplitude is large because there is a large mass of ventricular muscle. Depending on where you measure the voltage across the heart, the QRS complex can be either positive or negative. For any QRS complex, if the deflection at first is negative, then it starts with a Q wave. The first positive deflection is the R wave regardless of whether there was a Q wave or not. A negative deflection after an R wave is called an S wave.

As the wave of depolarization passes through the thickness of the ventricle, a voltage is still present. When the whole thickness of the left ventricle is totally depolarized, the surface charge of both the endocardium and epicardium is negative. Therefore, there is no longer any voltage difference across the ventricle and the recorded voltage is again zero. This is the end of the QRS complex. The QRS complex is the electrical signature of the wave of depolarization passing over the ventricle. The normal QRS complex lasts about 80 ms. The QRS complex occurs only when the ventricles are changing from resting to depolarized state.

The QT interval

The QT interval is measured from the beginning of the QRS complex to the end of the T-wave. Normal measurements for this interval are based on the heart rate. Generally it should be about 40 % of the total time between two QRS complexes, typically between 0.34 to 0.42 seconds.

The normal corrected QT interval (QTc) is between 0.34 and 0.44 seconds. The QTc is calculated as the QT interval divided by the square root of the RR interval (the RR interval is the time between subsequent QRS complexes) as in the following equation:

$$QT_c = QT / \sqrt{RR} \tag{2.1}$$

The T Wave

In normal hearts, the epicardial usually repolarizes first, despite having depolarized last. When the epicardium repolarizes, its surface charge becomes positive which produces a positive voltage, which is defined as the beginning of the T wave. When the repolarization reaches the endocardial surface, there are no longer any voltages and the T wave ends.

ST segment

When the wave of depolarization fully passes through the ventricle it produces no measurable potential on the surface electrodes. This represents ventricular depolarization and is called the ST segment. The ST segment contains information about myocardial ischemia and injury. Myocardial injury is when myocardial cells are dying (acute myocardial infarction) or if the epicardium is irritated. The hallmark of myocardial injury is ST elevation: the ST segment will have a higher voltage than the heart at rest. Acute MI is a focal process; therefore there will be focal elevation in the ST segment, frequently with the development of focal Q waves. However, early during an acute MI, Q waves are not always seen. The ST elevation of a classic acute MI is typically convex up. The TP segment, from the end of the T to the beginning of the P, is defined as zero voltage and represents the heart at rest.

2.3 Characteristics of ECG components, artifacts and noise

The theoretical frequency distributions of ECG signals are classified as lower frequency P and T waves, middle-to-high frequency QRS complex and high frequency late potentials when they exist. In this thesis we designate the P and T waves as medium-amplitude low-frequency signals (MALFS), the QRS complex as high-amplitude medium-frequency signal (HAMFS) and the VLP is as low-amplitude high-frequency signal (LAHFS). Fig. 2.2 shows a diagram of the different frequency components presented against their respective strengths (Mousa, Yilmaz, 2002) (Mousa, Yilmaz, 2004-a).

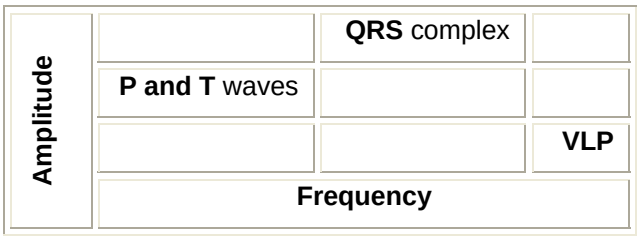

Figure 2.2 Theoretical frequency distribution of ECG signal components

The recorded signal usually contains the desired part plus other undesirable interferences added to the signal through the recording instrumentation and the environment including the patients. In Fig. 2.3 we show the approximate spectrum distribution of these different components. The parts not shown here, are the interferences caused by power lines and their possible harmonics. In the following subsection we present some of the ECG components and their properties since they make up the main concern in the work of isolating and detecting delayed potentials (DP).

The main components of the recorded ECG in addition to possible harmonics are:

- P, T waves: 0-10 Hz
- Motion artefacts: 0-10 Hz
- QRS complex: 0-40 Hz
- AC line: 50/60 Hz
- EMG: 0-10000 Hz
- VLP: 50-250

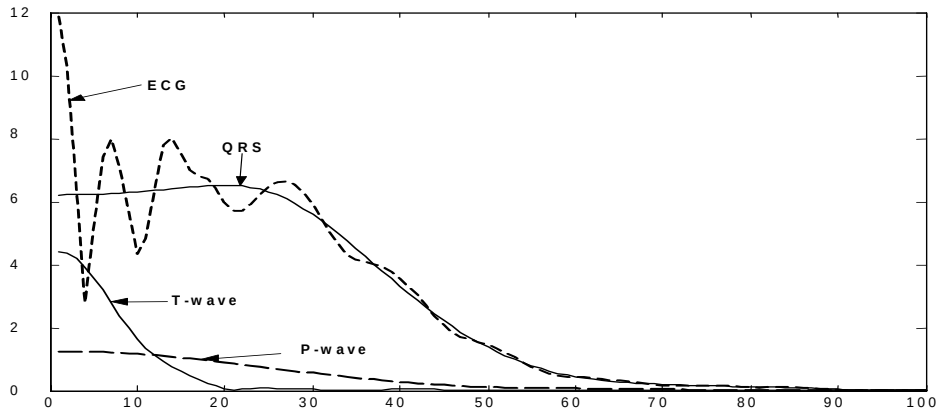

Figure 2.3 Frequency-amplitude relationships of different ECG components

2.4 Noise types and sources

An ECG signal may contain any or all of the following types of interferences (Friesen et al. 1990):

1. Power line interference
2. Electrode contact
3. Motion artefacts
4. Muscle contractions (EMG)
5. Baseline drift and ECG amplitude modulation with respiration
6. Instrumentation noise
7. Electrosurgical noise

A summary of the main noise types and their important properties including duration, amplitude and frequency is shown in table 2.1.

Table 2.1 Summaries of noise types and their properties

Noise type	Amplitude[1]	Frequency (HZ)	Duration (msec.)
Power line interference	Up to 50 %	50/60	Persistent
Electrode contact noise	Recorder gain	50/60	1000
Motion artifacts	500%	Base-line drift	100-500
Baseline drift	15%	0.15-0.3	Varies
Muscle contractions	10%	DC-to-10000	50
Electrosurgical noise	200%	Aliased high frequencies	1000-10000

1. Expressed as % of the peak-to-peak of ECG amplitude

A summary of the characteristics of the different ECG components including durations and frequencies are presented in Table 2.2 below.

Table 2.2 Durations and approximate frequencies of different Cardiac components

Wave	Duration (ms)	Frequency (Hz)
P wave duration:	60 ms to 110 ms	0-10
P-R interval:	120 ms to 200 ms	0-40
QRS duration:	60 ms to 100 ms	0-40
Q-T interval:	340 ms to 420 ms	0-40
T wave duration:	120 ms to 180 ms	0-10

2.5 Lead systems: viewing the heart from different directions

The standard ECG is collected from a series of electrodes attached to the body surface. These electrodes measure the electrical activity of the heart. In one type of configuration, three limb electrodes form a triangle called Einthoven's triangle and the fourth (right leg) is electrical ground. Einthoven's triangle is considered an equilateral triangle for measurement purposes. The voltage measured across the two arms is lead-I (the left arm is defined as positive). Lead-II is measured from the right arm to the left leg (the left leg is defined as positive). Lead III is measured from the left arm to the left leg (the left leg is defined as positive). Lead-III looks at the heart from the right of Lead-I.

Orthogonal X, Y, Z lead system is another type of configuration and is the one used in this study are assumed to be placed in perfect orthogonal configuration as shown in Fig. 2.4 (Malmivuo, Plonsey, 1995). The X electrodes are placed at opposite end in front and back of patient with the frontal lead at V_2 position. The Y lead is placed between the right and left midauxillary lines at the fourth intercostals space. The Z lead is placed at the superior aspect of the manubrium and the proximity of the left leg. In reality these leads are only approximately orthogonal and the assumption of perfect orthogonality does not exist resulting in some correlation in the different leads.

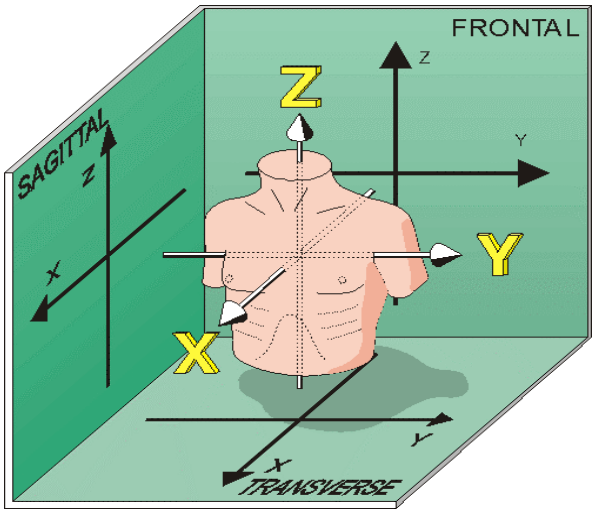

Figure 2.4 The orthogonal XYZ lead system , (Malmivuo, Plonsey, 1995)

2.6 Acute Myocardial Infarction (AMI)

The subject of myocardial infarction is introduced here in order to pave the way and introduce late potentials, which are thought to be a direct consequence of damaged portions of the heart. In the next section we introduce the concept of late potentials, which are considered as noninvasive markers that may help in saving of lives (Breithardt et al.1991)(Makuavi et al. 1994).

Heart attack is a condition technically known as a myocardial infarction MI. MI is a "plumbing problem" in which a blockage in a blood vessel interrupts the flow of blood to the heart causing an "infarct"; an area of dead heart muscle.

Sudden Cardiac Death (SCD), or Cardiac Arrest, kills half of all people who die of heart disease, the number one cause of death in the United States, accounting for more than 400,000 deaths each year. SCD is a catastrophe in which the heart abruptly and without warning ceases to function. It is an "electrical problem" caused by a heart rhythm disorder called Ventricular Fibrillation (VF). It is particularly terrifying because it kills its victims within minutes and often occurs in outwardly healthy people who have no known heart disease. Without emergency help, SCD leads to death within minutes. 95 percent of victims die before reaching the hospital. Victims of cardiac arrest can be saved if immediate medical care is provided.

Heart attacks or "acute myocardial infarction" (AMI), are very common and also very deadly. The underlying cause of a heart attack is usually "coronary thrombosis", which is a blockage of the blood vessels of the heart. The most common symptom is chest pain or discomfort, but in many cases even the patient is uncertain of having a heart attack.

However, many cases go undiagnosed even in the emergency department, and this diagnostic error makes AMI the single leading malpractice litigation-related condition. AMI is often under diagnosed in women or younger adults. In any age patients, AMI can have a variety of presentations, and diagnostic tests such as an ECG may still be normal (NHS 2003)(AIHW 2004).

2.6.1 Prevalence and Incidence of AMI

The term prevalence of heart attack usually refers to the estimated population of people who are managing heart attack at any given time. The term incidence of heart attack refers to the annual diagnosis rate, or the number of new cases diagnosed each year. Hence, these two statistics types can differ: a short-lived disease like flu can have high annual incidence but low prevalence, but a life-long disease like diabetes has a low annual incidence but high prevalence. Some of the available information about prevalence and incidence statistics are:

- **Prevalence of Heart attack:** 7.5 million people with acute myocardial infarction (NHLBI).
- **Prevalence Rate:** approximately 1 in 36 or 2.76% or 7.5 million people in USA.
- **Incidence (annual) of Heart attack:** 1.25 million annually USA (NHLBI); 1.1 million with 650,000 new events and 450,000 recurrences.
- **Incidence Rate:** approximately 1 in 217 or 0.46% or 1.2 million people in USA.
- **Incidence of Heart attack:** Each year, about 1.1 million Americans suffer a heart attack.

People who have had one heart attack are at much higher risk for a second attack. Cardiovascular disease is world's greatest health problem. It kills more people than any other disease (almost 51,000 deaths in 1998 in Australia) and creates enormous costs for the health care system. It also places a heavy burden on individuals and the community due to the resulting disabilities. Cardiovascular disease was estimated to account for 22% of the disease burden in Australia in 1996, 33% of premature mortality and 9% of years of equivalent 'healthy' life lost through disease, impairment and disability. Coronary heart disease and stroke accounted for almost 57% and 25% of the cardiovascular disease burden, respectively (NHLBI 2003).

2.6.2 Prognosis and recurrence of AMI

The prognosis of AMI usually refers to the likely outcome of heart attack which may include the duration of the attack, chances of complications, probable outcomes, and prospects for recovery, recovery period, survival rates, death rates, and other outcome possibilities in the overall prognosis of heart attack. Naturally, such forecast issues are by their nature unpredictable.

1-year survival rate for Heart attack: 24 out of 25 patients will survive if they survive the attack (1 in 25 dies within a year)

Deaths from Heart attack: 459,841 deaths in 1998 (NHLBI); 199,154 deaths for AMI reported in USA 1999 (NVSR Sep 2001)

The key to saving the life of a heart attack patient is immediate medical care. Doctors have clot-busting drugs and other artery-opening procedures that can stop or reverse a heart attack, if given quickly. These drugs can limit the damage to the heart muscle by removing the blockage and restoring blood flow. Less heart damage means a better quality of life after a heart attack. The odds of women having a second heart attack are relatively high. In fact, more women than men will suffer a second heart attack within four years after having their first attack.

2.6.3 Diagnosis errors of myocardial infarction

The most common medical diagnosis error is failure to diagnose, or a delay in diagnosing, an acute myocardial infarction. Infarction means "death of tissue" and a myocardial infarction occur when the heart muscle (tissue) dies.

Time is of the essence when a patient makes a trip to the emergency room complaining of chest pain. With immediate and proper care, the damage from a heart attack can be minimized. However, when an emergency room physician or other healthcare professional mistakes chest pain for indigestion and sends the patient home, the result is often catastrophic. More often than not, an otherwise preventable death occurs, all due to the negligence of the medical professional.

Statistics reveal that a heart attack victim is twice as likely to die if the attending physician significantly delays the diagnosis of myocardial infarction. Since such an unfortunate outcome is so easily avoided, medical malpractice lawsuits based on failure to diagnose often exact a heavy financial toll on the negligent doctor.

After a myocardial infarction (MI), there is a region of the heart with dead myocardium. The ECG undergoes some changes. In some people, the first ECG change is a high peaked T wave. Peaked T waves, if they occur, last only a short time. Convex ST elevation is the next typical change in the ECG. In many people, this occurs within 30 sec after occlusion of the coronary artery and is not preceded by peaked T waves. As the myocardial cells die, R wave voltage decreases and then Q waves develop. The key to diagnosis of an old or recent MI is the presence of abnormal Q waves. An abnormal Q wave is at least 0.04 seconds wide and at least ¼ of the total height of the QRS complex. For the diagnosis of MI, there should be Q waves in at least 2 leads. Q waves are present on the ECG because the scar of the myocardial infarction does not produce a wave of depolarization. If there is an ECG lead directly over the scarred tissue, the lead sees “through” the scar and detects the voltage of the opposite myocardial wall. For example, if there is an anterior MI, then a lead will see through the anterior LV wall and see the vector of the posterior LV wall. The posterior wall vector is pointed to the back away from the lead, producing a Q wave. In essence, the Q wave reflects absence of electrical activity in the region of the MI. The location of Q waves is a predictor of the location of the MI. This occurs over a variable time course of minutes to hours.

After several hours to days, the ST segments return back to their resting values, but the T wave remains inverted. This indicates that the injured cells are either dead (MI) or that blood flow has returned to the artery (reperfusion). Q waves with inverted T waves are consistent with a recent or old MI. After months to years, the heart scars and the T waves can return to their normal upright position. Q waves with normal upright T waves are consistent with an old MI. In some people with small MIs, the Q waves can disappear as the heart scar shrinks after few years. In a large anterior MI (AMI), large Q waves

are typically present. It is the large MI that frequently causes congestive heart failure from the loss of contractile myocardium.

Myocardial tissue does not regenerate once it is damaged. If an area of the myocardium becomes damaged from myocardial infarction, it goes through a 4- to 6- week healing process where it eventually becomes connective or scar tissue and never functions as cardiac tissue again. The electrical activity through this area of damaged tissue is altered and can only be detected on ECG by digital signal processing.

Delayed activations of myocardium, appear to generate delayed potentials (DP) on the body surface, which were previously termed as ventricular late potentials (VLP). These VLPs are low-amplitude high-frequency potentials that have been observed in ECG signals of patients after myocardial infarction (MI) and considered as a noninvasive indicator of Ventricular Tachycardia (VT). Ventricular Late Potentials are covered in more detail in the next section.

2.7 Ventricular Late Potentials

Ventricular late potentials (VLP) are low amplitude signals that occur in the ventricles. Also called Late Potentials (LP), these signals are caused by slow or delayed conduction of the cardiac activation sequence. Under certain abnormal conditions, there may be small regions of the ventricles within a diseased or ischemic region that generate such delayed conduction, Fig. 2.5. This results in depolarization signals that prolong past the refractory period of surrounding tissues and re-excite the ventricles. This re-excitement is known as reentry (Lander, Deal and Berberi, 1988)(Mousa, Yilmaz, 2001-a).

Due to their very low magnitudes, late potentials are not visible in a standard ECG. Moreover, factors such as increased distance of the body surface electrodes from the heart, and inherent noise in patients make identification of VLP beyond the resolution limits of a standard ECG. As a result, high-resolution recording techniques and computerized ECG processing are necessary for detection of late potentials (Rioul,Vetterli, 1991)(Raghuveer, et al 1992)(Thakor, et al. 1993.)(Mallat , 1989).

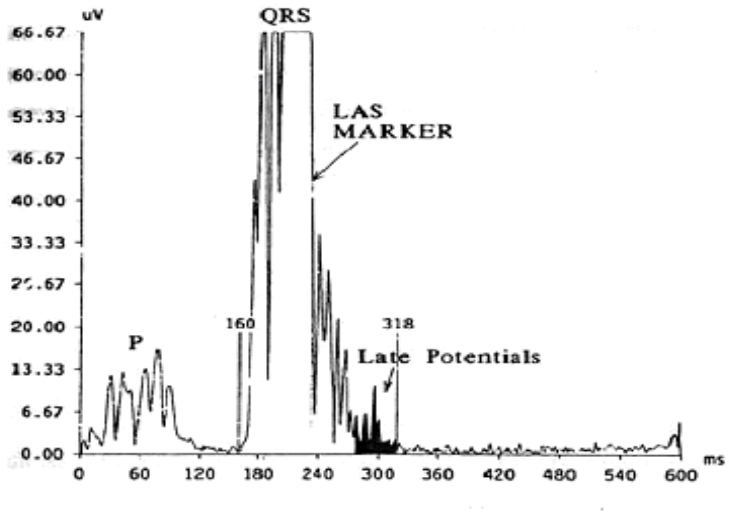

Figure 2.5 Vector magnitude of ECG signal showing the presence of VLP (source: Gang et al. 2000)

Such ECG signal processing includes techniques to improve the ability of detecting and identifying LPs include wavelet transform (WT), complex cepstrum analysis (CCEPS), artificial neural networks (ANN) and other. Some of these DSP tools have been used in this study as will be seen in later chapters.

2.7.1 Diagnostic values of VLP

Ventricular Late Potentials appear to arise from small areas of structurally abnormal myocardium in which ventricular activation is delayed and asynchronous. When surviving heart fibers are separated by connective tissue, delayed activation patterns may occur. The result is a low-amplitude, fragmented local potential. This activity can be recorded in most patients with remote myocardial infarction (heart attack), but is detected at fewer recording sites and is of shorter duration in infarction patients without clinical VT. Late potentials imply that the substrate for reentry is present, and then be precipitated by such triggers as premature ventricular beats, myocardial ischemia (lack of oxygen), or autonomic nervous system instability. Late potentials occur more frequently and are of greater duration in patients with sustained VT than in patients with ventricular fibrillation, a rhythm less associated with conduction delay (Simson 1981)(Vester, Strauer,1994).

Common criteria defining late potentials include the following:

1. The filtered QRS complex is longer than 114 ms
2. The terminal filtered QRS complex remains below 40 μ volt for more than 38 ms, and
3. There is less than 20 μ volt of signal in the last 40 ms of the filtered QRS complex.

2.7.2 Problems encountered in the detection of late potentials

The nature and exact cause of late potentials are not well understood and therefore not well defined. Late potentials are not present in all patients with recurrent VT. In some instances the fragmented activity may be too brief or the late potential may be masked by bundle branch block (BBB).

The signal amplitude is usually too low to be differentiated from noise. Therefore, advanced signal processing must employed in order to extract the needed information.

Detecting VLPs is a challenging task due to the nature of these potentials and the environment in which they exist. The next chapter deals with the limitations and drawbacks of the commonly employed methods in VLP detection.

CHAPTER 3

LIMITATIONS AND DRAWBACKS OF STANDARD DETECTION METHODS

3.1 Introduction

In this chapter we investigate some of the standard and widely accepted approaches employed in the detection of VLPs. We also examine their related assumptions and try to pinpoint the drawbacks and inaccuracies of these methods and their assumptions. The three widely accepted criteria; QRS duration, root-mean-square and duration of the signal at the end of QRS for VLP detection are used in the investigation (Simson 1981).

According to the mechanism of distorted myocardial activity important information to detect Ventricular Late Potentials (VLP) or simply Late Potentials (LP), may be extracted from high-resolution recordings through advanced signal processing techniques. These VLPs are low-amplitude high-frequency potentials that have been observed in ECG signals of patients after myocardial infarction (MI) and considered as a noninvasive indicator of Ventricular Tachycardia (VT). Previous studies have shown that patients with VLP in their ECG have a higher possibility to develop a cardiac event than those without VLPs. Several studies have reported an increased possibility of spontaneous VT or sudden cardiac death in patients with abnormal ECG. Myocardial activation may be delayed due to increased length of the pathway of excitation or due to slowing conduction velocity. Physical characteristics of the myocardium can be critical factors in the delayed activation. The amount of dead myocardium is variable and may be located anywhere in the heart. Regions of dead myocardium create barriers that lengthen the excitation pathway. The increased separation of myocardial bundles and disruption of their parallel orientation by fibrosis distort ventricular activation. Electrograms

recorded from such bundles usually have small amplitudes because of the intervening layers of nonconductive tissue and small diameter of the muscle bundles. When individual bundles are separated by nonconductive regions heterogeneous patterns of activation may occur and result in fragmentation of local electrograms. In regions bordering the infarct, abnormal ventricular conduction during sinus rhythm has been observed and appears to be related to the development of ventricular tachycardia (VT) (Meste,Rix,1994) (Mousa,Yilmaz,2001-a) (Mousa,Yilmaz,2001-b).

Delayed activations of myocardium, appear to generate delayed potentials (DP) on the body surface, which were previously termed as late potentials (Mousa,Yilmaz, 2004-a). Delayed potentials have been recorded from dogs with experimental infarction and corresponded in time with fragmented and delayed electrocardiograms recorded from the epicardium. Potentials recorded from the body surface of human patients, have been accompanied by late, fragmented electrograms recorded directly from the heart.

Although fragmented electrograms can be recorded from most patients with myocardial infarction, delayed activation is more profound and detectable in patients with, compared with those without sustained ventricular tachycardia. The finding of fragmented local electrograms or delayed potentials on the body surface may indicate that the substrate for reentry is present.

Since VLPs are of undefined nature and possibly varying frequency superimposed on a relatively high amplitude medium frequency QRS complex, time domain analysis alone did not yield sufficient diagnostic values and was not able to accurately detect these pathologic oscillations.

The relatively low positive predictive accuracy for identifying vulnerability to ventricular arrhythmias possibly caused researchers to look for other predictive means and almost abandon the subject of ventricular late potentials. This limited performance calls for the need for improved methods in VLP analysis rather than abandoning the subject entirely. These methods should be tested in a frame with wide range of possibilities that might occur.

The task is by no means an easy one due to the composite nature of ECG signals and the difficult environment in which they exist, let alone the unknown nature of these LPs themselves. The diversity of methods available in the analysis of VLP in ECG signals arises from the difficulty of the task. Unfortunately, no single approach has provided a satisfactory conclusion to the problem at hand. Wavelet transform is shown to be a possible alternative to approach the problem of identifying late potentials (LP) and in addition it is also able to detect (DP) that might occur anywhere in the cardiac cycle.

The study emphasizes that some standard methods are not capable of detecting DPs in general and limit their focus on LPs only.

3.2 Standard detection methods using Simson's parameters

Present studies in the field underlined a variety of methods and approaches and at times making assumptions about the nature of VLP. These studies have been using mainly adapted methods based on signal averaging of a large number beats in order to improve the signal to noise ratio (SNR). Then a vector magnitude is calculated using a three orthogonal lead system. High-pass filtering is then applied in order to remove the high-amplitude low to medium frequency components in the signal. Time domain analysis of filtered QRS (FQRS) is the most widely used method in the analysis of VLP. Simson has developed a technique, which is based on FQRS and is still widely used (Simson, 1981). The three parameters he suggested were introduced in section 2.7.1 of this thesis which will be revisited in the corresponding part of the wavelet transform. This method depends considerably on the accurate detection of the QRS endpoints, the correct detection of which is not always guaranteed. This detection process is the bottleneck of the entire analysis and any approximation errors can be projected onto the rest of the works and their results. The analysis procedure proposed by Simson is summarized as follows.

3.2.1 Signal averaging and digital filtering

The ECG signal from each lead is aligned and averaged after passing though a template program to reject ectopic beats and grossly noisy signals. Each averaged lead is filtered to remove the low-frequency content. The choice of the filter type, size and corner frequency, have a pronounced effect on the values of the calculated parameters. The filter used by Simson as well as in the first part of this work is a 4-pole high-pass Butterworth filter with corner frequency of 25-Hz (Rompelman, Ros 1989).

3.2.2 Vector magnitude calculation

The filtered signal from the three X, Y and Z leads are combined into a vector magnitude $M = \sqrt{(X^2 + Y^2 + Z^2)}$, which allows for the detection of high-frequency voltages in any lead. The vector magnitude of the filtered signals is referred to as the filtered QRS (FQRS) complex (Lander, Deal, Berberi, 1988).

The X, Y, Z leads used in this system are assumed to be placed in a perfect orthogonal configuration. The X lead is placed between the right and left midauxillary lines at the fourth intercostals space. The Y lead is placed at the superior aspect of the manubrium and the proximity of the left leg. The Z electrodes are placed at opposite end in front and back of patient with the frontal lead at V_2 position. In reality these leads are only approximately orthogonal and the assumption of perfect orthogonality does not exist resulting in some correlation in the different leads. This concept is detailed in section 5.4.2 of this thesis.

3.2.3 Extracted Parameter

Based on the vector magnitude, the three parameters calculated by Simson are given as follows:

- Duration of the QRS complex denoted as **QRSDUR:**

From the vector magnitude of the signal a noise sample was measured and its mean and standard deviations were calculated for use in the detection of

end points. A threshold value was defined as the mean plus three times the standard deviation of the noise sample. The noise sample for the QRS onset was chosen to be 20 msec wide and began about 50 msec before the approximate QRS onset. The noise sample for the QRS offset was 40 msec wide and began about 60 msec after the QRS. A search where the average of the samples exceeds the threshold value within a 5-msec segment was performed. When the sample average exceeds the required threshold, the midpoint of the 5-msec segment was called the endpoint (onset or offset).

- Duration of the low-amplitude signal in the last 40 msec, denoted as **LAS40** is calculated.
- The root-mean-square (RMS) value of **LAS40** denoted by **RMS40** is calculated.

The 40 msec value was chosen as the interval because it is the period of the 25-Hz used as a corner frequency of the filter.

A parameter is considered a positive indicator when it exceeds a certain threshold value. In Simson's method, the threshold value for the QRS duration was 120 msec, a 25 μ v for the RMS40 and about 100 msec for the duration of LAS40. A case is classified as VLP positive when any two of the three parameters are found to be positive indicators. For this work, a similar procedure is carried out with the threshold values extracted from the base ECG signal.

3.3 Problems encountered in the detection of VLP

Many observers have recorded VLPs and disorganized activations from infaracted myocardium. The source of VLP was attributed to the delay in activation due to the damaged myocardium region. These VLPs activities in the form of fragmented deflections are found in border zones surrounding the scar tissue of a myocardium infarct (MI). This border zone is composed of conducting and non-conducting regions, which slow and fragment the depolarization wave. This behavior resembles a capacitor composed of

dielectric placed between two conducting plates. One has to note that still little is known about VLP in terms of their occurrence.

Questions that still to be answered include:

- Do they occur periodically at every beat or do they occur at an interval of beats?
- Do they always occur at the exact location?
- Do they always have the same duration, frequency, and amplitude?

The exact answers to these questions are not yet addressed properly however, it is fair to say that they are important to form the prerequisite to isolate VLP from ECG signals and draw accurate conclusions.

The end of the QRS complex is a reasonable choice for detecting of VLP since it is the relaxation period of the myocardium and any signal in that portion can be detected easily, but not for other potentials occurring in other regions of the ECG signal such as DP. The effect of type of infarct and its variable manner is also reported by Simson in his work and is reproduced here in the table (3.1). Voltage in last 40 msec of the filtered QRS complex, are shown for two different types of infarctions, with values in μ volts listed as mean ± one standard deviation. This table shows the dependence of parameter values on the type of infarct. We can see the difference in both mean and standard deviations with change of infarct type even for the same type of patient.

Table 3.1 Voltage in last 40 msec of filtered QRS for two different types of infarctions (source: Simson 1981)

	Control Patients	**Patients with VT**
Anterior MI	86.6 ± 56.5 μV	20.6 ± 20.7 μV
Inferior MI	55.4 ± 25.2 μV	10.9 ± 5.2 μV

Table (3.1) shows an example of the dependence of parameter values on the type of infarct and in some sense supports our argument about the variability

of the occurrence of VLP. There are some other problems that exist in the detection process. In the next part we shall touch upon these difficulties.

3.4 General problems in some of the standard VLP detection methods

In addition to the particular parametric values of the desired signal, the different approaches used may influence the end results and can even reduce its prevalence. A sample of these different approaches is discussed below. One should note that we are not questioning the integrity of the three parameters set by Simson; rather, it is the method by which they are extracted.

3.4.1 Signal averaging

Signal averaging is a common method used for improving the signal to noise ratio (SNR) that is essential to detect low-level signals. High sampling frequencies (>1000 Hz) and high-resolution analog to digital conversion (12-16 bit or higher) are required. Signal averaging process is essentially statistical in nature and it is based on white noise assumption. Some studies have defined VLP as having a repetitive and deterministic in nature as opposed to periodic one (Lander, Deal, Berberi, 1988). Furthermore, in contrast to stationary processes, late potentials are a transient or short time phenomenon. Therefore, it would be expected that their statistical properties should change with time. Hence, late potentials are considered as non-stationary waveforms. Unless the desired signal repeats at every beat, averaging will tend to reduce its strength rather than improve its SNR. Therefore, we must know the repetition nature of the VLP before applying any averaging in order to get optimum improvement in SNR. Of course averaging every beat is optimal if the desired signal is repeated at every beat periodically, and results in SNR improvement equal to $\sqrt{N}$ where N is the number of averages. According to an expert consensus document:

"Current research is establishing the extent to which the terminal QRS complex and ST segment are optimal ECG intervals and orthogonal ECGs are the ideal leads for detecting signals generated by myocardial tissue responsible for sustained ventricular arrhythmias. Results of analysis of three dimensional, computer-assisted, ventricular

activation maps recorded during sustained ventricular tachycardia and sinus rhythm from patients with healed myocardial infarction undergoing arrhythmia surgery have shown that current methods of signal-averaged ECG analysis limiting interrogation to the terminal QRS/ST segment exclude detection of 95% of the signals generated by myocardium responsible for sustained ventricular tachycardia" (CAIN et al., 1996)

3.4.2 Vector magnitude

Calculation of the vector magnitude means taking the square root of the sum of squares of the bipolar X, Y, Z leads. Anatomically perpendicular leads on the body surface give no guarantee of electrical orthogonality as stated by the study of (Lander, Deal, Berberi, 1988).

Without perfect orthogonality of the leads, the vector magnitude distorts the signal content in these leads. When combining the three leads into a single vector magnitude, information in these individual leads is weakened in the transformation. The vector magnitude is not a unique representation of the three leads since we may have many signals making up the same vector magnitude. The standard way of calculating the vector magnitude produced undesirable cross terms that can overshadow the desired part and may even prevent their accurate detection. These cross terms arise from the different frequency components contained in the signal including noise and VLP when they exist (Mousa, Yilmaz, 2002).

3.4.3 Filtering and cutoff frequencies

The ECG is high-pass filtered to reduce the low frequency signals contained in the QRS complex. The high-amplitude low-frequency component may interfere with the measurement of the desired microvolt level signals, the VLP. The main problem seems to be the selection of a steep and linear phase filter causing little or no ringing in the QRS being examined while preserving signal morphology. In reality, bi-directional filtering is appropriate if one is considering the entire signal but if the interest lies in its end, as is the case of VLP, filtering a reversed version of the signal will be adequate. A bi-directional IIR filter may strongly influence signal morphology, whereas alternative FIR filters are difficult to optimize. A low number of taps results in

a poor frequency response, while a large number of taps increases filter ringing and obstructs precise detection of low-amplitude signals (Oppenheim and Schafer, 1989). No consensus has been established so far for any frequency band to extract reliable time domain parameters. The choice of filter cutoff as reported by some of the researchers is presented in Table (3.2), and as can be seen the choice will affect all resultant parameters where prevalence indicates the number of accurately detected cases (Gramatikov, 1993) (Makuavi et al., 1994).

Table 3.2 Effect of cutoff frequency of the filters on VLP prevalence.

Filter (Hz)	VLP prevalence (%)	QRSDUR (msec)	LAS40 (msec)	RMS40 (μVolts)
25	29.2	103.7±13.9	30.5±14.8	3.5±1.0
40	25.0	98.0±13.7	31.9±13.3	3.5±1.0
80	20.8	97.0±13.9	40.4±14.2	2.7±1.0

3.4.4 QRS duration and endpoint detection

Another fundamental problem in QRS detection is the accurate determination of RR intervals. The first difference in amplitude of successive samples of the ECG signal is one of the commonly used methods for this purpose. However, this method and many of the other methods used are very sensitive to motion artifacts and other interference and noise.

The detection of the QRS complex, as well as the T and P waves is the most important task in ECG signal analysis. In general, once the QRS complex has been identified, a more detailed examination of ECG signal, including the heart rate, the ST segment, etc., can be performed. There are many algorithms for QRS detection with different reported performance (Friesen, 1990).

Next chapter introduces the suggested signal processing tools to detect abnormalities occurring anywhere in the conduction path. This includes wavelet transform as the major tool supported by the application of the complex cepstrum and artificial neural network techniques.

CHAPTER 4

DSP TOOLS USED IN UNIFIED FRAME

4.0 Introduction

Digital signal processing uses sophisticated mathematical analysis and algorithms to extract information hidden in signals derived from sensors. In biomedical applications, these sensors, such as electrodes, accelerometers, optical imager's etc. record signals from biologic tissue with the goal of revealing their health and well being in clinical and research settings. Refining these sign-processing algorithms for biologic applications requires building suitable signal models to capture signal features and components that are of diagnostic importance. Since most signals of biologic origin, are time varying there is a special need for capturing transient phenomena in both healthy and chronically ill states. A critical feature of many biologic signals is frequency-domain parameters. Time localization of these changes is an issue for biomedical researchers who need to understand subtle frequency content changes over time. Certainly signals marking the transition from severe normative to diseased states of an organism sometimes undergo severe changes that can easily be detected using methods such as the short-time Fourier transform (STFT) for deterministic or energy signals and its companion, the spectrogram, for power signals. The basis function for the STFT is the complex sinusoid, which is suitable for analysis of narrow-band signals. For signals of biological origin, the sinusoid may not be a suitable analysis signal.

Biologic signals are often spread out over wide areas of the spectrum. Also as Rioul and Vetterli point out, when the frequency content of a signal changes in a rapid fashion, the frequency content becomes smeared over the entire frequency spectrum, as it does in the case of the onset of seizure spikes in epilepsy or a fibrillating heartbeat as revealed on an ECG. The use

of narrow-band basis function does not accurately represent wide-band signals. We would prefer that our basis function be similar to the function under study. In fact, for a compact representation using as few bases as possible, it is desirable to use basis functions that have a wider frequency spread, as most biologic signals do. There are a number of methods of transforming a 1-D signal in time into a 2-D distribution of signal strengths in time and frequency. The time frequency distribution (TFD) gives a measure of intensity of frequencies over time. Various transformation methods such as the short time Fourier transform, Wigner distribution, smoothed pseudo Wigner-Villa distribution and cone-shaped kernel are the well known ones. The properties of each of these time-frequency analysis methods are described elsewhere.

Wavelet theory, which provides for wide-band representation of signals, is therefore a natural choice for biomedical engineers involved in signal processing and is currently under intense study. These characteristics motivated our approach, which makes use of wavelet, transforms (WT) to be presented later in this thesis.

4.1 Wavelet transform

4.1.1 Introduction

Various digital-signal-processing methods are applied to the ECG to identify, extract and analyze the different ECG signal components. In this large set of signal-processing tools, a technique called wavelet transform proved to be a suitable one describing time and frequency characteristics of ECG waves. Here we present an overview of the wavelet technique applied to the area of ECG signal analysis. We will first give some rationale for the utilization of new ECG processing tools and then describe the contribution of the wavelet transform in the analysis of ECG signals.

This technique will be discussed and compared to the classical techniques using the time-domain and frequency-domain methods. The frequency representation of a signal can be obtained using different techniques including the most frequently used Fourier transformation that is able to decompose any temporal signal in an infinite set of sinusoid functions. This set of sinusoid functions is then represented in the frequency space using the amplitude and the phase of each of these functions thus provides a link between the time representation of a signal in seconds and the frequency representation in cycle/second. Theoretically these signals should be deterministic and periodic in nature (Oppenheim, Schafer, 1989).

As the digitized ECG is a finite signal, its boundaries are usually abrupt and these abrupt cuts of the signal make it discontinuous which introduces a smearing or a decrease and spread of all the estimated frequency peaks. In order to avoid this, the calculation of the FFT is applied to the windowed ECG.

Windowing aims at removing this discontinuity by smoothing and decreasing the boundary of the ECG signal to near zero which in effect reduce the frequency resolution and therefore lowers the quality of the estimation of the ECG signal frequencies. Another unavoidable limitation of the Fourier transformation for the ECG analysis is that this technique does not provide insight into exact location of frequency components in time.

The frequency content of the ECG varies in time; the QRS complex is a high frequency wave whereas the P and T waves contain low-frequency components, therefore, an accurate description and representation of the ECG frequency contents according to their location in time is needed. This kind of representation provides insight into three dimensions of the ECG signal: the time, the frequency and the amplitude. Utilization of time-frequency representation in ECG analysis is thus justified which be introduced in the next sections.

4.1.2 Wavelet basics

A wavelet is a small wave with its energy concentrated in time to give a tool for the analysis of transients, non-stationary or time-varying signals. The goal of most expansions of a signal is to have the coefficients of the expansion give more useful information about the signal than is directly obvious from the signal itself. A second goal is to have most of these coefficients be zero or very small. This is what is called sparse representation and is extremely important in applications for statistical estimation and detection, data compression, non-linear noise reduction and fast algorithms (Burrus, Gopinath and Guo, 1998).

4.1.3 Why Wavelets?

The basic properties that make wavelet transforms very useful, efficient and effective in analyzing a very wide class of signals and phenomena are:

1. The wavelet expansion allows the separation of components of a signal that overlap in time or frequency.

2. A wavelet expansion coefficient represents a component that is itself local and is easier to interpret and allows a more accurate local description and separation of signal characteristics.
3. Ideal for adaptive systems that adjust to suit the signal since they are adjustable and adaptable and can be designed to fit individual applications.
4. The size of the wavelet expansion coefficients drops off rapidly for a large class of signals a useful property in signal and image compression, denoising and detection.
5. Calculation of the discrete wavelet transform (DWT) is well suited for digital computers since only multiplications and additions are included in the defining equations of the wavelet transform.

4.1.4 Wavelets and Wavelet expansion systems

The wavelet transform decomposes a signal $f(t)$ into a set $\psi(t)$ of orthogonal basis functions that make the wavelet family (Mallat , 1989) (Rioul,Vetterli, 1991) . The general formula for representing the decomposition of the signal as a linear combination of this expansion set $\psi(t)$ is:

$$f(t) = \sum_k a[k]\psi_k(t) \tag{4.1.1}$$

If the expansion set is also orthogonal it forms a basis for that class of functions where orthogonality means:

$$\langle \psi_k(t), \psi_l(t) \rangle = \int \psi_k \psi_l(t) dt = 0 \qquad \text{k} \neq \text{l} \tag{4.1.2}$$

The $a[k]$s are the real valued expansion coefficients which can be calculated using the inner product

$$a[k] = \langle f(t), \psi_k \rangle = \int f(t)\psi_k(t)\, dt \tag{4.1.3}$$

The inner product for two functions $x(t)$ and $y(t)$ is defined as a scalar a obtained as:

$$a =< x(t), y(t) >= \int x^*(t) y(t) dt \tag{4.1.4}$$

where $x^*(t)$ is the complex conjugate of $x(t)$ with the range of integration depending on the signal class considered.

Two signals with nonzero norms are called orthogonal if their inner product is zero. Where the norm or length of a vector is defined as:

$$\|f\| = \sqrt{< f, f >} \tag{4.1.5}$$

In the Fourier transform, the orthogonal basis functions $\psi_k(t)$ are sin($\omega_0 kt$) and cos($\omega_0 kt$), for the wavelet expansion, a two-parameter system is constructed as:

$$f(t) = \sum_k \sum_l a_{j,k} \psi_{j,k}(t) \tag{4.1.6}$$

where both j and k are integers and the $\psi_{j,k}(t)$ are the wavelet expansion functions that usually form an orthogonal basis. The set of expansion coefficients $a_{j,k}$ are called the discrete wavelet transform (DWT) of $f(t)$.

The Fourier transform maps a one-dimensional signal into a one-dimensional sequence of coefficients; the wavelet expansion maps it into a two-dimensional array of coefficients. It is this two-dimensional representation that allows localizing the signal in both time and frequency in the wavelet transform. And the two-dimensional representation is achieved from a mother wavelet $\psi(t)$ by:

$$\psi(t) = \frac{1}{\sqrt{a}} \psi\left(\frac{t-b}{a}\right) \qquad a > 0 \tag{4.1.9}$$

The factor $\frac{1}{\sqrt{a}}$ is introduced to guarantee energy preservation and ***a*** represents the scale parameter and ***b*** represents the translation parameter producing the time-shift. The function $\psi_{a,b}(t)$ is obtained by scaling and translation of the mother wavelet $\psi(t)$ at time ***b*** and scale ***a***. Increasing the scale value will stretch the function $\psi_{a,b}(t)$, a useful form for the analysis of low frequency contents while lowering this factor will shrink the function $\psi_{a,b}(t)$ producing a form suitable for the analysis of high frequency contents of signals (Burrus et al, 1998).

There are many wavelet systems but all have some general characteristics as:

1. It is a two-dimensional set (a basis) for some class of one-dimensional signals.
2. Gives time-frequency localizations of the signal.
3. Calculation of the wavelet transform coefficients from the signal requires O(N log N) operations which is the same as for the fast Fourier transform (FFT).

While the Fourier series maps a one-dimensional signal into a one-dimensional sequence of coefficients, the wavelet expansion maps it into a two-dimensional array of coefficients. It is this two-dimensional representation that allows localizing the signal in both time and frequency.

Three more additional characteristics are more specific to wavelet expansion:

1. The two-dimensional representation is achieved from a mother wavelet $\psi(t)$ by:

$$\psi_{j,k}(t) = 2^{j/2}\psi(2^j t - k) \qquad j,k \in Z \tag{4.1.10}$$

the factor $2^{j/2}$ maintains a constant norm independent of the scale j.

2. Multi-resolution is useful property of wavelet systems. if a set of signals can be represented by a weighted sum of $\varphi(t-k)$, then a larger set (including the original) can be represented by a weighted sum $\varphi(2t-k)$.
3. Lower resolution coefficients can be calculated from higher resolution coefficients by a tree-structured algorithm called filter bank of the DWT.

The multi-resolution formulation needs closely related basic functions. In addition to the mother wavelet $\psi(t)$, we will need another basic function called the scaling function $\varphi(t)$. The simplest possible orthogonal wavelet system is generated from the Haar scaling function and wavelet. These are shown in Figure (4.1.1)

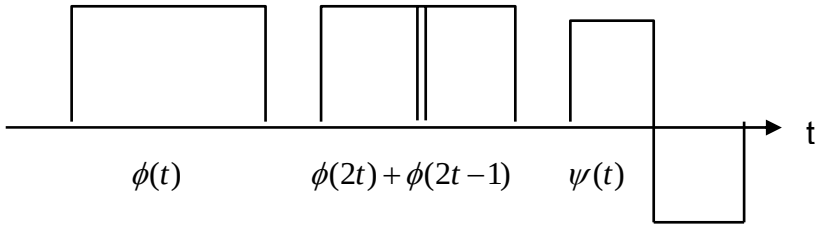

Figure 4.1.1 Haar scaling $\varphi(t)$ and wavelet $\psi(t)$ functions

Using the combination of these scaling functions and wavelets allows a larger class of signals to be represented by:

$$f(t)=\sum_{-\infty}^{\infty} C_k \varphi(t-k)+\sum_{-\infty}^{\infty}\sum_{j=0}^{\infty} d_{j,k}\psi(2^j t-k) \qquad (4.1.11)$$

4.1.5 Basics of the Daubechies wavelets

The function displayed in Figure 4.1.2 is the so-called wavelet function from the Daubechies family of wavelet functions which is only one of a number of wavelet families (Burrus, Gopinath and Guo, 1998).

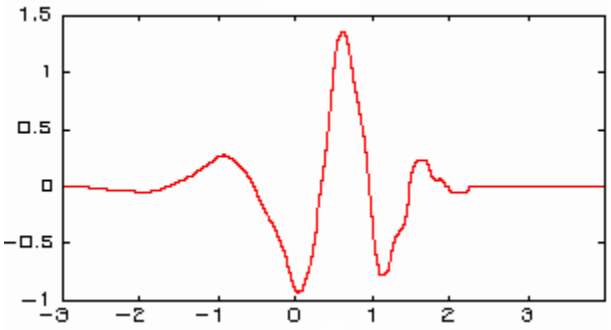

Figure 4.1.2 Daubechies wavelet

The wavelet function (mother wavelet) is orthogonal to all functions, which are obtained by shifting the mother by an integer amount. Furthermore, the mother wavelet is orthogonal to all functions, which are obtained by dilating (stretching) the mother by a factor of 2^j and shifting by multiples of 2^j units.

The orthogonality property means that the inner product of the mother wavelet with itself is one and the inner products between the mother wavelet and the aforementioned shifts and dilates of the mother are zero. The collection of shifted and dilated wavelet functions is called a wavelet basis. The grid in shift-scale space on which the wavelet basis functions are defined is called the dyadic grid. The orthonormality of the wavelets has a very important mathematical and engineering consequence: any continuous function may be uniquely projected onto the wavelet basis functions and expressed as a linear combination of the basis functions. The collection of coefficients, which weight the wavelet basis, functions when representing an arbitrary continuous function are referred to as the wavelet transform of the given function.

Representation of an arbitrary function by an infinite collection of wavelet transform coefficients may not, at first glance, appear to be worthwhile. The real strength of wavelet transform representations, however, is that functions (or signals or images) that look like the wavelet function at any scale may be well represented by only a few of the wavelet basis functions. The wavelet transform therefore provides an efficient representation for functions, which have similar character to the functions in the wavelet basis.

Decomposition of functions in terms of orthonormal basis functions has been known for centuries where continuous functions may be represented by an orthonormal basis of sinusoidal functions. The wavelet basis functions have what is called compact support. This means that the basis functions are non-zero only on a finite interval. In contrast, the sinusoidal basis functions of the Fourier expansion are infinite in extent (Rajoub B., 2002).

The compact support of the wavelet basis functions allows the wavelet transformation to efficiently represent functions or signals, which have localized features. Many real-world signals have these features, and decompositions such as the Fourier transform are not well suited to represent such signals. The efficiency of the representation is important in applications such as compression, signal detection, denoising, and interference excision. The common thread throughout all these applications is that the structured component of a signal is well represented by a relative few of the wavelet basis functions, whereas the unstructured component on the signal (e.g. noise) projects almost equally onto all of the basis functions. The structured and unstructured parts of the signal are then easily separated in the wavelet transform domain.

Even if a signal is not well represented by one member of the wavelet family, another may still very efficiently represent it. Selecting a wavelet function, which closely matches the signal to be processed, is of utmost importance in wavelet applications.

The Daubechies family is just one of a number of wavelet families. Some of the families are characterized by orthonormal basis functions as described above. Other wavelet families, for example the biorthogonal wavelets, are orthogonal in a more general sense than has been described. Still other families of wavelet basis functions are not orthogonal in any sense. The large number of known wavelet families and functions provides a rich space in which to search for a

wavelet, which will very efficiently represent a signal of interest in a large variety of applications.

The great interest in wavelets today is only partly due to their ability to efficiently represent functions with localized features. The interest is also due to the fact that it was discovered that some wavelets might be implemented in an extremely computationally efficient manner by means of what is called a multi-resolution analysis. Just as Fast Fourier Transform (FFT) algorithms made the Fourier Transform a practical tool for spectral analysis, the multi-resolution analysis has made the Discrete Wavelet Transform (DWT) a viable tool for computational time-scale analysis (Raghuveer, et al 1992).

4.1.6 Wavelet transform decomposition of ECG signals

To illustrate how wavelet decomposition works, Fig. 4.1.4 shows the decomposition of a signal into its wavelet components (Rioul,Vetterli, 1991) .

The signal is an actual vector magnitude of an ECG signal and below it are the eight separate sub-signals, which have been obtained by decomposing this ECG signal into its wavelet components. Each component is called a level and the levels are numbered from –1 upwards.

When the separate wavelet levels are added together, the original signal is regained. This is shown in Fig. 4.1.5. Starting at the top left-hand diagram, which shows level –1 alone, and moving down successive levels is added until finally, at the bottom diagram, the original signal has been regained.

Depending on the type of wavelet used the dividing line between frequency bands may overlap and frequency content of neighboring levels may also overlap. The number of levels n is related to the signal size N according to $N = 2^n$ therefore a signal of 128 samples will have a total of n = 7 levels.

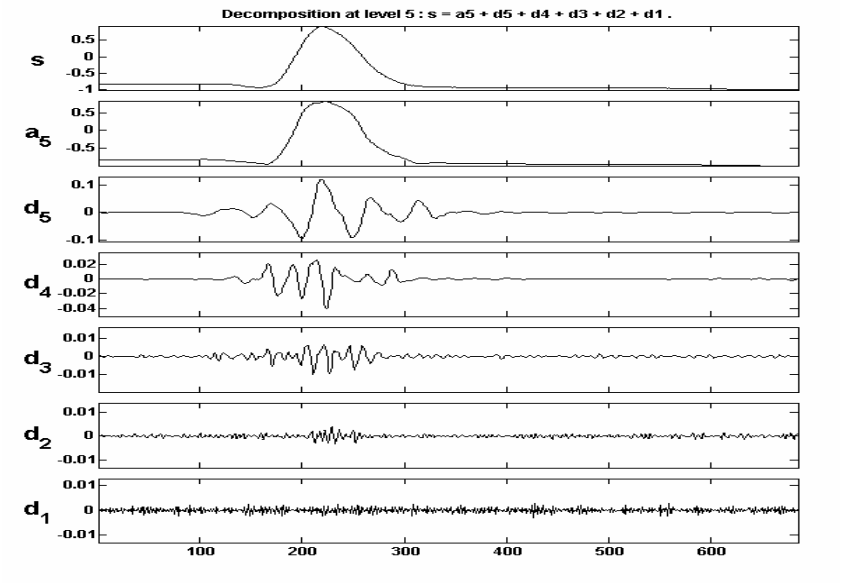

Figure 4.1.4 Wavelet decomposition of an actual ECG signal

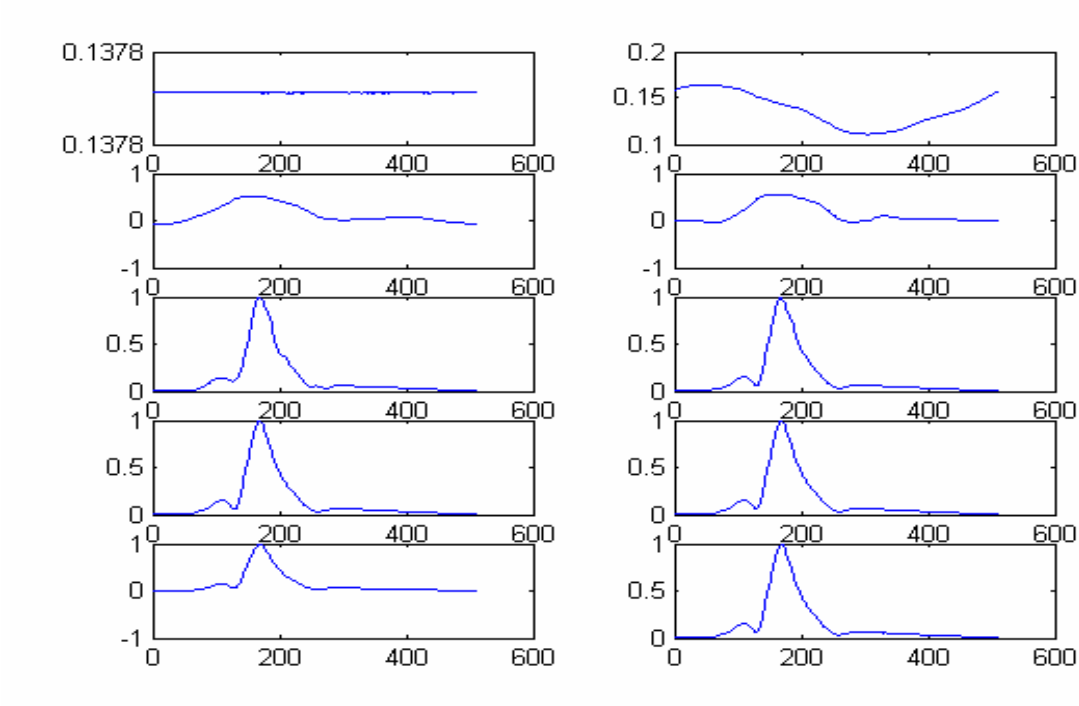

Figure 4.1.5 Step by step reconstruction of ECG signal from its levels

The frequency content of these levels is shown in table 4.1.1 computed for a sampling frequency f_s = 1024 Hz. We see that the highest frequency content falls in L7, which is equal to the Nyquist frequency.

Table 4.1.1 Frequency distribution of different levels

Level	L7	L6	L5	L4	L3	L2	L1
Frequency (Hz)	512 : 256	256 : 128	128 : 64	64 : 32	32 : 16	16 : 8	8 : dc

Due to the overlapping spectral components in the ECG signal, the WT provides some advantages in the analysis and in separating the P, QRS, and T waves since it looks at both time and frequency domains. As can be seen, P-wave, T-wave and motion artifacts are contained in levels L2 and L1 in this example. Muscle noise and QRS last for the entire spectrum of the ECG with the QRS having the higher relative strength.

Fundamental to the problem of rhythm monitoring is the detection and delineation of QRS complexes, and quite often the processes required for this purpose are more complicated than the classification scheme. In this part, a method for the detection of QRS complexes and a classification scheme using the wavelet transform is presented. The detection of the QRS complex, as well as the T and P waves is one of the most important starting points in ECG signal analysis. Once the QRS complex has been identified, a more detailed examination of ECG signal, including the heart rate, the ST segment, etc., can be performed.

Wavelet transform is a suitable technique for time-frequency analysis. By decomposing signals into elementary building blocks that are well localized both in time and frequency, the WT can characterize the local regularity of signals. This feature can be used to distinguish ECG waves from serious noise, artifacts and baseline drift. An algorithm based on the WT for detecting QRS complex, P and T waves have been used. A dyadic wavelet transform is used for extracting ECG characteristic points. The local maxima of the WT modulus at different scales can be used to locate the sharp variation points of ECG signals. The algorithm first detects the QRS complex, then the T wave, and finally the P wave.

Signal singularities often carry the most important information. It is important to find the location of singularity and characterize the singular degree in signal processing (Meste, Rix, 1994)(Mousa, Yilmaz, 2004-a).

4.1.7 WT filtering and detection of the R peak

A major task of the method; which is also sensitive to noise lies in the process of isolating independent beats. The WT method was employed in this process as well as other parts of the analysis by combining levels **L10** and **L11** which emphasize the presence of the R-peak, reduce and remove base-line drift as seen in Fig. 4.1.6. During this process the mid-point between two R-peaks is taken as the dividing point between two successive beats. The heart rate (HR) and RR intervals are then easily obtained (Mousa, Yilmaz, 2004-c).

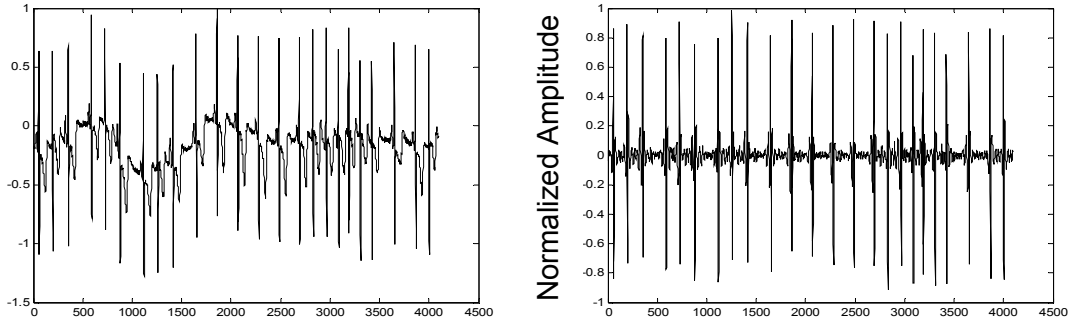

a. Original signal **b.** Appropriate WT levels

Fig. 4.1.6 Detection of R-peak using WT to remove base line variations

4.1.8 WT application in clustering of similar beats

As we will see later in chapter 6, the WT plays an important role in the process of clustering of similar ECG beats. Introduced here is a portion of that analysis. We begin by assigning the first beat as the template. The second beat received is compared to this template, aligned with template and averaged together if the correlation value exceeds the predefined threshold. If the beat and template are not similar (i.e., correlation value is less than the threshold), this new beat is appended to template increasing the size of template by one beat. This in effect

generates a multi-beat template. The process is continued to the end of the record. The resulting multi-beat template is then taken as the template for that patient that also summarizes the contents of the entire record.
Due to heart rate variability in the different data sets, these processes generate R-R intervals that are not all equal. The portions of signal falling between three R-peaks were separated and their lengths made equal by centering them in a zero-padded vector. A total of 13 different matrices resulted each containing corresponding levels from all beats and designated as {**L1, L2, … ,L13**}. A cross-correlation process generated the different templates. The size of the templates {**T1, T2, …, T13**} depended on the degree of similarity set by the threshold value, with high similarity giving a smaller size template.

To explain how the different templates labeled **T1, T2, …,T_n** are formed we will consider one of them since the process applies to the rest in exactly the same manner. The T may be regarded as column matrix with variable size that is decided by the number of beats appended to it. First the WT of a beat is performed producing a number of levels that is related to the number of samples in that beat.

As an example taking the WT of record of 4096 samples will produce 13 different levels. Each level in the decomposition of the first received beat is appended to the corresponding **T1, T2, …,T_n** to form the starting template. At this point we have 13 different column vectors each containing one level representing the first beat. When the second beat is received, it will go through the process of decomposition again producing a total of 13 different levels. The cross-correlation of each one of these levels is calculated with the corresponding entry contained in each T vector, i.e., **L1** with **T1, L2** with **T2** and so on. If the signal in a particular level say **L1**, meets the threshold value implying similarity, this level is aligned and averaged with that of **T1** otherwise **L1** is appended to **T1** increasing the size of **T1** by one, similarly for the rest of the levels and T vectors. This is continued until the last beat after which the T vectors will have different numbers of levels appended to them depending on their similarity.

4.1.9 WT-based vector magnitude calculation

The ECG leads may be composed of a number of different components such as:

$$X = X1 + X2 + \ldots + X9, \tag{4.1.12-a}$$

$$Y = Y1 + Y2 + \ldots + Y9, \tag{4.1.12-b}$$

$$Z = Z1 + Z2 + \ldots + Z9, \tag{4.1.12-c}$$

With X, Y and Z defined as above where the numbers indicate the level number and represent a signal with different frequency content. The lower numbers are the low levels, which contain low frequencies, and the higher numbers are the high levels containing high frequency part of the signals. For a signal with 512 samples, the WT decomposes the three X, Y and Z leads into nine different levels. When taking the vector magnitude we will have:

$$M = \sqrt{(X^2 + Y^2 + Z^2)}$$

$$\begin{aligned} M^2 = {} & X1^2 + X2^2 + \ldots + X9^2 + \\ & Y1^2 + Y2^2 + \ldots + Y9^2 + \\ & Z1^2 + Z2^2 + \ldots + Z9^2 + 2CT \end{aligned} \tag{4.1.13}$$

The CT component in (4.1.13) represents the product of cross-terms between all different frequencies in the signal as shown in (4.1.14).

$$\begin{aligned} CT = {} & X1X2 + X1X3 + \ldots + X8X9 + \\ & Y1Y2 + Y1Y3 + \ldots + Y8Y9 + \\ & Z1Z2 + Z1Z3 + \ldots + Z8Z9 \end{aligned} \tag{4.1.14}$$

$$X^2 = (X1^2 + \ldots + X9^2) + 2\left[X_j \left(\sum_{k=j+1}^{9} Xk \right) \right] \tag{4.1.15-a}$$

$$Y^2 = (Y1^2 + \ldots + Y9^2) + 2\left[Y_j \left(\sum_{k=j+1}^{9} Yk \right) \right] \tag{4.1.15-b}$$

$$Z^2 = (Z1^2 + \ldots + Z9^2) + 2\left[Z_j \left(\sum_{k=j+1}^{9} Zk \right) \right] \tag{4.1.15-c}$$

To simplify the presentation let us combine some of the levels to form a frequency separation similar to that defined for (P, T), QRS and VLP. With this division we have signals, which are composed of three frequency bands. When these signals are used in the calculation of the vector magnitude we have:

$$X = X_T + X_Q + X_V \tag{4.1.16-a}$$

$$Y = Y_T + Y_Q + Y_V \tag{4.1.16-b}$$

$$Z = Z_T + Z_Q + Z_V \tag{4.1.16-c}$$

$$\begin{aligned} M^2 = {} & (X_T^2 + Y_T^2 + Z_T^2) + \\ & (X_Q^2 + Y_Q^2 + Z_Q^2) + \\ & (X_V^2 + Y_V^2 + Z_V^2) + 2\,C\,T \end{aligned} \tag{4.1.17}$$

Where:

$$\begin{aligned} CT = {} & (X_T X_Q + X_T X_V + X_Q X_V) + \\ & (Y_T Y_Q + Y_T Y_V + Y_Q Y_V) + \\ & (Z_T Z_Q + Z_T Z_V + Z_Q Z_V) \end{aligned} \tag{4.1.18}$$

The desired part of this composite signal is the square root of the term containing the square terms of signals with V subscripts i.e.,

$$DS = \sqrt{(X_V^2 + Y_V^2 + Z_V^2)} \tag{4.1.19}$$

As we have seen in the different formulae, the classical way of calculating the vector magnitude produced undesirable terms that can overshadow the desired part and may even prevent their accurate detection. Therefore, the proposed method presents the vector magnitude in a decomposed form that enables us to choose the exact regions of interest. The method, however, requires more calculations since a WT decomposition of each level has to be carried out. When calculating the vector magnitude directly in the classical method or using all levels in WT method, we observe the reduced strength of the desired signal (VLP) from the O (10^{-6}) to O (10^{-12}) due to squaring. Another term is introduced

which is HALFS modulated by the LAHFS; the degree of modulation may be an indication of the presence and strength of VLP in the signal (Mousa, Yilmaz, 2000-a).

We have demonstrated that the desired signal components X_V, Y_V and Z_V can be isolated prior to the calculation of the vector magnitude. Our method uses WT (see section 6.2) to decompose the three X, Y and Z leads and choose the appropriate levels based on their frequency content which are then defined as X_V, Y_V, and Z_V.

The two methods show exact match when the non-filtered vector magnitude is calculated adding all levels of the WT and compared to that of the normal method as shown below in Fig. 4.1.7.

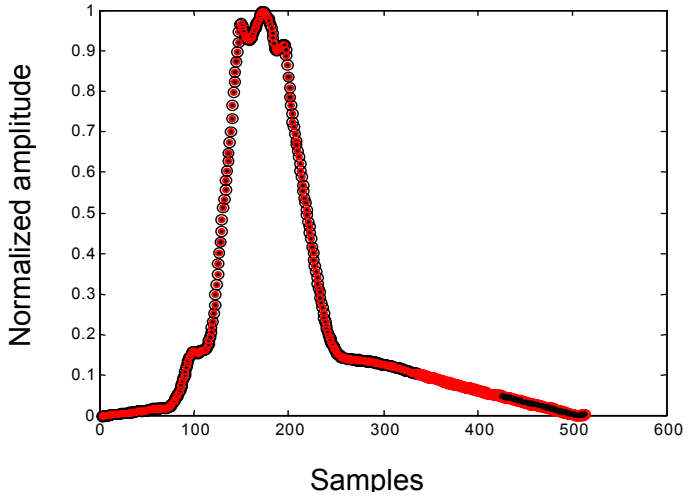

Figure 4.1.7 A plot of the non-filtered vector magnitudes

4.1.10 QRS onset and offset detection

For the first part of the analysis to minimize variations from the Simson's method, the QRS detection in the first part of this work followed the same method outlined by Simson as introduced in section 2.3. Since the result is directly related to the correct QRS end points detection, one can argue that this is also a weak point of this type of methods.

For the detection of *R* peaks, the onset and offset of the QRS complex are also detected. The onset of the QRS complex is defined as the beginning of the Q wave (or R wave when Q wave is not present), and the offset of the QRS complex is defined as the ending of the S wave (or R wave when the S wave is not present). Ordinarily, the Q and S waves are high frequency and low amplitude waves and their energies are mainly at small scale.

T and P wave detection

After the detection of the QRS complex, the peaks, onsets, and offsets of *T* and *P* waves are also detected. The peak, onset, and offset of the P wave are detected similarly to those of the T wave within a time window before the detected R wave.

4.2 Cepstrum analysis and homomorphic deconvolution

4.2.1 Introduction

In this chapter we introduce the concepts of the complex cepstrum and homomorphic filtering techniques for their abilities to separate signal components in ways that could be utilized in the analysis of late potentials. A variety of signal processing applications use the collection of nonlinear techniques known as complex cepstral analysis. The complex cepstrum rearranges the power spectrum of the signal in such a way that the slowly varying components of the signal are represented by the low frequencies or early coefficients and the fine detail by the high frequencies or late coefficients. The complex cepstrum of a signal is defined in terms of its z-transform while the z-transform of the cepstrum, is defined as the logarithm of the z -ransform of the sequence. The full complex cepstrum is computed with the complex logarithm (Oppenheim, Schafer, 1989).

Given the complex cepstrum, we can use techniques similar to frequency-domain filtering methods to deconvolve the signal into its constituents. The low-time portion of the cepstrum coefficients corresponds to the low frequency of the input signal, so by windowing the signal with an appropriate filter, we can separate it from the high-time portion of the signal. (See, for example, Section 12.8.4 of Oppenheim and Schafer for more details.) This technique is called homomorphic deconvolution.

It can be seen that most of the detail occurs near the origin and in peaks higher up the cepstrum. Thus the lower numbered coefficients provide the envelope information. The remainder of the detail is mostly contained in the peaks. Therefore, using the complex cepstrum enables the separation of signals combined through the operation of convolution.

The cepstrum and homomorphic deconvolution systems satisfy the principle of superposition; i.e., input signals and their corresponding responses are combined by an operation having the properties of addition. These systems have proved useful in signal analysis and have been applied with success in processing signals, and in particular biomedical signals. The complex cepstrum has found broad application in speech processing, seismic analysis, and many other fields. A number of researchers in the field of ECG analysis have reported some success when applying complex cepstrum and signal length methods (Murthy, Rangaraj, Udupa, Goyal 1997)(Murthy, Rangaraj, 1997). In this work we incorporate their methods as a further support to the wavelet transform method in order to achieve the maximum accuracy possible.

The transformation of a signal into its cepstrum is a homomorphic transformation, and the concept of the cepstrum is a fundamental part of the theory of homomorphic systems for processing signals that have been combined by convolution. Homomorphic filtering is very general, but it has been studied most extensively for the combining operations of multiplication and convolution because many signal models involve these operations.

These properties are described in full detail in Oppenheim and Schafer (1989).

The complex cepstrum can be difficult to compute analytically, however, we can define the cepstra in terms of the discrete Fourier transform. Given the Fourier transform, we can find the real cepstrum of the data sequence quite easily. The real cepstrum while not as useful for deconvolution applications is applied where the energy in various parts of the signal needs to be computed.

Computation of the inverse cepstrum is simpler than the cepstrum, since special care is not required with respect to the phase. The inverse cepstrum is computed by taking the inverse transform of the exponent of the Fourier transform.

4.2.2 The cepstrum and the complex cepstrum

The z-transform of a given stable sequence x[n] defined as:

$$X(Z)=\sum_{n=-\infty}^{\infty} x[n]z^{-n} \qquad (4.2.1)$$

or represented in polar form :

$$X(z) = |X(z)|\, e^{j\angle X(Z)} \qquad (4.2.2)$$

where $|X(z)|$ is the magnitude and $\angle X(z)$ is the angle, of X(z). For a stable x[n], the region of convergence for X(z) includes the unit circle, and the Fourier transform of x[n] exists and is equal to $X(e^{j\omega})$.

The complex *cepstrum of* x[n] is defined as the stable sequence $\hat{x}[n]$ with z-transform:

$$\hat{X}(z)=\log[X(z)] \qquad (4.2.3)$$

With

$$\text{Log } [X(z)] = \log [|X(z)|e^{\angle X(z)}] = \log|X(z)| + j\angle X(z) \text{ s} \qquad (4.2.4)$$

The complex cepstrum exists if log[X(z)] and has all the properties of the z-transform of a stable sequence has a convergent power series representation as:

$$\hat{X}(z)=\log[X(z)]=\sum_{n=-\infty}^{\infty}\hat{x}[n]z^{-n} \qquad |z|=1 \qquad (4.2.5)$$

Therefore the sequence of coefficients of the power series corresponds to the complex cepstrum of x[n]. The complex cepstrum can be represented using the inverse Fourier transform since we require $\hat{x}[n]$ being stable and the region of convergence includes the unit circle.

4.2.3 Homomorphic deconvolution

An important property of the cepstrum is that it is a homomorphic transformation. A homomorphic system is one in which the output is a superposition of the input signals, *i.e.*, the input signals are combined by an operation that has the algebraic characteristics of addition. Under a cepstral transformation, the convolution of two signals becomes equivalent to the sum of the cepstra of the signals (Murthy, Rangaraj, Udupa, Goyal 1997)(Murthy, Rangaraj, 1997) (Oppenheim, Schafer, 1989).

The operations that defined the complex cepstrum were the same as those shown in block diagram form in Fig. 4.2.1.a. The cascade of z-transform, complex logarithm, and inverse z-transform can be thought of as a representation of the characteristic system $D_*[.]$. Since we are assuming that all sequences and their complex cepstra are stable, the associated z-transform always include the unit circle in their regions of convergence; consequently the z-transforms in Fig. 4.2.1 can also be specialized to Fourier transforms as in (4.2.8). Each of the three basic component transformations is also homomorphic, and the corresponding input and output operations are indicated in Fig. 4.2.1 (a). The z-transform maps convolution to multiplication; the complex logarithm converts multiplication to addition; and the inverse transform is a linear transformation.

The third system Fig. 4.2.1 is the inverse of the characteristic system for convolution; its input must be the complex cepstrum of its output, i.e.

$$y[n]=D_*^{-1}\left[\hat{y}[n]\right] \tag{4.2.6}$$

The basic operations that define the inverse characteristic system for convolution are depicted in Fig. 4.2.1 (b). The linearity of the z-transform takes a sum of complex cepstrums into a sum of transforms; the complex exponential maps a sum into a product; and the inverse transform maps a product into a convolution.

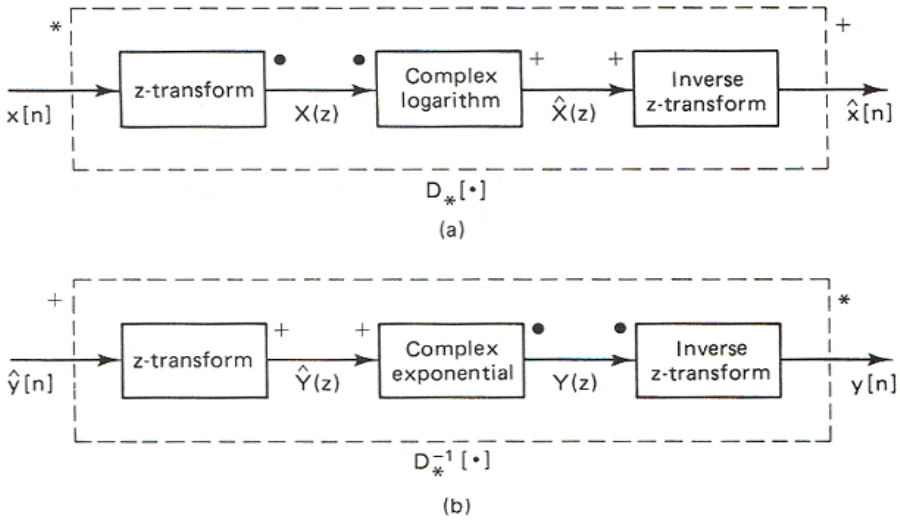

Figure 4.2.1 (a) Characteristic system for convolution and (b) its inverse.

Properties of the complex cepstrum

Some of the properties of the complex cepstrum are:

PROPERTY 1: The complex cepstrum decays at least as fast as $1/|n|$.

PROPERTY 2: If x[n] is real, $\hat{x}[n]$ is also real.

PROPERTY 3: The complex cepstrum $\hat{x}[n] = 0$ for $n < 0$ if and only if x[n] is minimum phase, i.e., X(z) has all its poles and zeros inside the unit circle.

PROPERTY 4: The complex cepstrum $\hat{x}[n] = 0$ for $n > 0$ if and only if x[n] is maximum phase, i.e. X(z) has all its poles and zeros outside the unit circle.

4.2.4 Minimum-phase and maximum-phase sequences

Minimum-phase sequences are real, causal, and stable sequences whose poles and zeros are inside the unit circle. Since we require that the region of convergence of log[X(z)] include the unit circle so that $\hat{x}[n]$ is stable, and since causal sequences have a region of convergence includes $|z| = \infty$ it follows that there can be no singularities of log[X(z)] on or outside the unit circle if $\hat{x}[n] = 0$ for $n < 0$, conversely, if all the singularities of $\hat{X}(z) = \log[X(z)]$ are

inside the unit circle, then it follows that $\hat{x}[n] = 0$ for $n < 0$. Since the singularities of $\hat{X}(z)$ are the poles and the zeros of X(z). The complex cepstrum of x[n] will be causal ($\hat{x}[n] = 0$ for $n < 0$) if and only if the poles and zeros of X(z) are inside the unit circle. In other words, x[n] is a minimum-phase sequence if and only if its complex cepstrum is causal.

Causality of the complex cepstrum is equivalent to the minimum phase lag, minimum group delay, and minimum energy delay properties that also characterize minimum-phase sequences. This property motivated the use of the complex cepstrum in order to try to separate envelopes that contain little changes from components that include delayed activities such as VLPs.

Maximum-phase sequences are stable sequences whose poles and zeros are all *outside* the unit circle. Thus, maximum-phase sequences are left-sided, and, it follows that the complex cepstrum of a maximum-phase sequence is also left-sided. Our initial hypothesis was that any delayed activities should be of the maximum-phase type and by separating the two types of signals, we can gain better insight into the concept of VLP.

4.2.5 Minimum-phase/maximum-phase decomposition by homomorphic filtering

If no poles or zeros lie on the unit circle, then

$$X(Z) = X_{mn}(Z).X_{mx}(Z) \tag{4.2.7}$$

where $X_{mn}(z)$ is minimum phase and $X_{mx}(z)$ is maximum phase.
a sequence of the form

$$x[n] = x_{mn}[n] * x_{mx}[n] \tag{4.2.8}$$

having a complex cepstrum:

$$\hat{x}[n] = \hat{x}_{mn}[n] + \hat{x}_{mx}[n] \tag{4.2.9}$$

Then $x_{mn}[n]$ and $x_{mx}[n]$ may be extracted from x[n] by homomorphic filtering using:

$$\hat{x}_{mn}[n] = l_{mn}[n]\hat{x}[n] \tag{4.2.10a}$$

where

$$l_{mn}[n] = u[n] \tag{4.210b}$$

and

$$\hat{x}_{mn}[n] = l_{mx}[n]\hat{x}[n] \tag{4.2.11a}$$

where:

$$l_{mx}[n] = u[-n-1] \tag{4.2.11b}$$

And $x_{mn}[n]$ and $x_{mx}[n]$ can be obtained from $\hat{x}_{mn}[n]$ and $\hat{x}_{mx}[n]$. The operations required for the decomposition of (4.2.8) are depicted in Fig. 4.2.2 with $l_{mn}[n]$ and $l_{mx}[n]$ representing the frequency invariant filters.

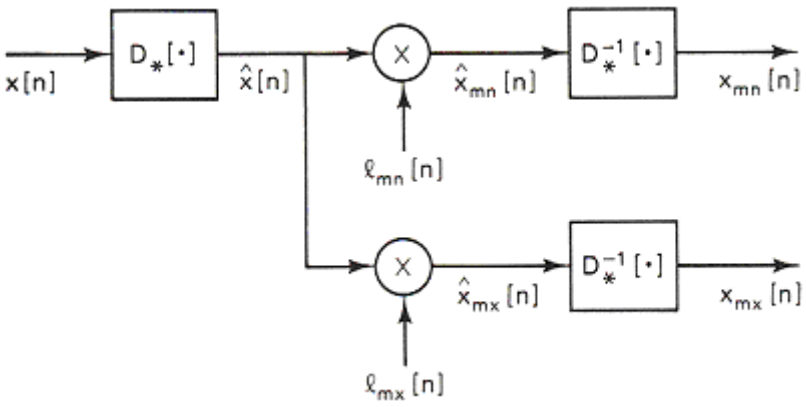

Figure 4.2.2 Minimum-phase / Max-phase decomposition

4.2.6 Minimum-phase correspondence (MPC)

While there exists only one minimum phase signal for given amplitude spectrum, a number of non-minimum phase signals can exist with varying degrees of phase lags. Homomorphic filtering can be employed to convert a non-minimum phase signal into its minimum-phase correspondence (MPC). Some of the important properties of a minimum phase signal are presented in section 4.2 of this thesis. Of all energy bounded one-sided signals with identical amplitude spectra the energy of minimum phase signal is optimally concentrated towards the origin and the signal has the smallest phase lag and phase-lag derivative for each frequency. The resultant y(n) is the MPC of x(n), having an amplitude spectrum identical to that of x(n), but with energy concentrated optimally towards the origin (Murthy, Rangaraj, Udupa, Goyal 1997)(Murthy, Rangaraj, 1997).

4.2.7 Signal length

Signal length is a quantity, which gives information about distribution of energy over the duration of the signal. For a given amplitude spectrum, signals which have their energy optimally concentrated at the origin have minimum signal length while signals with distributed energy have greater signal lengths. More often, an abnormal signal has a much wider than a normal QRS complex and while the amplitude spectra of the two are almost identical, they are known to differ in phase. Signal length implicitly takes into account the phase of the signal. Hence, depending upon the type of the abnormality, its signal length could be quite different from that of a normal ECG complex. It is shown that better feature separation and parameter extraction is achieved in some cases when the signal length of the minimum phase correspondent of the signal is considered and classification can be performed using a Neural Networks. Signal length and signal duration are two different concepts while signal duration gives the interval outside which the signal is zero, signal length gives information as to how the energy of the signal is distributed within its duration. Signal length depends on both amplitude and phase spectra of the signal, and for one sided signals minimum

length implies minimum phase and vice versa. The signal length (*SL*) of a one-sided signal x[n] of duration *L* is defined as

$$SL = \frac{\sum_{n=0}^{L-1} w[n][x[n]]^2}{\sum_{n=0}^{L-1} [x[n]]^2} \qquad (4.2.12)$$

where w[n] is an increasing series in n, the choice of which depends upon the application. Here it is chosen as the index *n* itself. As can be seen from (4.2.12), sample points away from the origin (n = 0) receive progressively heavier weighting. For a given amplitude spectrum and hence total energy, the signal that has its energy concentrated optimally at the origin has minimum length, while signals with added delay have greater lengths. Thus, an ECG that has a wider QRS complex with larger phase lag than a normal ECG complex can be expected to have greater signal length.

4.2.8 Application of the Complex cepstrum analysis to recorded data

Presented here is a sample of applying the complex cepstrum to two different real ECG signals from our own data base. The first signal comes from a normal subject used for control and the other signal is from a patient classified as having anterior myocardial infarction.

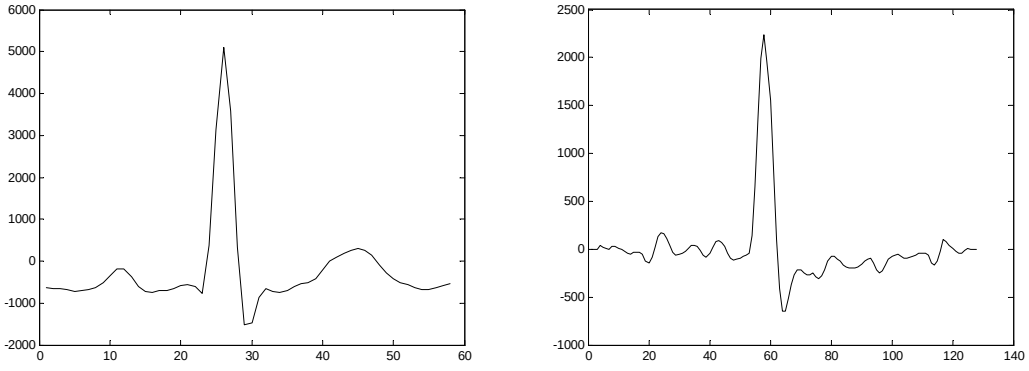

a. Normal b. Anterior MI

Figure 4.2.3 Two sample signals from the Hacettepe database

The different properties of the complex cepstrum outlined in this chapter will be used in our unified approach to the problem of identifying delayed potentials. The ability of the complex cepstrum to separate a signal into its minimum-phase and maximum-phase components will be used in the calculation of the additional parameters such as the signal length as shown in Table 4.2.1.

Table 4.2.1 Complex cepstrum related parameters

Signals and parameters		Anterior MI	Normal
MPC	SL	47.7786	47.2568
	rms	3.1638	2.7603
Min-PH	SL	98.8368	36.3296
	rms	1.6137	2.0417
Max-PH	SL	60.7077	34.2436
	rms	2.1781	2.5675
Signal	SL	59.9564	61.8233
	rms	0.5038	0.4008

Using the original signals the SL parameter failed to classify the differences as expected since there were no rearrangement of coefficients but the rms parameter showed a small difference between the two signals. After calculating the MPC both parameters performance showed improvement and were able to detect the two signals correctly. The SL parameter differences were not wide with only differences in the fraction parts. The minimum-phase and maximum-phase portions showed a clear margin in differences as can be seen in their corresponding entries.

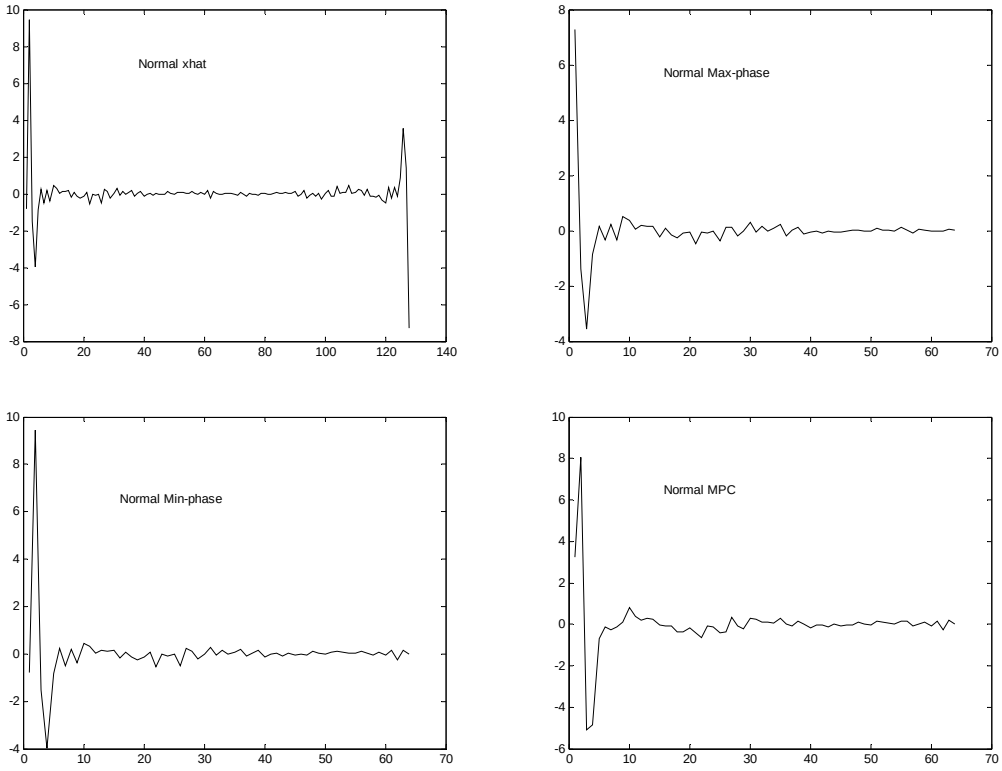

Figure 4.2.4 Normal signal results

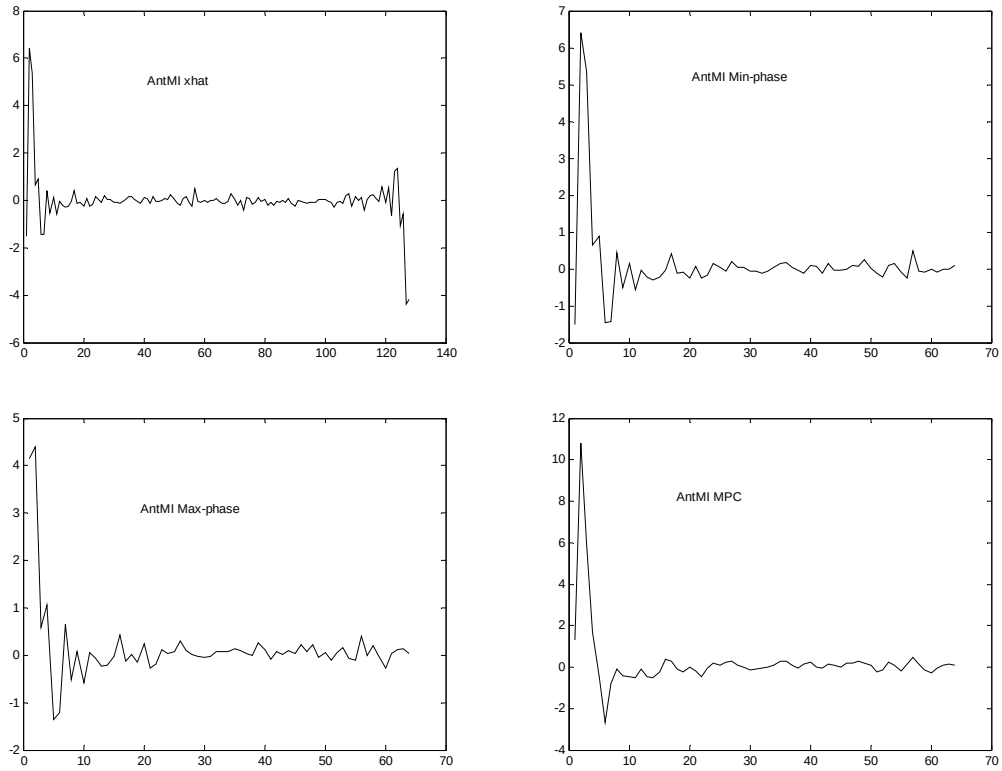

Figure 4.2.5 Anterior MI signal results

4.3 Artificial neural networks

4.3.1 Introduction

Artificial neural networks (ANN's) have been widely used over the past few years as pattern and statistical classifiers in many application areas including medicine. ANN's were used for QRS/PVC classification or for the detection of atrial fibrillation. Neural network-based ST segment analysis has been used for automated detection of the J-point to identify hypothermic patients and the onset of the T-wave, using adaptive theory, and also for the classification of ST-T segments. Classical back propagation (BP) NN using inputs of measured ST-T data such as ST slope, ST-J amplitude, and positive and negative amplitudes of the T wave with emphasis in data coming from myocardial infarction patients have been employed. Only recently, some algorithms for ischemia detection and analysis were tested with varying degrees of success. This chapter describes the implementation of a BP NN for VLP detection. The performance of the algorithm was tested on the ECG database, which has been described earlier with sample results presented here. The approach in this part differs considerably from previously used algorithms in that it avoids reliance on the QRS region, because of its problematic detection, concentrating instead on information coming from the whole ECG pattern (Mousa, Yilmaz, 2001-b)(Gang, Wenyu, Ling, Qilian, Xuemin, 2000)(Xue, Reddy, 1997).

The artificial neural network structure is based on our present understanding of biological nervous systems. Although a great deal of biological detail is eliminated in these computing models, the artificial neural networks retain enough of the structure observed in the brain to provide insight into how biological neural processing may work. These models are composed of many non-linear computational elements operating in parallel and arranged in patterns similar to biological neural nets.

Computational elements or nodes are connected via weights that are typically adapted during use to improve performance. Neural networks utilize a parallel processing structure that has large numbers of processors (neurons) and many interconnections between them. Each processor is linked to many of its neighbours so that there are many more interconnections than processors. The power of the neural network lies in the tremendous number of interconnections.

4.3.2 Computing with neural networks

A neural network is a system that is designed to model the way in which the brain performs a particular task or function of interest. A neural network is a massively parallel-distributed processor, which is able to store knowledge and making it available for use. It resembles the brain in two respects:

1. Knowledge is acquired by the network through a learning process,
2. Inter-neuron connection strengths known as synaptic weights are used to store the knowledge.

The procedure used to perform the learning process is called a learning algorithm, the function of which is to modify the synaptic weights of the network in an orderly fashion so as to attain a desired design objective. The modification of synaptic weights provides the method for the design of neural networks (Haykin 1999)(Fu 1994).

Nodes

Computational elements or nodes used in neural net models are non-linear. The simplest node sums N weighted inputs and passes the result through a non-linearity. The node is characterised by an internal threshold, or offset, and by the type of non-linearity. There are three common types of non-linearities: hard limiters, threshold logic elements and sigmoidal non-linearities.

Topology

Neural networks are specified by the net topology node characteristics and training or learning rules. These rules specify an initial set of weights and indicate how weights should be adapted during use to improve performance. Neural networks typically provide a greater degree of robustness or fault tolerance because there are many more processing nodes each with primarily local connections. Damage to a few nodes or links thus need not impair overall performance significantly.

Network training

The ability to adapt and continue learning is essential in areas such as biomedical signal analysis and processing. Adaptation also provides a degree of robustness by compensating for minor variabilities in characteristics of processing elements. Neural network classifiers are also non-parametric and make weaker assumptions concerning the shapes of underlying distributions than traditional statistical classifiers.

4.3.3 The neuron model

A simple description of the operation of a neuron is that it processes the electric currents, which arrive on its dendrites, and transmits the resulting electric currents to other connected neurons using its axon. The classical biological explanation of this processing is that the cell carries out a summation of the incoming signals on its dendrites. If this summation exceeds a certain threshold, the neuron responds by issuing a new pulse, which is propagated along its axon but If it is less than the threshold the neuron remains inactive.

The three basic elements of the neuron model are:

1. A set of synapses, each of which is characterised by a weight or strength of its own. A signal x, at the input of synapse ***i*** connected to neuron j is multiplied by the synaptic weight w_{ij}. The first subscript refers to the neuron in question and the second subscript refers to the

input end of the synapse to which the weight refers. The weight w_{ij} is positive if the associated synapse is excitatory, it is negative if the synapse is inhibitory.

2. An adder for summing the input signals, weighted by the respective synapses of the neuron (a linear combiner).

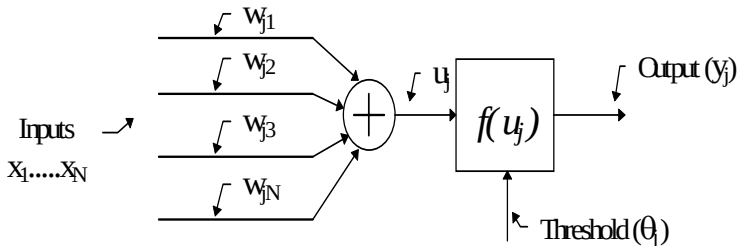

Fig. 4.3.1 Computational model of a neural network

3. An activation function for limiting the amplitude of the output of a neuron. The activation function is also referred to as a squashing function in that it squashes the permissible amplitude range of the output signal to some finite value.

$$u_j = \sum_{i=1}^{N} w_{ji} x_i \tag{4.3.1}$$

$$y_j = f(u_j - \theta_j) \tag{4.3.2}$$

4.3.4 Network architectures

4.3.4.1 Single-layer feed forward networks

A layered neural network is a network of neurons organised in the form of layers. The simplest form of a layered network has an input layer of source nodes that projects onto an output layer of neurons but not vice versa. In other words, this network is strictly of a feed forward type. The designation 'single-layer' refers to the output layer of computation nodes. The input layer of source nodes does not count, because no computation is performed there.

A linear associative memory is an example of a single-layer neural network. In such an application, the network associates an output pattern (vector) with an input pattern (vector), and the information is stored in the network by virtue of modifications made to the synaptic weights of the network.

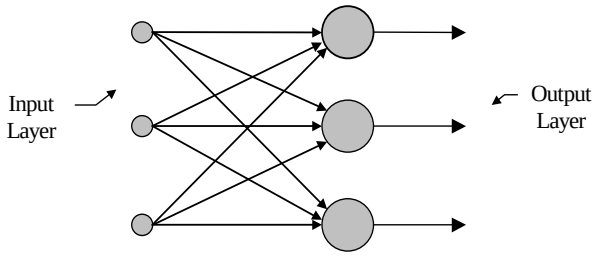

Fig. 4.3.2 Single layer feed-forward network

4.3.4.2 Multi-layer feed-forward networks

Multi-layer perceptrons are feed-forward nets with one or more layers of nodes between the input and output nodes. These additional layers contain hidden units or nodes that are not directly connected to both the input and output nodes. Multi-layer perceptrons overcome many of the limitations of single-layer perceptrons, but were generally not used in the past because effective training algorithms were not available.

The neural network is fully connected in the sense that every node in each layer of the network is connected to every other node in the adjacent forward layer. If, some of the synaptic connections are missing from the network, then the network is partially connected. Each neuron in the hidden layer is connected to a local set of source nodes that lie in its immediate neighbourhood. Likewise, each neuron in the output layer is connected to a local set of hidden neurons. Thus, each hidden neurons responds essentially to local variations of the source signal.

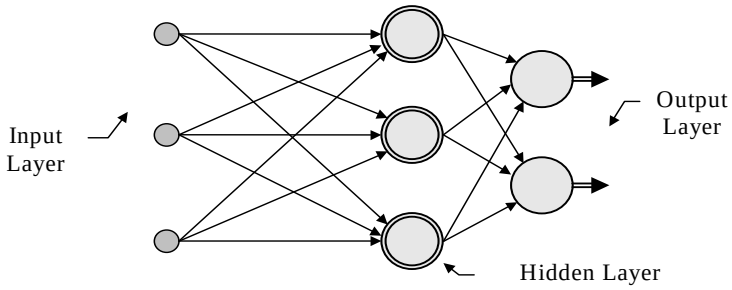

Fig 4.3.3 Multi-layer feed-forward network

4.3.5 Non-linearities of multi-layer perceptron

The capabilities of multi-layer perceptrons stem from the non-linearities used within nodes. If nodes were linear elements, then a single-layer net with appropriately chosen weights could exactly duplicate those calculations per formed by any multi-layer net. A single-layer perceptron forms half-plane decision regions. A two-layer perceptron can form any, possibly unbounded, convex region in the space spanned by the inputs. Such regions include convex polygons sometimes called convex hulls. Here the term convex means that any line joining points on the border of a region goes only through points within that region.

4.3.6 Required nodes and layers

The number of nodes must be large enough to form a decision region that is as complex as is required by a given problem. It must not, however, be so large that the many weights required cannot be reliably estimated from the available training data. No more than three layers are required in perceptron-like feed-forward nets because a three-layer net can generate arbitrarily complex decision regions. The number of nodes in the second layer must be greater than one when decision regions are disconnected or meshed and cannot be formed from one convex area. The number of second layer nodes required in the worst case is equal to the number of disconnected regions in input distributions.

4.3.7 Multi-layer perceptron with sigmoidal on outputs

The above discussion centred primarily on multi-layer perceptrons with one output, which utilise hard limiting non-linearities as activation functions. Similar behaviour is exhibited by multi-layer perceptrons with multiple output nodes when sigmoidal non-linearities are used and the decision rule is to select the class corresponding to the output node with the largest output. The behaviour of these nets is more complex because decision regions are typically bounded by smooth curves instead of by straight-line segments and analysis is thus more difficult.

4.3.8 Back propagation

The back-propagation algorithm is a generalisation of the LMS algorithm. It uses a gradient search technique to minimise an error function equal to the mean square difference between the desired and the actual net outputs. The desired output of all nodes is typically "low" (0 or <0.1) unless that node corresponds to the class the current input is from in which case it is "high" (1.0 or >0.9). Initially selecting small random weights and internal thresholds and then presenting all training data repeatedly train the net.

Weights are adjusted after every trial using side information specifying the correct class until weights converge and the cost function is reduced to an acceptable value. An essential component of the algorithm is the iterative method described in Table 4.3.1 that propagates error terms required to adapt weights back from nodes in the output layer to nodes in lower layers.

Table 4.3.1 Back-propagation training algorithm

Step 1.	Initialise weights and offsets: Set all weights and node offsets to small random values.
Step 2.	Present input and desired outputs: Present a continuous valued input vector $x_0, x_1, ..., x_{m-1}$, and specify the desired outputs $d_0, d_1, ..., d_{m-1}$. If the net is used as a classifier then that desired output is 1. The input could be new on each trial or samples.
Step 3.	Forward Calculation: Use the sigmoid non-linearity from above and calculate outputs $y_0, y_1, ..., y_{m-1}$
Step 4.	Backward calculation: The local gradient δ is calculated as: $\delta_j[n] = e_j[n]o_j[n](1-o_j[n])$ for output layer $\delta_j[n] = y_j[n](1-y_j[n])\sum_k \delta_k[n]w_{kj}[n]$ for other neurons Adapt weights: Use a recursive algorithm starting at the output nodes and working back to the first hidden layer. Adjust weights by $W_{ji}[n+1] = W_{ji}[n] + \alpha\{W_{ji}[n] - W_{ji}[n-1]\} + \eta\delta_j[n]y_i[n]$ Where: α = momentum constant, δ's = local gradients, η = learning rate
Step 5.	Repeat by going to step 2

4.3.9 The back-propagation training algorithm

The back-propagation training algorithm is an iterative gradient algorithm designed to minimise the mean square error between the actual output to a multi-layer feed-forward perceptron and the desired output. It requires continuous differentiable non-linearities. The following assumes a sigmoid logistic non-linearity is used where the function f (v) is:

$$f(v) = 1/(1+e^{-av}) \tag{4.3.3}$$

One of the major problems with the error back-propagation learning algorithm is it runs the risk of being trapped in a local minimum. These are points where the gradient goes to zero but the network is not at the global minimum. As the network trains, the algorithm will get stuck at these points because the error gradient goes to zero.

The error back-propagation learning algorithm will not always find the global minimum, even though it is present. Then the network must be restarted and a new search is carried out. This is typically done with a new random set of starting weights and by presenting the training data in a different order. This allows the network to find an alternative route to an optimum set of weights avoiding the local minima.

4.3.10 Matlab algorithm

Feed-forward backpropagation networks are created using the Matlab command NEWFF according to:

net = newff(PR,[S1 S2...SNl],{TF1 TF2...TFNl},BTF,BLF,PF)

which returns an N layer feed-forward backprop network.

with:

PR - Rx2 matrix of min and max values for R input elements.
Si - Size of ith layer, for Nl layers.
TFi - Transfer function of ith layer, default = 'tansig'.
BTF - Backprop network training function, default = 'trainlm'.
BLF - Backprop weight/bias learning function, default = 'learngdm'.
PF - Performance function, default = 'mse'.

The feed-forward network consists of layers set by Nl and using the DOTPROD weight function, NETSUM net input function, and the specified transfer functions.

The first layer has weights coming from the input. Each subsequent layer has a weight coming from the previous layer. All layers have biases set to default values. The last layer is the network output.

Each layer's weights and biases are initialized with INITNW. Adaptation is done with TRAINS which updates weights with the specified learning function.

Training is done with the specified training function. Performance is measured according to the specified performance function.

The differentiable transfer function TFi was either the sigmoid tLOGSIG or the TANSIG function. The training function BTF was TRAINLM and the learning function BLF was the backpropagation learning function LEARNGD. The performance function was the differentiable performance functions MSE. The data consisted of inputs P and targets T to be solved with a neural network.
After the two-layer feed-forward network was created. The network's input ranges from [min to max]. The first layer has five TANSIG neurons, the second layer has one PURELIN neuron. The TRAINLM network training function was used. The network was simulated and trained for 50 epochs and the network's output was plotted.

Once the parameters are extracted, they are used as inputs to a feed-forward neural network (ANN) for classification as shown in Fig. 4.3.4.

Fig 4.3.4 Classification of extracted parameters

The process is composed of 1) taking the wavelet transform of the three X,Y and Z leads , 2) parameter extraction, 3) design, train and test neural networks.

4.3.11 Application of ANN in VLP classification using WT parameters:

A feed-forward neural network containing two hidden layers was designed and trained using the back-propagation learning algorithm. The network was trained for a number of times and the best result was chosen. The hyperbolic tangent function was used as the activation function.

The extracted three classical parameters, i.e., QRS duration, voltage in the terminal of the QRS and the duration of the low amplitude terminal signal were used as input to ANN. A sample of the training error performance is

shown in Fig. 4.3.5 while the result of ANN classification is presented in Fig. 4.3.6 and as can be seen did not give acceptable classification results.

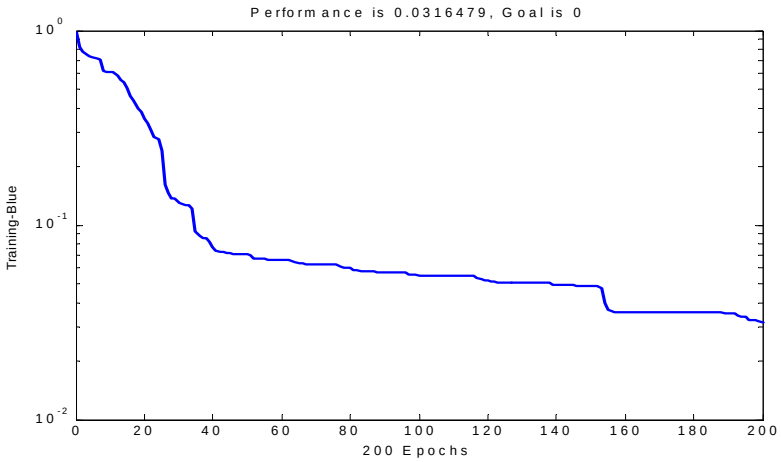

Fig. 4.3.5 A sample of the training performance for the network.

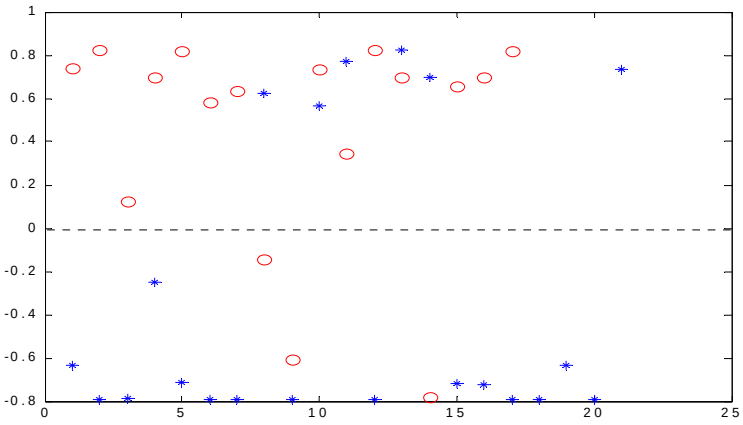

Fig. 4.3.6 Classification using classical parameters.
normal (o) and abnormal signals (*).

The symbol (o) represents signals for normal subjects while; symbol (*) represents those with VLP in their ECG recordings.

Due to the small number of data size and limiting the region of analysis to the end of the QRS complex, results obtained here were not satisfactory and did not give acceptable classification results. This problem will be dealt with in the upcoming chapters through introducing more data and enlarging the region of analysis to include the entire cardiac cycle.

CHAPTER 5

INSTRUMENTATION AND DATA ACQUISITION

5.1 Introduction

In this chapter we introduce the work carried out in the design and implementation of our ECG recording system. We start by presenting the basic theories involved and concluding with the complete data acquisition system. A great deal of time and effort were devoted to the development of an appropriate device according to our specification but the task was at last completed.

The system can be divided into two main parts, the analog part and the digital part integrated together to give the complete acquisition system in addition to the software needed for acquisition and analysis. The block diagram shown in Fig 5.1 depicts the main components of ECG recording instruments.

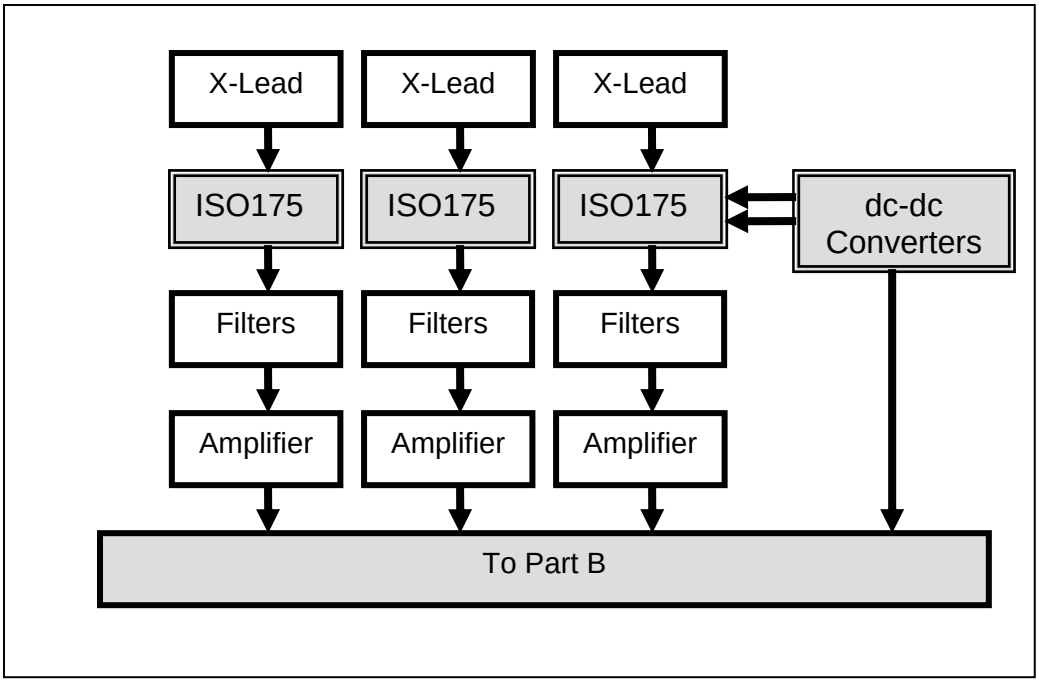

Fig 5.1-a The analog part of the system

Part A is the analog part which records, amplifies and band-limit the signal prior to digitization. Part B is the digital part that receives its input from part A. This part samples the signals at a preset sampling rate and sends it through to the laptop for display, processing and storage for future use. The recording system connects to laptop via the USB port that can also supply the necessary power to run the system. The device is capable of recording three separate channels simultaneously or 12 channels multiplexed using the special properties of the three onboard ADC converters.

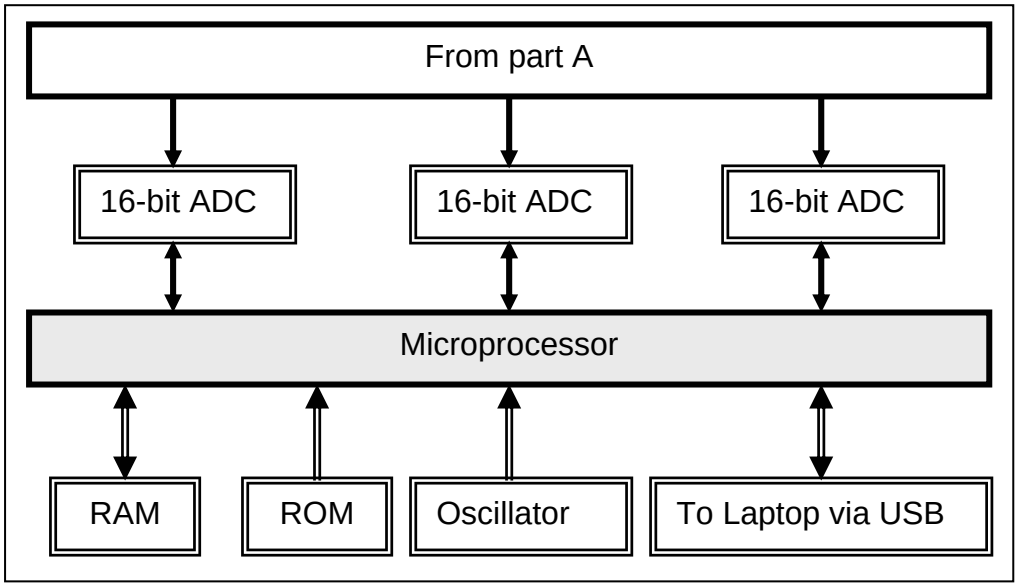

Fig 5.1-b The digital part of the system

Recording of ECG signals for the purpose of VLP analysis is a very challenging task due to a number of factors. One such factor is the fact that ECG signals as well as any signal of biologic origin are very weak with magnitudes in the range of 1-10 mV. Furthermore, these signals have very low drive, i.e. source has very high output impedance. Another important factor is the noise that can corrupt the recorded signal in addition to the fact that recordings are carried out in a noninvasive manner. The use of equipment with very good specifications does not guarantee interference free recordings as will be seen in section 5.3.

In the following sections we introduce the different parts making up the acquisition system and some of the theories behind their operation.

5.2 Bio-potential amplifiers

An ECG amplifier is usually required to have the following properties:

- Ability to sense low amplitude signals in the range of 0.1 - 10 mV or less
- Very high input impedance, usually more than 5 Mega-Ohms
- Very low input leakage current, 1 micro-Amps or below
- Flat frequency response of 0.1 - 100 Hz
- High common mode rejection ratio (CMRR).

Input leakage current is defined as the current an amplifier sends to the unit connected to its input terminals (human body in our case) (Webster, 1998).

Common Mode Rejection Ratio (CMRR) is defined as the ratio of the magnitude of the differential gain to the magnitude of the common mode gain, as given below:

$$CMRR = \frac{A_D}{A_C} \tag{5.1}$$

where A_D is the differential gain of the amplifier and is given by

$$A_D = \frac{V_{OUT}}{V_{IN+} - V_{IN-}} \tag{5.2}$$

where $V_{IN+} \neq V_{IN-}$ and A_C is the common gain of the amplifier and is given by

$$A_C = \frac{V_{OUT}}{V_{IN+}} \tag{5.3}$$

where $V_{IN+} = V_{IN-}$

A high CMRR is essential since the capacitive coupling from the external electrical sources such as power lines would create a strong common mode signal in comparison to the differential ECG signal. A high CMRR would mean that the A_D is much larger than A_C, and the differential amplification of low amplitude ECG signals would be possible in the presence of common 50/60 Hz signal coupled from the power mains (Winter, Webster, 1983-a).

Common mode voltage reduction remains important because differences in electrode impedance cause differential mode interference, even if the impedances of the amplifier inputs are equal. Although good preparation of the electrodes and the skin may reduce this type of interference, electrode impedances differ with every new recording and are inherently an uncertain factor. Some reduction of the common mode voltage can be obtained by a good isolation of the amplifier circuit, i.e. the capacitances of the amplifier to mains and ground should be much smaller than the capacitances of the body to mains and ground. However, these low capacitances are usually not easy to achieve and isolation must therefore be regarded mainly as a way to improve patient safety. A special class of interference is the high frequency interference caused by for instance fluorescent tubes or switching power supplies. Common mode voltage reduction is less effective at higher frequencies since circuit gain decreases with frequency. Moreover, at high frequencies the input impedance of an amplifier will decrease because of its capacitive component, increasing the effect of the common mode interference voltage. Although high frequencies are usually filtered out in bioelectric measurements, amplifiers can easily saturate or produce low frequency distortion components. High frequency interference therefore remains a factor of great concern (Winter, Webster, 1983-a) (Winter, Webster, 1983-b).

5.2.1 The differential amplifier

To improve the signal to noise ratio (SNR), we use the configuration shown below in Fig. 5.2. This is called a differential amplifier, because it amplifies the difference between the two input voltages.

The gain is given by:

$$Gain = \frac{R_2}{R_1}(V_{IN+} - V_{IN-}) \tag{5.4}$$

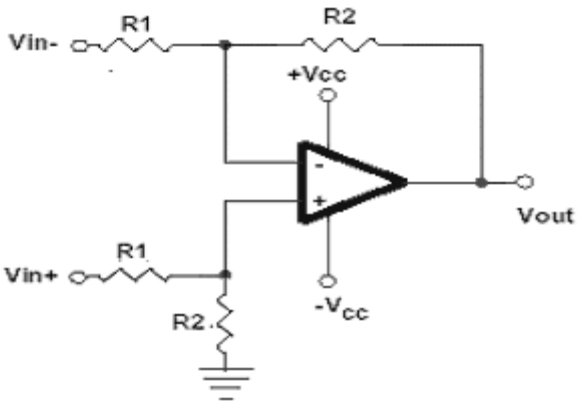

Figure 5.2 The differential amplifier

Since the output is proportional to the difference between the two input voltages, this circuit has the advantage of good common mode rejection. This means that any input present on both terminals will be cancelled out. So, only a signal, which is different on the two, inputs will be amplified, which of course is exactly what we want. The ISO175 used in our instrument contains a differential amplifier similar to the one introduced here with a controllable gain using a single resistor connected between the negative inputs as shown in the next section (Webster, 1998).

5.2.2 The instrumentation amplifier

The differential amplifier is limited in its performance because of the low input impedance. To improve this, two bootstrapped buffer amplifiers (which are simply op-amps with unity gain) are commonly added, which results in the simple instrumentation amplifier. Basically the instrumentation amplifier is made up of a buffer and a differential amplifier in cascade as shown in Fig. 5.3. In practice, it is difficult to precisely match resistors that are discrete components. To overcome this problem the entire circuit is put on a single integrated circuit, since IC manufacturing technology enables precise resistor ratios to be obtained. Chips such as Analog Devices AD620 or Texas instruments ISO175 find widespread use in working with low-level signals with large common-mode components in noisy environments and in particular in biomedical engineering application and measurements of bio-potential signals.

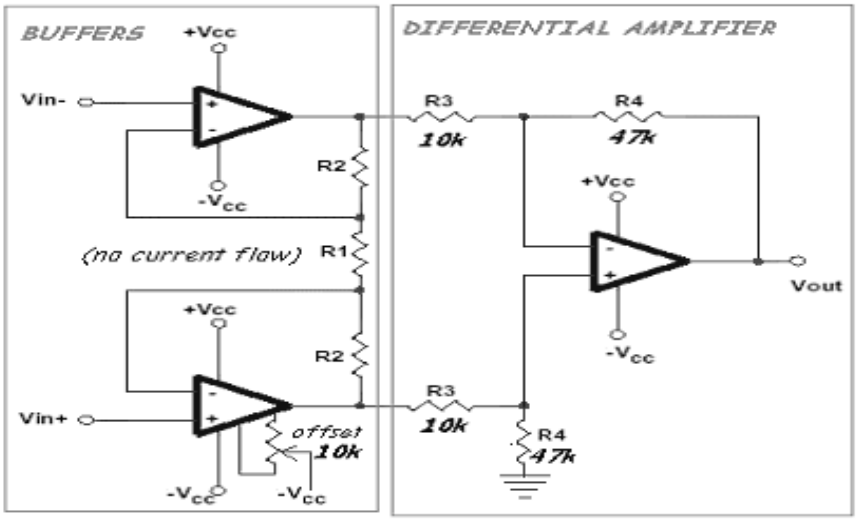

Figure 5.3 The three op-amp instrumentation amplifier

The most commonly applied ways of acquiring ECG signals are described in the following paragraphs.

5.2.3 AC coupling

DC voltage offsets present on the body or electrodes will be amplified. These are quite common, especially if the electrodes are moved (motion artifact). The effect is to cause the baseline of the ECG to wander around, and it can be so serious to saturate the amplifier. To avoid this, a high-pass filter with a very low cutoff frequency (block DC) can be used.

5.3 Noise and interference

An excessive level of interference often disturbs bioelectric recordings and degrades the quality of the recorded signal. In many cases very sophisticated equipment is needed even though interference free recordings cannot be guaranteed and one has to settle for a compromise. In most bioelectric measurements an interference level of 1 - 10 μV or less than 1% of the peak-peak value of an ECG is acceptable. As the noise of a typical electrode is also several μV, in most circumstances 10 μV can be accepted as the upper level of interference (Pickering P. 1999).

5.3.1 Interference currents through the body

The capacitances between the patient, the power lines and ground cause a small interference current to flow through the body. These capacitances cause an interference current of approximately 0.5 μA_{p-p} to flow from the power supply lines through the body to ground. If an amplifier is connected to the patient, part of the current from mains to patient will flow to ground.

5.3.2 Interference currents into the amplifier

In an isolated bioelectric measurement (i. e. no galvanic connection between the amplifier common and ground) the capacitances between the amplifier common and mains and between amplifiers common and ground should also be considered. These capacitances can cause additional interference currents to flow from the amplifier to ground, which contribute to the common mode voltage.

5.3.3 Interference currents into the measurement cables

A major source of interference in bioelectric measurements results from the capacitive coupling of the measurement cables with the mains. The currents induced in the wires flow to the body via the electrodes and from the body to ground. Because both the currents induced in the wires and the electrode impedances generally differ significantly, a relatively large differential voltage $\mathbf{V_{ab}}$ is produced between the amplifier inputs.

A typical situation with a mean current of 10 nA_{p-p} in the wires, a mean electrode impedance of 20 $K\Omega$ and a relative difference in interference current and electrode impedance of 50%, leads to an unacceptable high interference level of 200 μV_{p-p}. Given the inherent variability of the electrode impedances and the level of interference among recordings, there is only one practical way to reduce interference currents in the wires: shielding of the measuring cables.

5.3.4 Magnetically induced interference

Magnetically induced interference is easily distinguished from other types of interference because it varies with the area and orientation of the loop formed by the measurement cables. Suppression is easy in theory by reducing this area as much as possible through twisting of the measurement cables. In practice, this is not always feasible. For example, the usual electrode configuration in ECG measurements with electrodes placed at the extremities of the body might cause a considerable area between the input cables.

5.4 Influence and reduction of common mode voltage

There are two ways by which a high common mode voltage may cause interference. The first, obvious way is when the common mode rejection ratio (CMRR) of the amplifier is limited. This mechanism is not often problematic with modern differential amplifiers: a common mode rejection ratio of 80 - 120 dB is customary. A second and much more important way a high common mode voltage may cause interference is when there are differences in electrode impedances and/or input impedances which convert common mode voltage into a differential input voltage. This mechanism is the main reason for the need to reduce the common mode voltage as much as possible (Winter, Webster 1983-a)(Winter, Webster 1983-a).

The usual electrodes may show a mean impedance of 20 kΩ at 50 Hz and impedance differences of up to 50 %. Differences in input impedances should not exist in a carefully designed amplifier system, but often these differences are not easy to avoid.

An isolated measurement is very safe if the capacitance between the amplifier common and ground and the capacitance between the amplifier common and mains are kept sufficiently small.

5.5 Isolation and patient safety

Recording ECG signals means low-level signals must be detected and amplified in the presence of potentially dangerous voltages. An isolation

device acts as an interface between external devices and the data acquisition system. It provides galvanic isolation between the input and output. It also rejects large common-mode signals appearing at the input and breaks ground loops since the input and output are floating relative to each other.

In the medical field, patients are susceptible to electrical shock hazards. A normally harmless 50 Hz current can cause cardiac arrest under certain circumstances. As a result, manufacturers of bioelectric amplifiers, especially EEG and ECG equipment, use isolation amplifiers that provide appropriate isolation between the patient and the **AC** power line mains cord.

The effect of AC current passing through the body is a potentially dangerous situation and may lead to death. A 30 mA current can cause stopping of breath while a current as low as 20 μA directly applied to the heart would cause ventricular fibrillation and possible death.

There are several other key parameters that define the performance of an isolation device. A wide variety of isolation devices are available in fields ranging from industrial process control to medical instrumentation to PC-based data acquisition systems.

An isolation device passes a signal, either analog or digital, from input to output across an isolation barrier. This barrier ensures that there is no galvanic (ohmic) connection between input and output. To be effective, the isolation barrier must have high breakdown voltage, low **DC** leakage (high barrier resistance), and low **AC** leakage (low barrier capacitance).

The isolation voltage, the parasitic resistance, and the capacitance specify the barrier. The isolation voltage is a measure of the device's ability to protect itself and the surrounding circuitry against physical damage resulting from different voltage potentials. An isolation amplifier rejects the common-mode voltage and allows the signal of interest to be accurately measured.

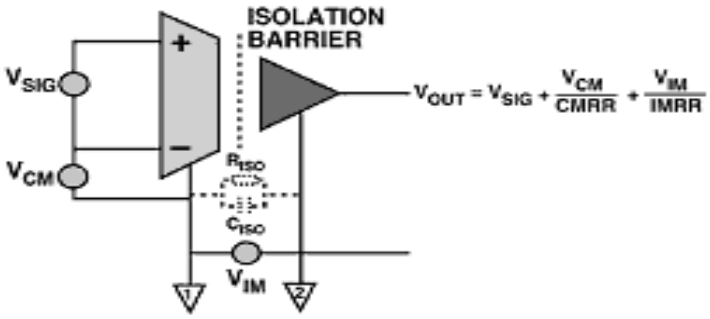

Figure 5.4. An ideal isolation device (source: Pickering P. 1999)

An ideal isolation device would transmit the input signal $\mathbf{V_{SIG}}$ across the barrier and reproduce it perfectly at the output. Real-world devices introduce errors due to the common-mode voltage, $\mathbf{V_{CM}}$, and the isolation-mode voltage, $\mathbf{V_{IM}}$. The barrier resistance and capacitance are modeled as shown.

5.6 Isolation device techniques

The three techniques commonly used are optical isolation, inductive isolation, and capacitive isolation. In the optical isolation the barrier consists of an LED and a photodetector. The input signal modulates the LED and the photodetector converts the light back into current. In inductive isolation the signal modulates a high-frequency carrier and is transformer-coupled from input to output. Transformer-coupled devices are the most effective at transmitting power in a given volume and are invariably used in dc-dc converters. The capacitive isolation modulates a high-frequency carrier and is capacitively coupled from input to output. Either duty-cycle or frequency modulation techniques are used, and then the signal is passed differentially across the barrier. The capacitors can be formed from elements of the IC package lead frame, reducing the overall cost.

5.7 Data acquisition methodology

5.7.1 Filtering

In a first order filter, the roll-off is very gradual (20 dB/decade, or 6dB/octave). This results in the cutoff between signal and noise being rather poor and noise will still continue to exist even with a low cutoff frequency.

To improve this, we need to make the cutoff cleaner. There are several common filters used in practice and they each have their relative advantages and disadvantages. The Butterworth filter was used due to the following properties:

1. Flat response in the pass band - minimal distortion
2. adequate rate of rolloff
3. large transition region
4. good all-round filter
5. simple to understand
6. Suitable for such applications as audio processing

In practice, higher-order filters are difficult to make with purely passive components (resistors and capacitors). Instead ***active*** filters are used, based around op-amps as seen in Fig. 5.5 and in Fig. 5.6.

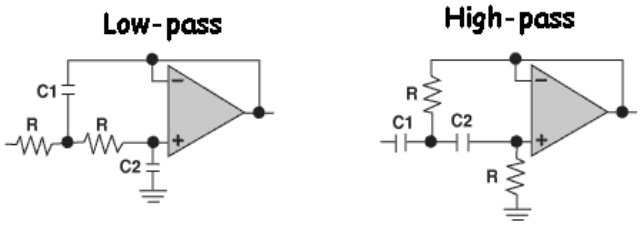

Fig 5.5 A single op amp realizations of active filters

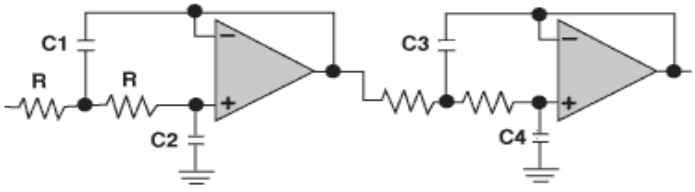

Fig 5.6 A two-op amp realizations of active filters

5.7.2 Analog to digital conversion (ADC)

In the process of analog to digital conversion, an analogue signal is converted into a digital signal, which can then be stored in a computer for further

processing. Analog signals are "real world" signals as is the case of the ECG signal recorded by the instrumentation amplifier. In order for these signals to be stored and manipulated by a computer, these signals must be converted into a discrete digital form.

The main advantages are

1. Data is easily transported and manipulated
2. Computer analysis of signals can be far more efficient
3. Real-time analysis can be performed

A number of important factors must be considered when converting analog signals into their digital equivalent. These include factors such as:

- Sampling and aliasing
- Resolution
- Saturation
- Quantization
- Dynamic range

Sampling and aliasing

The object of A/D conversion is to convert this signal into a digital representation, and this is done through sampling the signal. The sampling rate is the frequency expressed in Hertz (Hz) at which the ADC samples the input analog signal.

If the sampling rate is insufficient, the rapidly rising phase of a waveform may not be represented as well in the sampled waveform as is the more slowly changing part. In fact, it can be proven mathematically that the sampling rate to be used must be greater than twice the highest frequency contained in the analog signal. This critical sampling rate is called the Nyquist Frequency. If sampling rate is lower than the Nyquist, an artifact called aliasing can result. To allow for underestimates and give a margin of error, it is traditional in practice to use a figure of four times the maximum frequency.

For a signal of given frequency content, increasing the sampling rate beyond a certain point does not significantly increase the fidelity with which the signal is rendered. There is a tradeoff between fidelity of reproduction on the one hand, and computer storage space, computing time, and cost on the other.

As far as the ADC is concerned, noise is also a signal, so to prevent aliasing, the sampling rate calculation should allow for any noise in the signal. It is a usual to pass the analog signal through a low-pass filter before the ADC. This filter acts to remove some of the high-frequency content of the signal that would otherwise alias down in frequency. Note that this anti-alias filtering could remove high frequency information of physiological importance to the phenomenon under investigation. If it is important to retain these higher frequencies, one has no choice but to use a better data acquisition system that has a higher sampling rate.

Resolution

Resolution refers to the ability of the ADC to capture the smallest variations or changes in the voltage levels. This factor depends on both the span and the number of bits (N) used. The span is the maximum voltage used in accordance to the following formula:

$$\text{Resolution} = \text{Span} / 2^N$$

The type of ADC used forms an important factor since the number of bits the converted binary number can take is one of 2^N values, where N = number of bits in the ADC. For N=12, then there can be 4096 values, representing the integers from 0 to 4095. The ADC also has an input range (span), measured in volts. Thus, the input voltage range is divided into 4096 levels, with each level being Span/4096. So, with a span of 10 V, the resolution is 0.0024 volts. Our choice for this part of the circuit was the ADC since it provides a 16-bit resolution and which could be used to record up to 12 channels of ECG data.

Saturation

When carrying out A/D conversion it is important to keep the input signal within the span of the ADC. If the input signal exceeded the supply voltage $\mathbf{V_S}$, a 12 bit binary number with an equivalent decimal number of the maximum value would be still returned to the computer. The computer would thus interpret the voltage being sent to be the same value, which would be in error. This error is called saturation of the ADC. However, the input signal should span as much of the ADC input voltage range as possible, without saturating the ADC, since this increases the signal to noise ratio. Thus if the voltage range of the input signal is much smaller than $\pm$ $\mathbf{V_S}$ volts, the signal should be amplified before being fed to the input of the ADC.

Quantization Noise

The uncertainty introduced by rounding the sample amplitudes to discrete levels adds noise, called *quantization noise*, to the signal. The amount of this 'noise' decreases with increasing resolution. Because a sample is stored as a binary number, the total number of values that can be stored = 2^N, with N being the number of bits in the ADC. It can be shown that the RMS amplitude of the quantization noise = q / $(12)^{0.5}$ (or 0.29 q) where q is the resolution of the ADC.

Dynamic Range

Dynamic range refers to the range of values between the high and low values that can be recorded by the ADC. A 16-bit ADC with more bits was chosen to reduce the effects of quantization noise. In addition to our desire to represent both low and high amplitude signals with reasonable fidelity. The need for this dynamic range can result in more bits. Using an 8-bit ADC, then 255 correspond to the highest amplitude and the lowest amplitude is 0.255 represented by the least significant bit (LSB). For a 12-bit ADC, the lowest amplitudes are allocated about 2 bits; and for a 16-bit ADC, about 6 bits.

5.8 The complete data acquisition system

The instrumentation developed for this thesis is meant to provide the high-resolution high-sampling rate data needed for the analysis of VLP. It consists of an analog part and a digital part. The analog part is dedicated to record the ECG signal directly from the body surface of the patient. It provides the necessary patient safety through the use of special components designed for this purpose. It includes components such as the ISO175 isolation instrumentation amplifier and dc-dc converters. There are three isolation amplifiers that can provide a 12-channel data recording through the use of three 4-channel ADC. The role of the dc-dc converters is twofold; they provide supply isolation for patient safety and the needed positive and negative voltages needed to operate the circuit.

5.8.1 Isolation instrumentation amplifiers

The ISO175 is a precision isolated instrumentation amplifier incorporating a novel duty cycle modulation/demodulation technique and excellent accuracy. A single external resistor sets the gain. Internal input protection can withstand up to ±40V without damage. The signal is transmitted digitally across a differential capacitive barrier. With digital modulation the barrier characteristics do not affect signal integrity.

This results in excellent reliability and good high frequency transient immunity across the barrier. Both the amplifier and barrier capacitors are housed in a 24-pin plastic DIP that is only 0.3" wide.

The ISO175 is easy to use and its gain is set with a single external resistor placed between pins 2 and 22. A power supply range of ±4.5V to ±18V makes this amplifier ideal for a wide range of applications. The device has a CMRR of 115dB and a non-linearity of less than 0.01%. The stages of this amplifier are shown in Fig.5.7 along with the pin distribution and numbers.

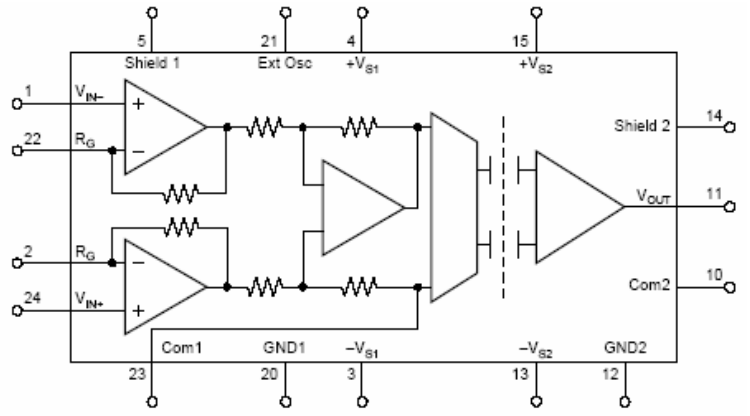

Fig. 5.7 ISO175 instrumentation amplifier pin distribution
(source: Texas Instruments)

5.8.2 The dc-dc converter

The DCP01B series is a family of 1W, unregulated and isolated dc-dc converters. Requiring a minimum of external components and including on-chip device protection, the DCP01B series provides extra features such as output disable and synchronization of switching frequencies. The internal structure of the device is shown in Fig 5.8.

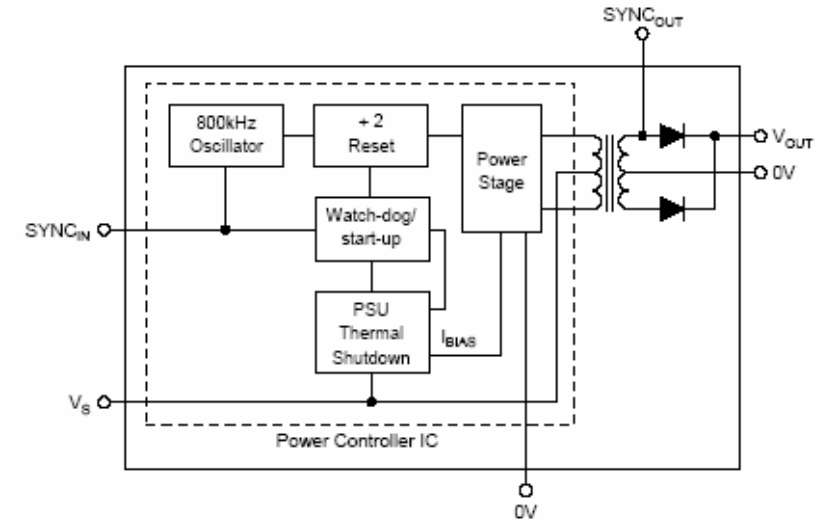

Fig. 5.8 Internal structure of the dc-dc converter
(source: Texas Instruments)

To generate a bi-polar supply, the dc-dc converter was used according to the configuration shown in Fig 5.9.

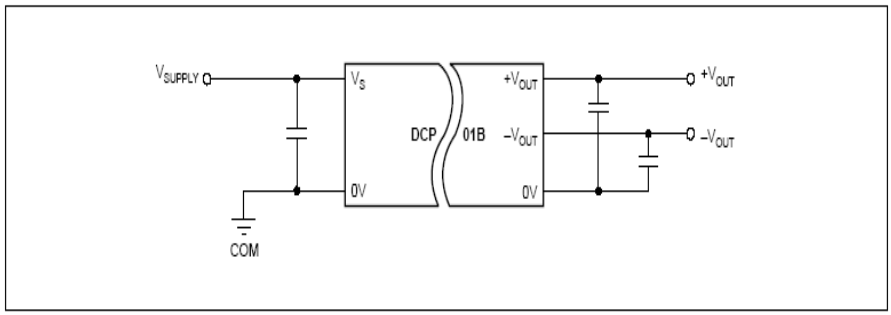

FIGURE 2. Connecting Dual Outputs in Series.

Fig. 5.9 Bi-polar supply structure of the dc-dc converter
(source: Texas Instruments)

The material discussed up to this point was utilized to produce the portable high-resolution system shown in Fig. 5.10. The system connects to laptop via the versatile USB port.

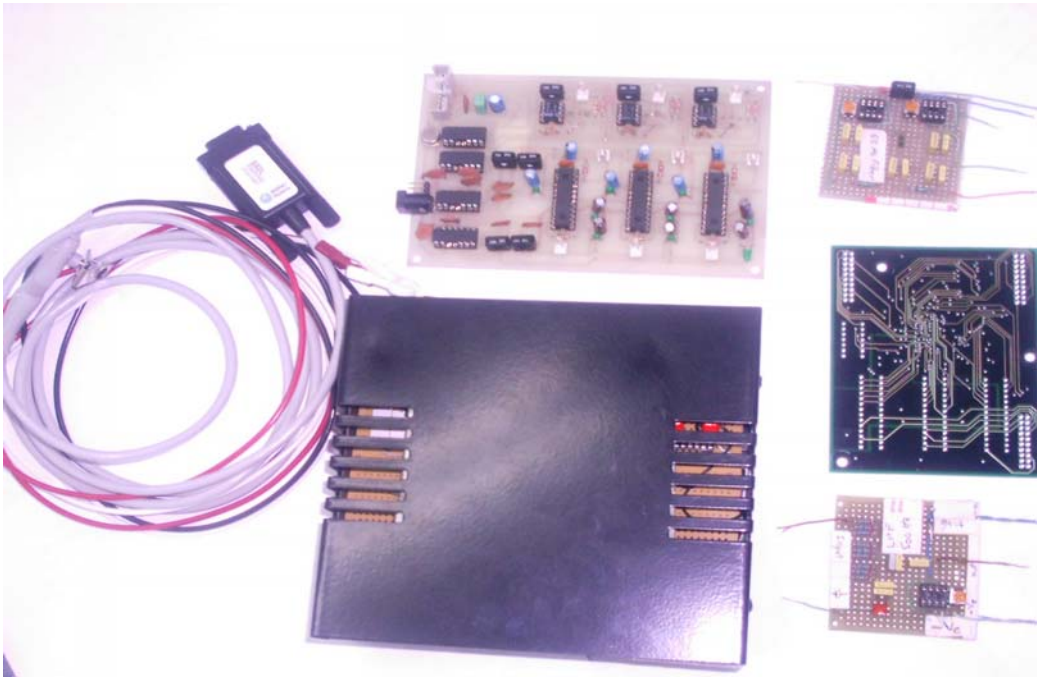

Fig. 5.10 A snapshot of the system components

CHAPTER 6

CLUSTERING OF PATIENT DEPENDENT FEATURES

6.1 Introduction

Material presented in this chapter follows the path of minimizing drawbacks of commonly used methods such as alignment, averaging of uncorrelated beats and the rest. It should serve as a preprocessing operation to the input data for and is part of the unified method. The preprocessing operation clusters ECG beats into templates that have common characteristics. Templates are usually employed in the analysis of ECG signals in order to control the quality of the incoming beats as they are recorded or during the classification stage. A possible application area of the method is in Holter recordings with higher sampling rates and better resolutions. Recording a long-term record generates large sizes of data records and analyzing such records is only approximate and is usually done in a short time through visual inspection. In Holter recordings, a 24-hour or sometimes more is usually recorded. The recorded signal is normally sampled at less than 250 samples per second and a resolution of 10 bits or less to keep the data size within a manageable range. The rates used represent a minimum requirement and must be increased in order to capture important hidden information in biological signals such as the ECG. Increasing these values will definitely increase the size of data collected. To be useful and give better insights into many abnormalities these values need to be increased to sampling rates of 1000 Hz or higher and resolutions of 12 to 16 bits. At a heart rate (HR) of 60 beats per minute (BPM), which is one beat/second, when sampled at 1000 samples/second and a resolution of 10 bits results in a data size of 10000 bits/second. For a 24 hour Holter recording this means, 864 mega-bit or 54 mega-byte of data. Even though today's storage devices are capable of storing large quantities of data in small and portable media such as flash cards, the problem remains at the doctor's end. Any cardiologist analyzing such data will only sample and

approximate these records with the possibility of unintentionally missing important details. It is impossible for any cardiologist to examine the complete long time records such as those of the Holter recordings. At best they will sample these records to try to spot distinguishing features that may have medical value in a laborious way (Mousa, Yilmaz, 2004-c).

The template may be a universal one representing a particular illness applied to all patients or might be extracted from individual patients by visually inspecting a clean beat, which is then used as the template. However, all these techniques come with their associated drawbacks and the currently applied methods may not be the best implementation possible. All incoming beats will be categorized with respect to this template regardless of their information content. In addition, a small variation that may not occur at every beat will be masked out by such methods in present. The universal template is not an accurate one since it attempts to mach all patients to common beat, which may be appropriate for general inspection and rejection of ectopic beats, but such a method is definitely inappropriate for detailed analysis of abnormalities such as ventricular late potentials (VLP) as microvolt signals used for prognosis of ventricular tachycardia (VT).

A major difficulty in averaging a number of beats to generate the improved template is alignment of the beats to a certain reference point. It has been found that the existence of a timing error or trigger jitter in the synchronization process causes a low-pass filtering effect in the averaged signal (Jane et al1991)(Rompelman and Ros,1986). Noise constitutes another major challenge to any working procedure especially if the desired signal is in the same range as that of the noise as the case of VLPs (Friesen et al., 1990).

What is presented here is an improved method for patient-dependent template generation that takes into account the possible variation in ECG signals from patient to patient and even from beat to beat for the same patient. In addition to template generation, the method allows for good reduction of data size without loss of information. The method shows good performance even for noisy signals since it isolates noise in a separate wavelet transform (WT) level.

To help in the diagnosis and summarize this large data with minimum or no loss at all, we introduce a method that extracts templates from patient data rather than using a general golden template. This approach uses a simple method named as dynamic averaging. Dynamic averaging allows for real time computation of the average of beats as they are recorded or received. The size of the template refers to how many different beats are clustered together to form the overall multi-beat template. A template of a user-defined size is generated for each patient and extracted from her/his own data. Data reduction is accomplished through the resulting size of data while cross-correlation values are used in the coding process in order to preserve information about all averaged beats that contributed to the generated templates.

In the following section we present a brief background on some of the tools employed in this study. Other sections introduce the methodology followed and finally their results are presented followed by some conclusions about the introduced method.

6.2 Theory and tools

6.2.1 Normal and dynamic signal averaging

Signal averaging is a common method used for improving the signal to noise ratio (SNR) and is essentially statistical in nature based on white noise assumption (Rompelman and Ros,1986). Unless the desired signal repeats at every beat, averaging will tend to reduce its strength rather than improve its SNR. Therefore, we must know the repetition nature of the desired part of the signal before applying any averaging in order to get optimum improvement in SNR. Of course averaging every beat is optimal if the desired signal is repeated at every beat and results in SNR improvement equal to $\sqrt{N}$ where N is the number of averages. The usual averaging process waits for an ensemble of data to be collected before averaging. This prohibits online averaging and renders the calculated average to static. On the other hand, dynamic averaging, which we have suggested here, allows for real time of beat averaging as they are acquired and allows for continuous updating of the

calculated average. The usual averaging scheme sums up N-points and divides that sum by the total number of data points N according to the following formula:

$$\bar{x} = \left(x[1] + x[2] + ... + x[N\}\right)/ N \tag{6.1}$$

Dynamic averaging introduced here in this work is a variation from the normal averaging process. The dynamic averaging process recalculates the average as new beats are received under predefined conditions at a sample k as:

$$M_k = \frac{\left[(k-1)M_{k-1} + x[k]\right]}{k} \tag{6.2}$$

where M_k is the k^{th} average and its initial value M_1 is set equal to the first sample received.

6.2.2 Wavelet transform

The forward and inverse WT are implemented as a tree-structured perfect reconstruction bank as illustrated in Fig 6.1.

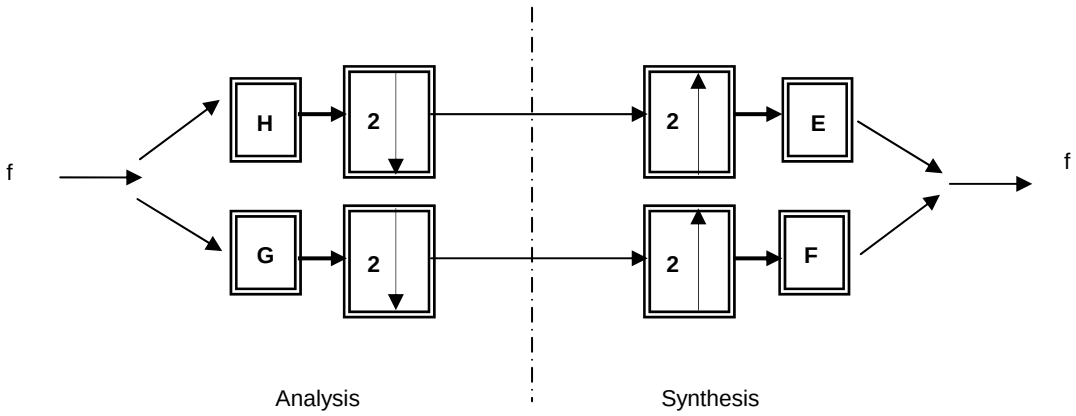

Fig. 6.1 Forward and inverse WT

The process takes an input signal $f(t)$ and applies a pair of analysis filters **G** and **H**. The **G** is a high pass filter while **H** is a low pass filter. The resulting signals are then down sampled by a factor of two, which forms the output of the analysis stage. Usually this process is continued for a number of stages where the output of the low pass filter becomes the input to the next stage,

while the output of the high pass filter is retained. The synthesis stage is comprised of the opposite operations carried out in the analysis part where the full signal is regained using the pair of filters **E** and **F** where **E** is a time-reversed version of **H** and **F** is a time-reversed version of **G** as required by the orthogonal wavelet system. Any processing of the signal f(t) has to take place between the two stages (Burrus, Gopinath and Guo, 1998).

6.3 Methods of analysis

E. Laciar et al. applied a similar method which they called multi-scale cross-correlation for the alignment process and concentrated their work on the alignment of noisy signals (Laciar et al, 2003). In this work, cross-correlation is used for several purposes such as alignment of individual levels, improving template generation and data size reduction. Using WT decomposition further extends this method.

The cross-correlation is a measure of the similarities or shared features between two signals (Oppenheim and Schafer, 1989). It is frequently necessary to be able to quantify the degree of interdependence of one process upon another, or to establish the similarity between one set of data and another. The existence of a finite sum will indicate a degree of correlation. The cross-correlation between two data sequences $x_1[n]$ and $x_2\{n\}$ each containing N data might be written as:

$$r_{12}[k] = \frac{1}{N}\sum_{n=0}^{N-1} x_1[n]x_2[k-n] \qquad for\ k = 0,1,... \tag{6.3}$$

The correlation is computed for a number of different lags, *k* in order to establish the largest value of the correlation, which is then taken to be the correct value.

Once the cross-correlation coefficient is calculated, it can be used for the alignment process for coinciding two beats properly. In this case the sample number of maximum lag value is taken as the alignment point. The correlation process is applied to each level and the alignment process is then carried out.

The overall process clusters the different information contained in ECG records into separate groups that could be utilized in further analysis and illness classification in a way similar to the usual template except instead of having a single beat as a template we have multiple beats.

The diagram in Fig 6.2 shows the flow of analysis of ECG signals under WT and the correlation process. The choice of record size and degree of similarity can be set according to the particular application at hand. Analysis for the detection of finite duration, low amplitude activities require a larger record size and a higher degree of similarity. Since these levels represent signals with certain frequency content and they fall in the same frequency range, individual levels are tested for correlation.

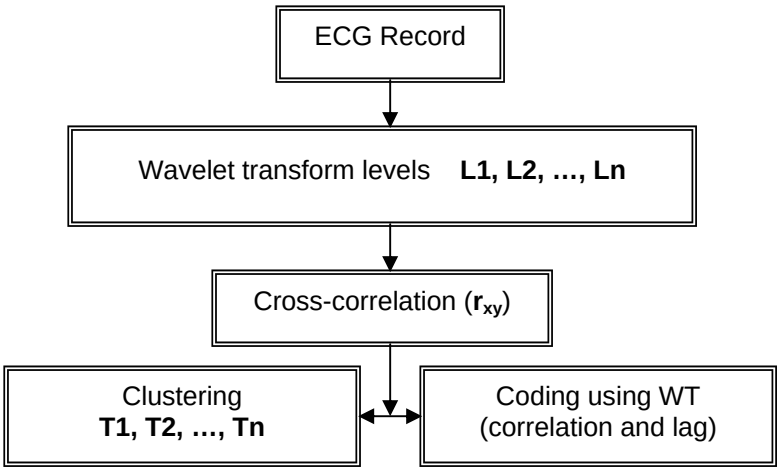

Fig. 6.2 Flowchart of analysis

The wavelet type used in this analysis was the Daubechies (D-20) wavelet shown in Fig. 6.3 below. Applying the WT to each beat produces a set of levels each containing a time signal with certain frequency characteristics (Mousa and Yilmaz, 2001). After the correlation process the new level, if there is any, is properly aligned and averaged with the previous average result using the dynamic averaging process producing a new and improved template including that particular level. One has to note that this process is performed according to a condition defined by correlation stage. When the process described above is applied to these levels then we have another dimension or signal added to the multi-beat template.

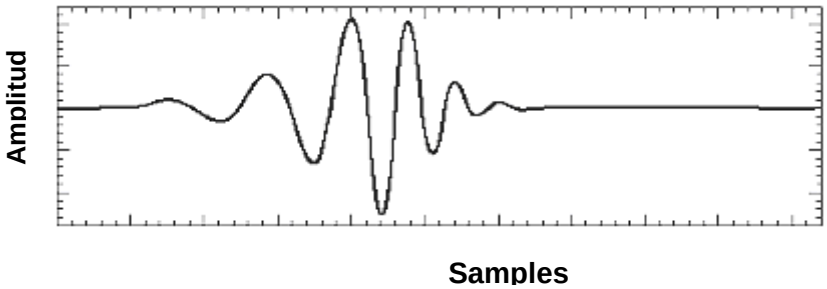

Fig.6.3 Daubechies D-20 wavelet

Only similar levels are aligned and averaged which ensures better association of contents. Cross-correlation values are used in both the measure of similarity and in alignment of beats prior to averaging to gain better results.
After generating the final template, the cross correlation process is recalculated. The auto correlation of the final template is used as the threshold for comparison. A two-parameter scheme is used in the coding process. The first parameter is the maximum correlation value between each beat and the beats in the templates and the second is the lag value at which the cross correlation is maximum.

Using WT coding, the template entry that resulted from averaging the highest number of signals was used as the representative template for cross-correlation. Using that template, the correlation coefficient and lag values, for the coding scheme is generated as mentioned above.

6.3.1 Clustering patient dependent features

Averaging is based on the assumption that the signal of interest is periodic and repeats itself with every beat, a situation that cannot be guaranteed in the case of VLPs. The threshold chosen for correlation as a similarity criterion for features in comparison stage can be set as tight as the application requires for better beat association and feature discrimination. In order to cluster some features in different ECG waveforms, a number of records from signals with different abnormalities were used in the analysis.

The signals included normal sinus (**NS**), Atrial fibrillation (**AF**), partial epillipsy (**PE**) and heart failure (**HF**), sample plots from each signal are shown in Fig.

6.4. The entire 4096-sample signal was wavelet transformed and a detection process for R-peaks was performed. As an example taking the WT of record of 4096 samples will produce 13 different levels {**L1, L2, … , L13**}.as calculated from the length of the sequence as $2^n = 4096$ or n=13. The L1 level contained the lowest frequency while the L13 level contained the highest frequency. At this point we have 13 different column vectors each containing one level representing the first beat. When the second beat is received, it will go through the process of decomposition again producing a total of 13 different levels each containing corresponding levels from all beats. A cross-correlation process generated the different templates. The size of the templates {**T1, T2, …, T13**} in cluster table depended on the degree of similarity set by the threshold value.

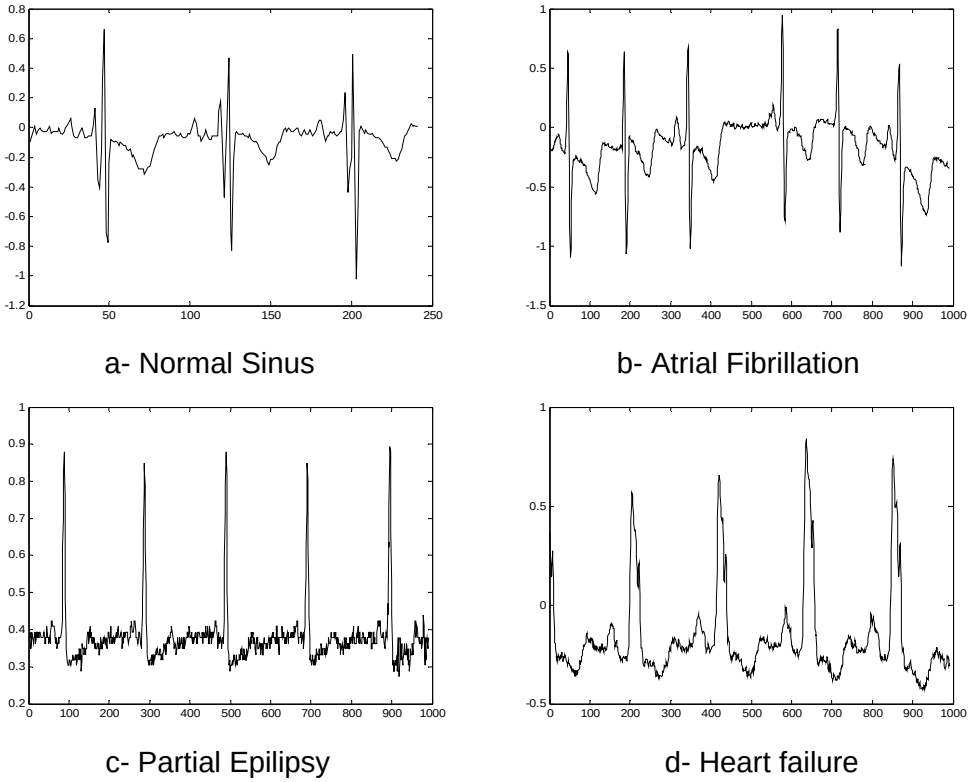

a- Normal Sinus

b- Atrial Fibrillation

c- Partial Epilipsy

d- Heart failure

Fig.6.4 Parts of the original signals, a-NS, b-AF, c- PE, d-HF.

The process begins with assigning the first beat as the initial template. The second beat received is compared to this template, aligned and averaged together if the correlation value exceeds the predefined threshold as an accepted degree of similarity. If the beat and template are not similar (i.e., correlation value is less than the threshold), this new beat is appended to

template increasing the size of template by one beat generating a multi-beat template. The resulting multi-beat template is then taken as the final feature clusters for that patient that also summarizes the contents of the entire record. Each level in the WT decomposition of the first beat in the signal is assigned to the corresponding cluster table of that level which are labeled as **T1, T2, …,T_n** to form the starting template. The content of each cluster table is compared with appropriate levels of other newly decomposed beats, (e.g. **L1** with **T1, L2** with **T2** and so on) by calculating their cross-correlation values. If a particular WT level with calculated correlation value exceeds the predefined threshold, this level is properly aligned and averaged with the corresponding T cluster (e.g. L1 with T1). Otherwise the WT level is accepted as new template and is appended to the same T cluster without averaging; increasing the size of the corresponding **T** cluster by one more beat.

The process is similar for the rest of the WT levels and T levels in clustering table. This is continued until the last beat after which the T vectors will have different numbers of levels appended to them depending on their similarity.

A major task of the method, which is sensitive to noise, lies also in the process of isolating independent beats. The WT method was employed in this process as well as other parts of the analysis by combining levels **L10** and **L11** which emphasize the presence of the R-peak, reduce and remove base-line drift as seen in Fig. 5. During this process the mid-point between two R-peaks is taken as the dividing point between two successive beats. The heart rate (HR) and RR intervals are then easily obtained.

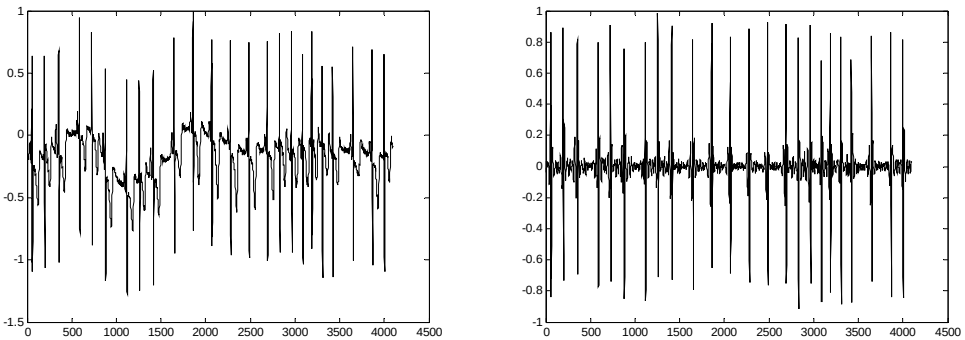

a. Original signal **b.** Appropriate WT levels

Fig. 6.5 Detection of R-peak using WT to remove base line variations

6.4 Results

A summary of the performance of the method as applied to the set of data is presented in Table (6.1). In this summary we record the effect of different signal categories on the number of beats within the chosen length of 4096 samples. The other important observation is that the degree of reduction varies from patient to patient and from level to level. The first two template entries, T1 and T2 produced equal reduction for the same patient but different for different patients. These levels represent the low frequency content in the data records. There is no particular pattern that can be seen from the values in the table therefore the results are signal-dependent.

The table presents the overall results of the method as applied to the four test signals with a middle value for the threshold of 0.5 chosen and presenting the sizes in terms of the number of beats in that portion. Each signal contained different number of total beats within the same chosen record length of 4096 samples per record indicated as N in the table. Since the WT produced 13 different levels we had a similar number for the multi-beat templates marked as **T1**, **T2**, and so on. The entries in these tables represent the size in beats of the resultant template.

Without data reduction the entries in the table should be equal to index N the size of each type of signal used.

Table 6.1
Size of each cluster level expressed as the number of beats at a threshold value of 0.5 for all signals.

Signal	T1	T2	T3	T4	T5	T6	T7	T8	T9	T10	T11	T12	T13
NS(N=50)	1	1	1	1	1	1	1	1	1	1	2	1	2
AF(N=22)	1	1	2	1	1	1	1	1	1	1	1	2	3
PE(N=22)	1	1	1	1	1	1	1	1	2	2	2	10	12
HF(N=20)	2	1	2	1	1	1	1	1	1	1	2	6	3

Level **L12** and **L13** show less similarity and therefore vary the most. This is reflected on the number of entries retained in the resulting template (**T12** and **L13**) especially for **PE** and **HF** which is reflected in the calculation of the overall performance as shown in Table.

The reduction percentages are calculated based on the number of beats in the original signal and that of the resultant individual templates as in:

$$Value = \frac{size\ of\ original\ signal\ (beats) - size\ of\ each\ template\ (beats)}{size\ of\ original\ signal\ (beats)} x\,100$$

The normal signal (NS) had the most reduction (98%) while partial epilepsy signal (PE) was the least reduction (87%) but still shows the efficiency of the method as in Table 6.2.

Table 6.2 Comparisons of size reduction values

Average Reduction Values	**NS**	**AF**	**PE**	**HF**
	98%	94%	87%	91%

The average reduction in cluster levels as applied to all signals expressed as percentage values is shown in Table 6.3. It can be seen that most levels achieved very high reduction values ranging from 93 to 96%. The least reduced clusters were **T12** and **T13** with a reduction value of 78%, which as we mentioned earlier contains mostly noise.

Table 6.3 Average compression of individual levels

T1	**T2**	**T3**	**T4**	**T5**	**T6**	**T7**	**T8**	**T9**	**T10**	**T11**	**T12**	**T13**
95%	96%	94%	96%	96%	96%	96%	96%	95%	95%	93%	78%	78%

It was also observed that lowering the threshold values of the correlation coefficient to zero resulted in combining all beats in the template into a single beat as expected while setting the value to one resulted in preserving the entire record without any averaging. These two situations are extremes and are included only as a control to process.

A sample of the reconstruction process is shown in Fig. 6.6-a where the original signal beats can be reconstructed using the generated templates. The plot shows an arbitrary beat superimposed on one of the generated cluster templates. The system is also registering the number of beats involved in the averaging of individual templates to reveal the overall weight of contributions in each cluster. Fig. 6.6-b displays two beats from the NS which were

classified as different beats in the same patient as indicated by the entry under **T11** in Table 6.1 with 48 out of 50 beats were associated with one of the templates while 2 beats were associated with the other.

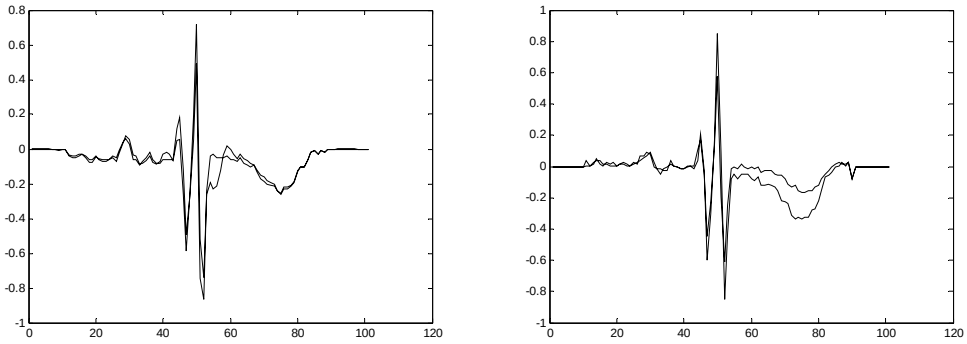

(a) (b)

Fig. 6.6 (a)-Sample plot of a reconstructed beat superimposed over one of the cluster templates and (b)- two beats from the NS which were classified as different beats in the same patient

A composite signal made up from a combination of **NS** and **AF** signals was also applied to test the performance of the method. Results obtained using the composite signal show that all clusters produced one template at the threshold value of 0.5 while **T11**, **T12** and **T13** produced two templates with varying number of beats averaged in each template as in Table 6.4. Examples of rebuilding beats from these templates are shown in Fig 6.7.

Table 6.4 distribution of averaged beats in each cluster

Cluster Template	**T11**	**T12**	**T13**
Number of beats averaged	23	35	34
	14	2	3

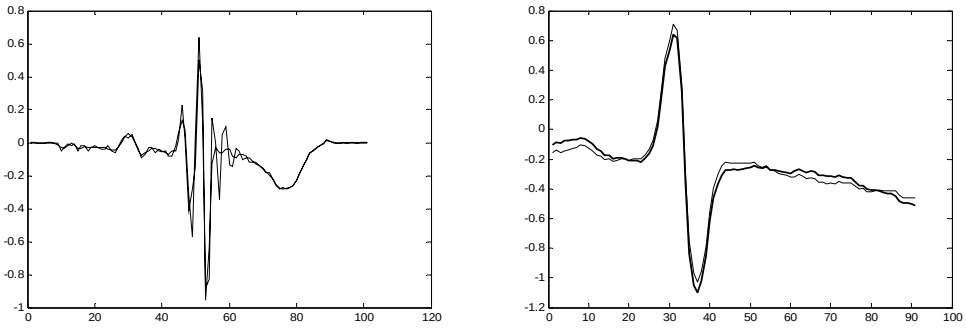

Fig. 6.7 Example of rebuilding beats from templates

6.5 Analysis of the method's performance

The method was tested and the results are presented in Table 6.5 and Table 6.6 for both noise and correlation threshold sensitivity respectively. Each normalized signal is corrupted with different levels of white noise and different correlation values set as thresholds and the proposed method applied. These signals were not free of noise to begin with so the added noise was in addition to that originally contained in the signal. A sample of both original signal and the noise-corrupted versions are shown in Fig. 6.8. Noise levels from zero to 0.2, representing signal to noise ratios of up to 20% of signal amplitudes have been used. The correlation values were varied from perfect match or a value of one to zero match.

Table 6.5
Results of different noise levels[1]

NS with noise n=0.05:0.05:0.2 and a threshold = 0.5													
Noise	**T1**	**T2**	**T3**	**T4**	**T5**	**T6**	**T7**	**T8**	**T9**	**T10**	**T11**	**T12**	**T13**
5 %	1	1	1	1	1	1	1	1	1	1	2	1	2
10 %	1	1	1	1	1	1	1	1	1	1	2	1	2
15 %	1	1	1	1	1	1	1	1	1	1	2	1	2
20 %	1	1	1	1	1	1	1	1	1	1	2	1	2

AF with noise n=0.05:0.05:0.2 and a threshold = 0.5													
Noise	**T1**	**T2**	**T3**	**T4**	**T5**	**T6**	**T7**	**T8**	**T9**	**T10**	**T11**	**T12**	**T13**
5 %	1	1	2	1	1	1	1	2	1	1	1	2	1
10 %	1	1	2	2	1	1	1	2	1	1	1	1	1
15 %	1	1	2	2	1	1	1	2	2	1	1	1	1
20 %	1	1	2	2	1	1	1	2	3	2	2	1	1

PE with noise n=0.05:0.05:0.2 and a threshold = 0.5													
Noise	**T1**	**T2**	**T3**	**T4**	**T5**	**T6**	**T7**	**T8**	**T9**	**T10**	**T11**	**T12**	**T13**
5 %	1	1	1	1	1	1	1	1	2	2	3	1	1
10 %	1	1	1	1	1	1	1	1	1	2	2	5	8
15 %	1	1	1	1	1	1	1	1	2	2	2	9	11
20 %	1	1	1	1	1	1	1	1	2	2	2	10	11

HF with noise n=0.05:0.05:0.2 and a threshold = 0.5													
Noise	**T1**	**T2**	**T3**	**T4**	**T5**	**T6**	**T7**	**T8**	**T9**	**T10**	**T11**	**T12**	**T13**
5 %	1	1	2	1	1	1	1	1	1	1	3	1	1
10 %	2	1	2	1	1	1	1	1	1	1	2	4	4
15 %	2	1	2	1	1	1	1	1	1	1	2	5	4
20 %	2	1	2	1	1	1	1	1	1	1	2	5	6

1. Size of each averaged level expressed as the number of beats at a threshold value of 0.5. T is the number of differences detected and considered as templates based on the given threshold.

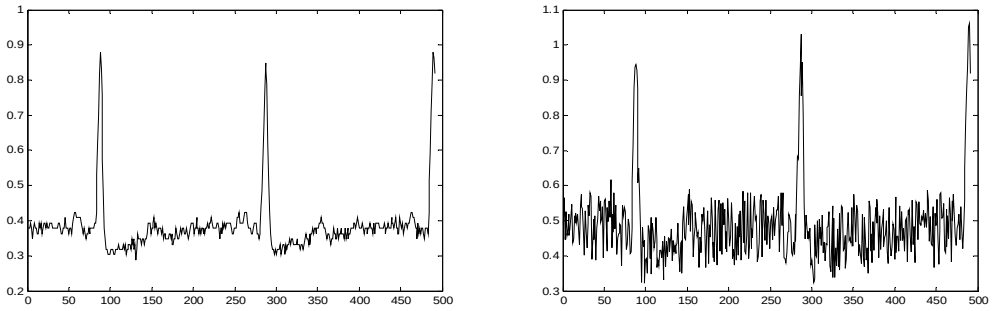

(a) (b)

Fig. 6.8 Samples of (a) original signal and (b) signal plus noise

The method kept a constant behavior even when the noise levels were increased to 20% of the signal amplitude.

Table 6.6
Cluster level sizes expressed as the number of beats at different threshold values.

NS with different threshold values (THD)													
THD	**T1**	**T2**	**T3**	**T4**	**T5**	**T6**	**T7**	**T8**	**T9**	**T10**	**T11**	**T12**	**T13**
0.6	1	1	1	1	1	1	1	1	1	1	2	1	3
0.7	1	1	1	1	1	1	1	1	2	1	2	1	3
0.8	1	1	1	1	1	1	1	1	2	1	3	3	4
0.9	1	1	1	1	1	1	1	1	2	3	6	4	8

AF with different threshold values (THD)													
THD	**T1**	**T2**	**T3**	**T4**	**T5**	**T6**	**T7**	**T8**	**T9**	**T10**	**T11**	**T12**	**T13**
0.6	1	2	2	1	1	2	1	2	2	1	1	4	7
0.7	1	2	2	2	2	2	2	4	4	2	2	6	14
0.8	1	2	2	2	2	2	4	6	8	5	4	11	19
0.9	1	2	3	3	3	3	5	10	14	12	18	14	22

PE with different threshold values (THD)													
THD	**T1**	**T2**	**T3**	**T4**	**T5**	**T6**	**T7**	**T8**	**T9**	**T10**	**T11**	**T12**	**T13**
0.6	1	1	1	1	1	1	1	1	2	2	4	15	16
0.7	1	1	1	1	1	1	1	1	3	4	6	16	18
0.8	1	1	1	1	1	1	1	2	3	4	7	17	19
0.9	1	1	1	1	1	1	2	2	6	7	10	19	19

HF with different threshold values (THD)													
THD	**T1**	**T2**	**T3**	**T4**	**T5**	**T6**	**T7**	**T8**	**T9**	**T10**	**T11**	**T12**	**T13**
0.6	2	2	2	1	1	1	1	1	1	2	4	5	6
0.7	2	2	2	2	2	2	1	1	1	2	4	9	8
0.8	2	2	2	2	2	2	1	1	1	2	5	10	13
0.9	2	2	2	2	2	2	1	2	1	4	9	14	17

Threshold values were varied in steps of 0.1 from zero to one and some of the results from this part are presented in Table 6.6. The size of the resultant cluster template increases with the increase in the threshold value, especially in the upper levels. This property can be utilized depending on the accuracy required.

The algorithm presented in this chapter is well suited for real time ECG preanalysis, classification and data size reduction. It retains the clinically significant details of the individual ECG signal. It provides cardiologists and doctors with a summary of the signal characteristics to ease the analysis and bring their attention to the portions that may be of clinical value. This approach does not attempt to reduce the sampling rate, as is the case with other compression algorithms.

This chapter serves as a preprocessing step to the unified method, which is introduced, in the next chapter. The unified method is applied to different sets of data with their results compared to previously gained results using common methods.

CHAPTER 7

DATA PREPARATION, ANALYSIS AND RESULTS IN UNIFIED FRAME

7.1 Introduction

In this chapter we present the results obtained using the processes and methodologies outlined in the previous chapters. Conclusions, comments and plans to be followed in the future for this subject will be introduced in the next chapter.

It is clear at this stage that current methods and approaches suffer from certain drawbacks due to some of the assumptions that limited their performance and resulted in low prediction rates to the problem of VLP identification. Itemized here are some of drawbacks to serve as a frame for the accomplished work in this thesis and these are:

1. Absence of exact properties and definitions of what constitutes VLP
2. Limited region of analysis
3. Low number of parameters
4. Cross-term generation in the calculation of the vector magnitude
5. Orthogonality assumption of the XYZ leads
6. Overlap of noise and VLP ranges
7. Averaging of uncorrelated beats and the need for beat rejection
8. Requirement for suitable data (high-resolution, high-sampling rates)
9. Need to minimize human involvement in classification
10. Importance of the Use of modern technology
11. Alignment problems
12. Lack of real time processing

7.2 Parameter extraction and analysis methods

A set of parameters is extracted from each process and is used as inputs to a feed-forward neural network for classification. Once the parameters have been extracted, they are used as inputs to a feed-forward neural network (ANN) for classification as shown in Fig. 7.1.

The roadmap for the analysis and extraction of appropriate parameters for the proposed method is as follows:

- WT decomposition and analysis including detection of characteristic points
- Complex cepstrum and homomorphic deconvolution
- Minimum-phase, Maximum-phase, MPC, and SL calculation
- Parameter extraction
- Neural Network classification of the extracted parameters

Fig. 7.1 Classification of extracted parameters

Snapshots of some of the GUI windows designed to organize the data acquisition and analysis processes using different DSP techniques are shown in Fig. 7.2 and Fig. 7.3 below.

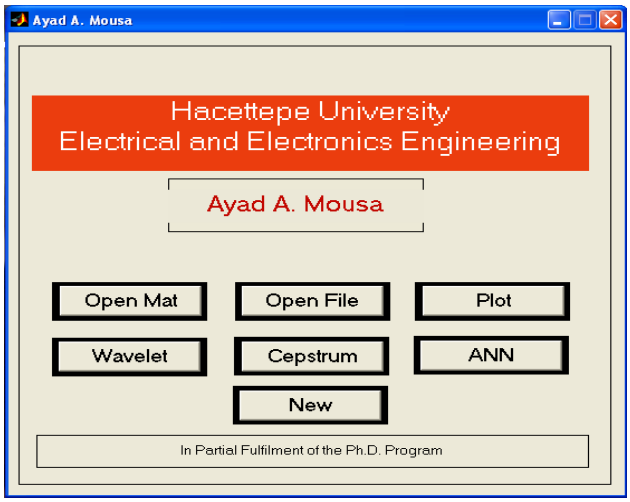

Figure 7.2 Snapshots of the user interface windows

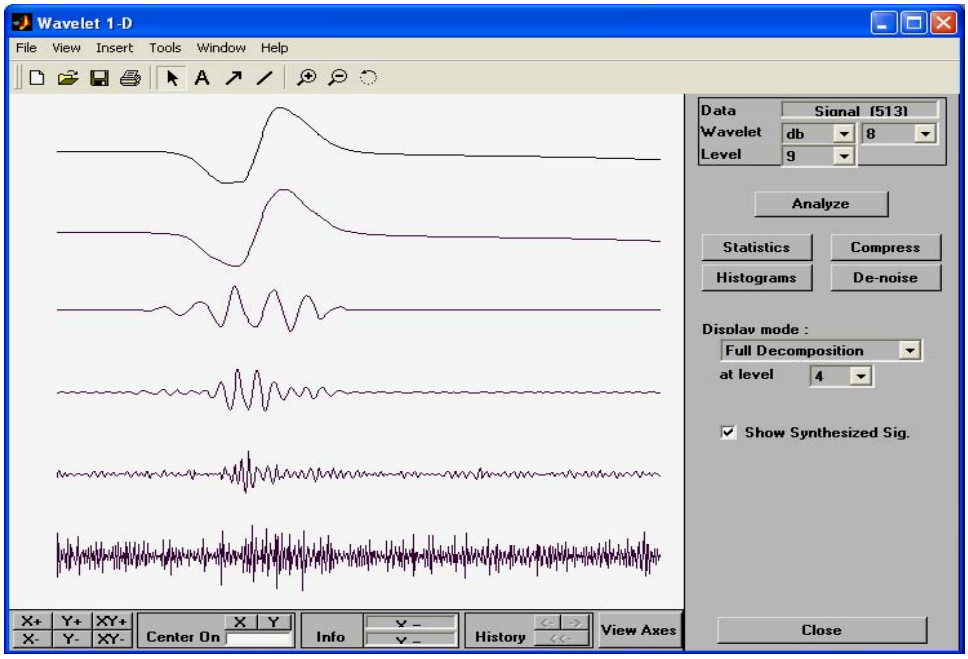

Figure 7.3 Snapshots of some of the analysis GUI using Matlab

Parameters can either be extracted from the vector magnitudes or directly from individual beats based on beat-to-beat analysis. The flowchart shown in Fig. 7.4 shows the application of the WT to the individual leads prior to calculating the vector magnitudes, while the flowchart of WT parameter extraction from the individual beats is illustrated in Fig 7.5 and the flowchart of CC parameter extraction from the individual beats is illustrated in Fig 7.6. The vector magnitude MQ is calculated based on the individual vector magnitudes MX, MY and MZ which were calculated using the WT method introduced in chapter three of this thesis and is defined as:

$$MQ = \sqrt{MX^2 + MY^2 + MZ^2} \tag{7.1}$$

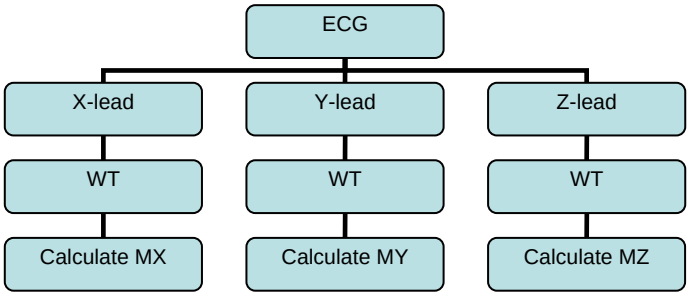

Fig.7.4 WT based vector magnitude calculation flowchart

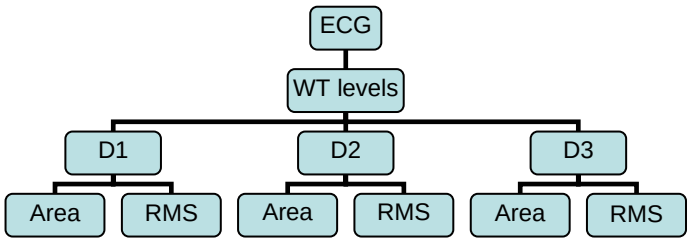

Fig. 7.5 Extraction of different WT parameters

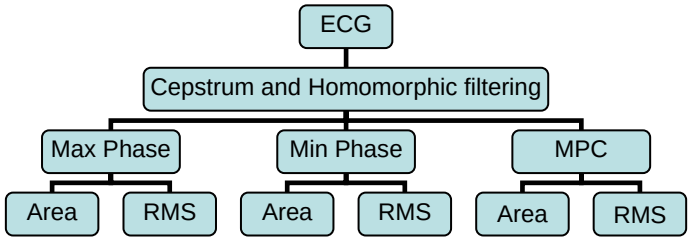

Fig. 7.6 Extraction of different Complex Cepstrum parameters

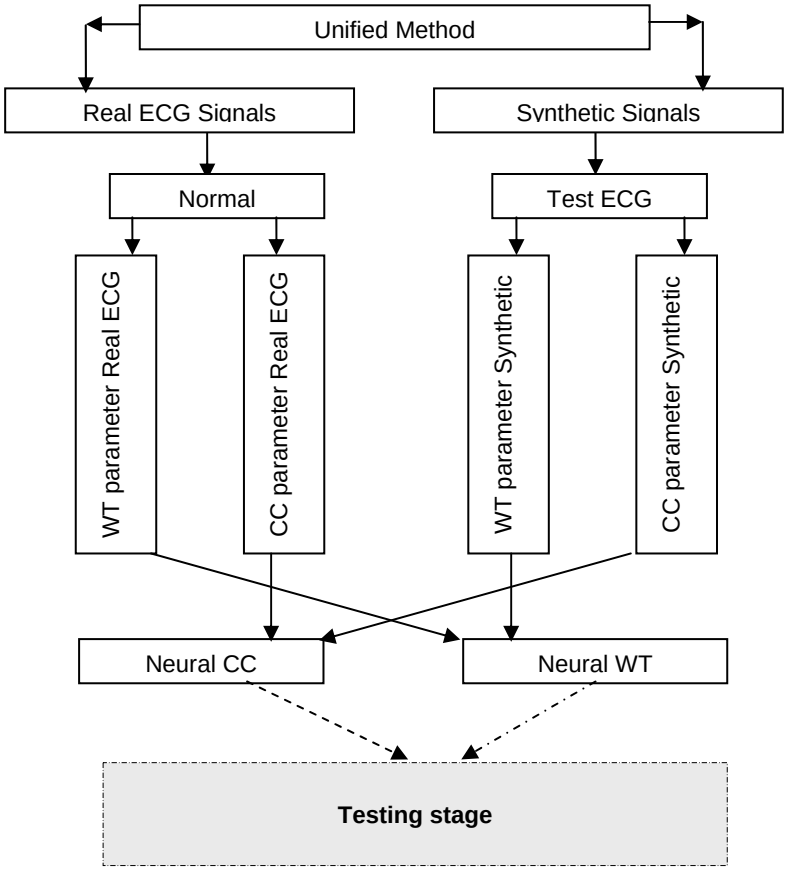

Fig. 7.7 Unified method parameter extraction and training stage

Parameters extracted for the WT employed the first three details D1, D2 and D3 resulting from the application of the wavelet transform. They included the area under the curve and its RMS values. For the complex cepstrum the parameters were the signal lengths and the RMS values for the derived minimum-phase correspondence (MPC), the minimum-phase and maximum-phase components of the signal. The flowchart presented in Fig. 7.7 shows the process of training the neural network using the extracted parameters prior to classification.

7.3 Data used in the analysis

The data used in this work is composed of different sets. The first is a synthetic set and is comprised of 1100 different signals. The synthetic signals were generated based on variations of a real ECG signal. The second data set is comprised of a number of actual ECG signals from Sussex University and those recorded at the Cardiology department of the Hacettepe University, Ankara. The system developed and built specially for this project was employed in the recording process. The full detail of the system is described in chapter 5 of this thesis.

7.3.1 Real ECG signals

This set contains data from two different sources. The first set comes from the database of the Sussex University, England and our team at the Hacettepe University recorded the other set. The Sussex database contained a total of 156 different ECG signals. There were 78 signals classified as VT and 78 classified as normal while the rest contained different abnormalities. Orthogonal X, Y, and Z-leads were recorded during sinus rhythm over a bandwidth of 0.0-500 Hz and amplified (1500) times, using techniques reported previously. Signals were digitized at 3000 samples per second with 16 bit of precision. The X, *Y,* and *Z* leads were monitored continuously in real time enabling display of the entire cardiac cycle in each patient. The sample points were stored in a digital form for future analysis and to be used as our own database.

7.3.2 Delayed potentials approximation (synthetic)

An infarct is a physical damage that has certain physical characteristics. These physical characteristics include the Size of the damage, Orientation, Type and Position or in general, (**SPOT**) parameters. The resultant delayed and disorganized activities will depend on the severity of these parameters. Because, the signal named in literature as VLP may be located anywhere along the conduction path and may not be restricted to the end of the QRS complex, we have defined a wider set to include the entire cardiac cycle. Since this large set includes LP as a subset, we have defined another name covering this range, and will be denoted as delayed potentials (DP). The duration, frequency, amplitude, position and periodicity are possible candidates for the characterization of DP in our set (Mousa, Yilmaz 2004-a).

Sufficiently large set of synthetic signals underlying the behavior of physical characteristics of the infarct parameters was employed to represent the effect of physical size, position, orientation and time of the infarct. The approximated signals are variations from real ECG signals by convolving signals representing late potentials based on duration, frequency, amplitude and position. The aim is not to exactly model VLP but rather generating an approximate set of signals to examine the performance of the standard methods for different possibilities in infarct dynamics. The position of this added signal was varied in steps to cover a range from 50 to 450 samples and added to the ECG signal extending outside the QRS complex at various durations ranging from 2 percent (8 sample in 512 signal length) to 5 percent (24 samples). These durations are based on the sampling rate of 1000 samples per second and a 12 bit resolutions used by Simson in his work. The amplitude was approximated according to usual recorded ECG signal of 1mV to 10mV as reported by Simson and compared to that used in the Hacettepe cardiology department. In order to compare the different approaches the same data set was used in all analysis stages (Simson, 1981).

The signals generated for this part are based on the fact that the accepted definition of VLP is a low-amplitude, high frequency, short-duration potential. The magnitude of VLP is thought to be in the μ volt range (0-20 μV), a value

close to noise and a wide frequency range of (40-200 Hz). These are the standards set by several international committees, including the European society of cardiology. This definition is used to generate a sinusoidal signal with amplitude (A), a frequency (F) and duration (D). The position (P) of this model signal is varied and the resultant signal is convolved with the base ECG signal. All values (A, F, D, P) are varied according to Table 7.1 to give the 1100 different signals defining delayed potentials. The base signal was an actual ECG signal taken from the Sussex university database sampled at 2200 samples per second. The Nyquist frequency was 1100 Hz and time increment of 0.45 ms.

Table 7.1 Different parameters used to generate the set of test signals

Duration (Samples)	8 – 24
Amplitude (of signal max)	0.01 – 0.1
Frequency (Hz)	80 – 150
Positioned (sample number)	10 – 450

As a first attempt, those potentials and the base signal were combined through the operation of addition. The resultant signals were examined and put through a neural network to search for commonalities between synthetic DP and real VLP but the outcome was unsatisfactory. Secondly, convolution was employed as the operation of combining these potentials and the base signal. The convolution-based approximation was compared to that of the addition-based one. Parameters of the common methods were used in the comparison process which included the QRS duration, the LAS40 and RMS40 as defined before. The convolution approach was found to be a better approximation to VLPs than directly adding the small variations representing the DPs. This time the neural network was able to detect commonalities and identify all VLP positive signals based on prior knowledge of synthetic signals only. The plots in Fig. 7.8 show the effect on the QRS duration as a result of adding potentials through convolution. The top vector magnitude is the normal base signal while the bottom graph represents on of the synthetic signals. The plots clearly present the success of the model in reflecting the effect of the presence of DP including VLP on the QRS duration parameter.

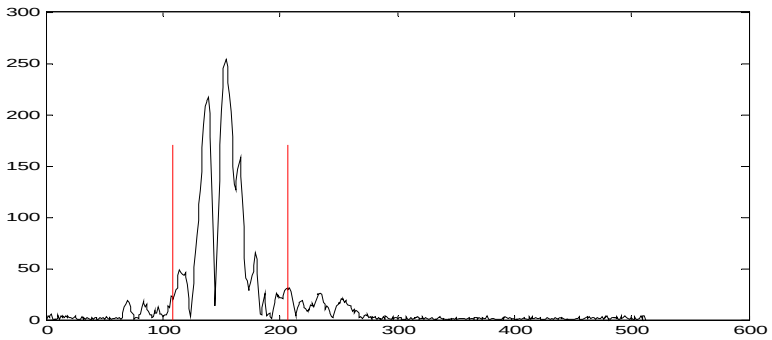

a-Normal

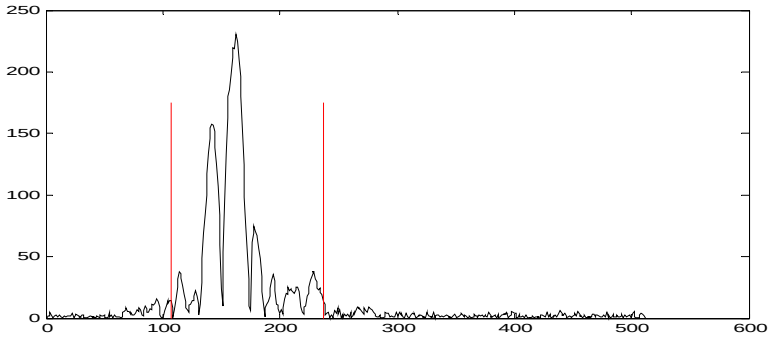

b. Synthetic DP

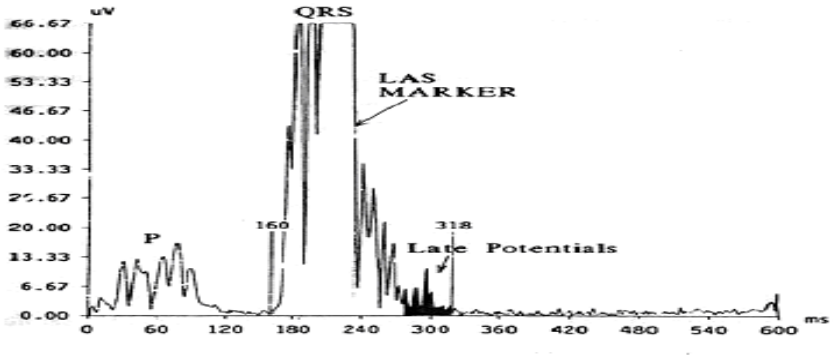

c. Real ECG previous work

Fig. 7.8 Vector magnitudes of (a) Normal (b) Synthetic (c) vector magnitude of ECG signal showing the presence of VLP (source: Gang et al. 2000)

7.4 Artificial data set tested using Simson's methods

The Simson's method is first applied to the synthetic data then the same method is applied to the set of real ECG signals. For Simson's method, any two of the following parameters imply VLP positive when FQRS > 114 ms, RMS40 < 20 µV and LAS > 38 ms.

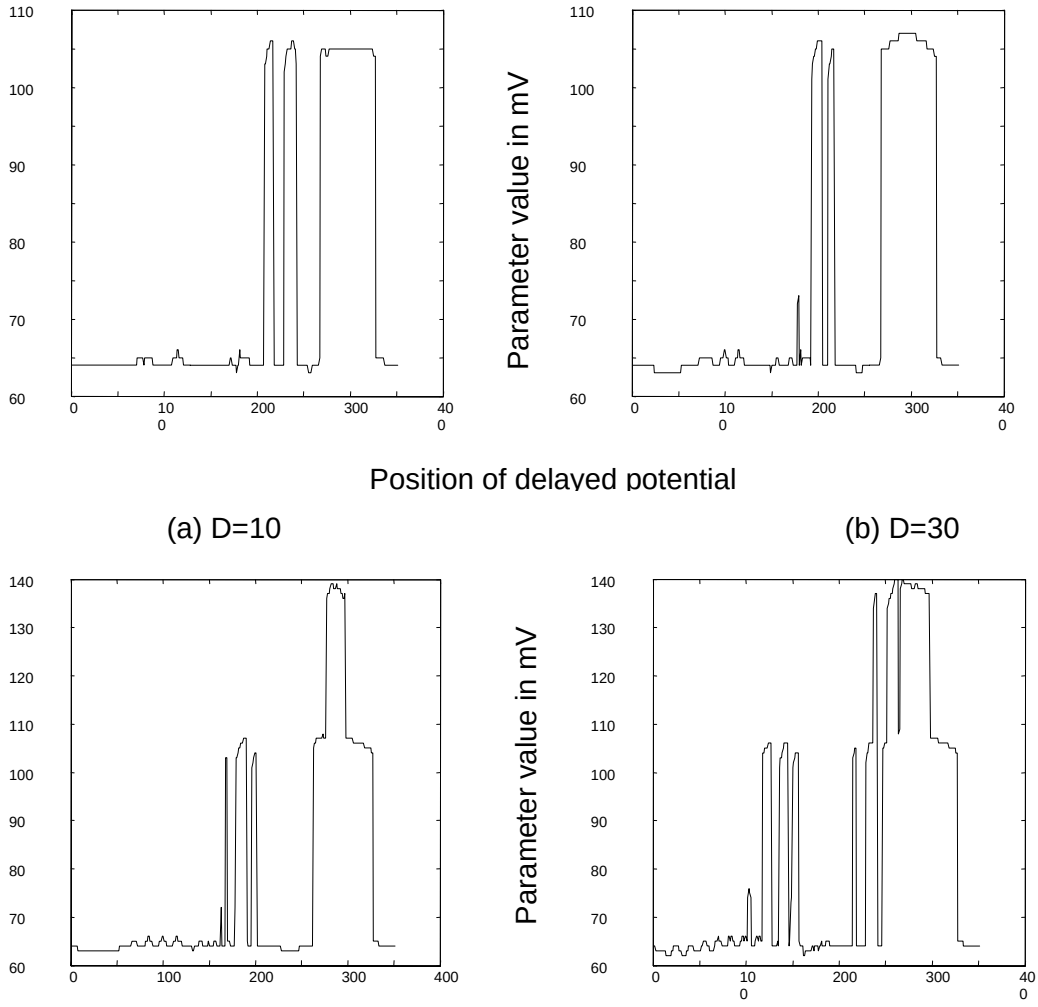

Fig. 7.9 QRSDUR[1]

1.Duration of the QRS complex for added signals of different durations (D) as the position is varied. The horizontal axis represents position and the vertical axis the calculated parameter value.

The plots in Fig. 7.9 represent the duration of the QRS and are for an added signal with an amplitude of one percent of the base ECG signal and a frequency of 100 Hz. Fig. 7.9-a is for an added potential with duration of 2 percent, shows no variation from the base value up to sample number 205. Fig. 7.9-b is for duration of 30 samples or 6 percent of base signal, shows a small peak around sample 180. This peak grows with increased duration of the added signal but around the same region only, which is around sample number 300 as can be seen. In other regions, we see that this parameter shows a drop especially as the position is after the QRS end-point.

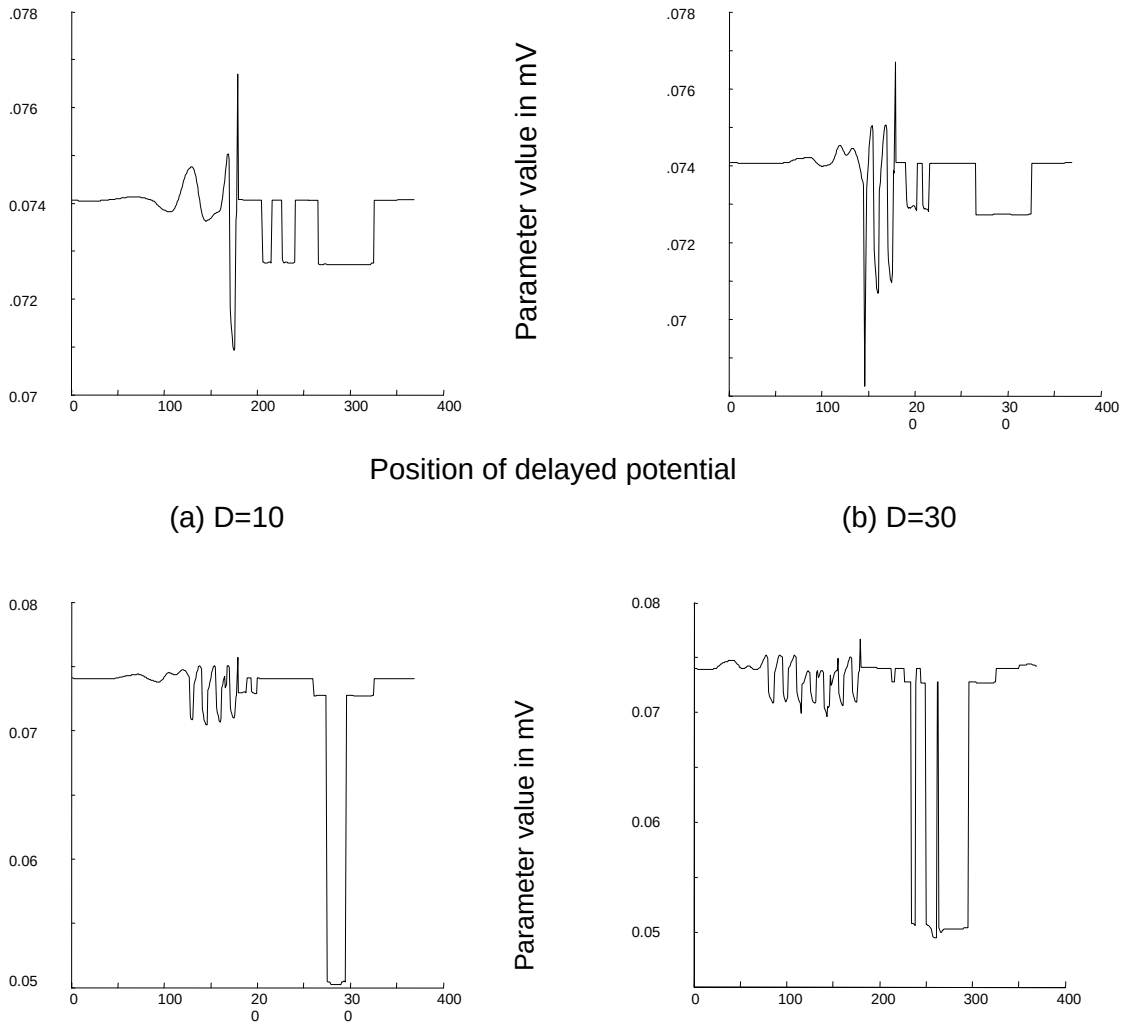

Fig. 7.10 RMS40[1]

1.RMS value of the last 40 ms of the QRS for signals with different durations (D) as the position is varied. The horizontal axis represents position and the vertical axis represents the calculated parameter value in mV.

The plots in Fig. 7.10 represent the RMS40 at the end of the QRS and are for an added signal with an amplitude of one percent of the base ECG signal and a of 100 Hz. Frequency. Fig. 7.10-a for an added potential with duration of 2 percent, shows a drop in variation from the base value at sample value 150. Fig. 7.10-b is for a duration of 30 samples or 6 percent of base signal, shows more oscillatory variations around the same sample. This variation grows with increased duration of the added signal but around the same region as can be seen in the other parts of this figure. In other regions, we see that this parameter shows a drop especially if the position is after the QRS end-point.

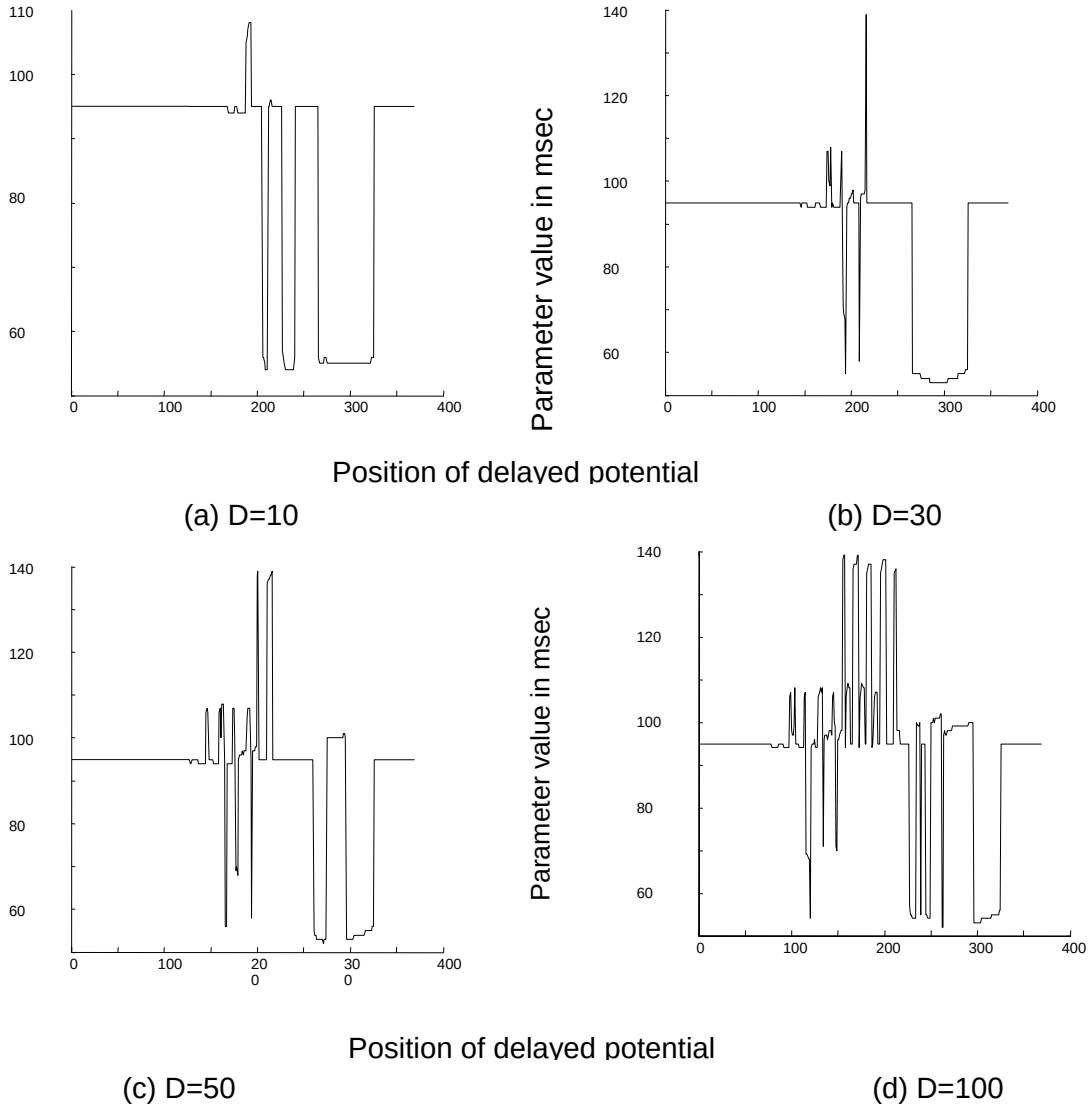

Fig. 7.11 The LAS40[1]

1.Different durations (D) of low amplitude signal as the position is varied. The horizontal axis represents position and the vertical axis the calculated parameter value in msec.

The plots in Fig. 7.11 represent **LAS40,** the duration of the low amplitude signal at the end of the QRS and are for an added signal with amplitude of one percent of the base ECG signal and a frequency of 100 Hz. Fig. 7.11-a is for an added potential with duration of 2 percent, shows small variation from the base value. Fig. 7.11-b is for duration of 30 samples or 6 percent of base signal, shows a small peak around sample number 180 with more decreasing values. This parameter shows a drop at other positions as can be seen and this parameter in general does not show significant variations from the base value of the normal ECG signal. In most regions, we see that this parameter shows a drop especially as the position is after the QRS end-point.

The overall observation in the Simson's method is the ability of these standard parameters to accurately detect signals falling at the end of the QRS. However, these parameters fail to detect delayed potentials even when they actually exist. The overall performance of common methods as applied to the set of 1100 different signals is summarized in Table 7.2. The table shows the percent of positive identification of delayed potentials for individual parameters and the overall performance when any two parameters are satisfied at the same time as required by Simson's method.

Out of the 24% signals correctly classified, 28.57% of signals fall in the first half of the signal and 71.44% fall in the second half (i.e., region that includes the QRS complex).

Table 7.2 Percent of positive identification of delayed potentials using Simson's method.

QRSDUR	LAS40	RMS40	Overall performance
38 %	22 %	39 %	24 %

7.5 Artificial data set tested using wavelet transform

There exist a large number of wavelets that can be used in the wavelet transform. The results of applying Daub-4 type of wavelet are presented in the sample given in Fig. 7.12.

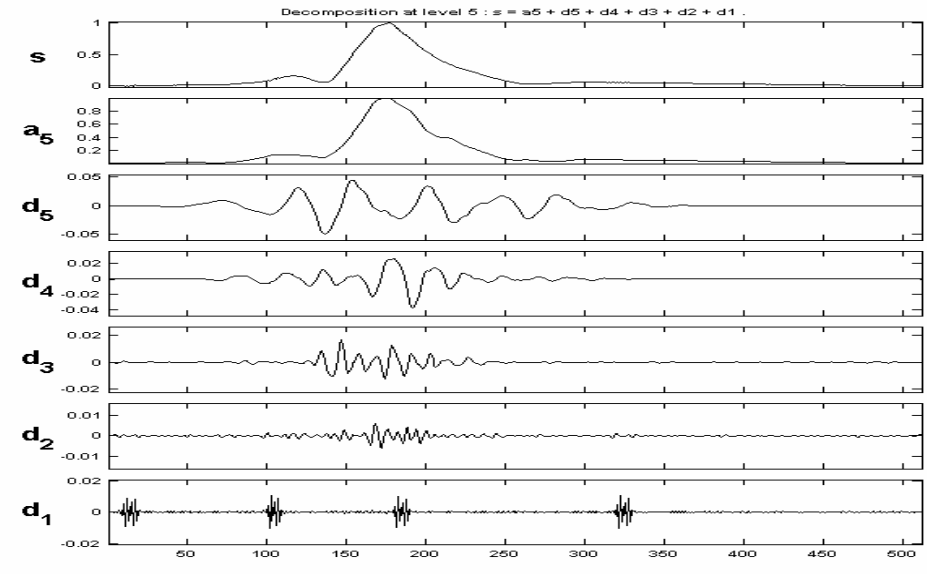

Fig. 7.12 A sample plot of WT analysis.

In Fig 7.12, the horizontal axis represents time and the vertical axis represents the different frequency scales.

The WT was applied to the same set of signals used in the previous part. The WT method was able to classify and detect all added potentials even at lower amplitudes than the 0.1 % used in the common methods analysis.

All added signals with a frequency of 125 Hz with a sampling rate of 2200 Hz and an amplitude as low as 0.1 % from base signal have accurately been identified as can be seen from the figure. In addition, the amplitude, time position and durations were detected reliably. In addition, the strength, duration and position can clearly be seen.

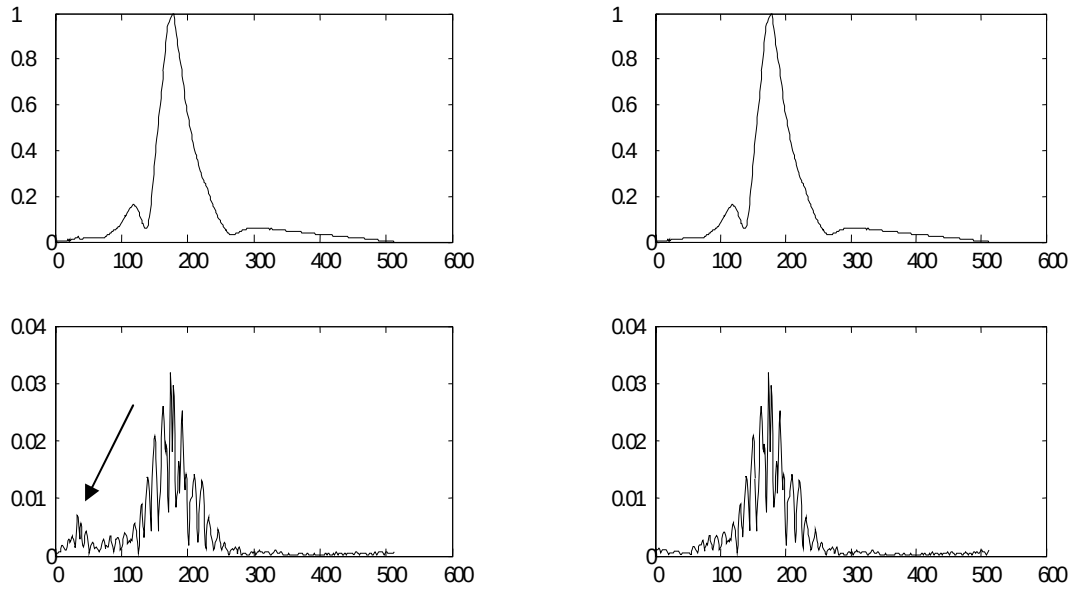

Fig 7.13 A sample of WT decomposition: the sum of level-7 and level-8.

The sum of level L7 and level L8 is presented in Fig 7.13 where the existence of added potential is clearly apparent at the left between sample number (1) and sample number (100). The plots to the right are for the base signals without added potentials presented here for comparison.

7.6 Simson's parameters using WT filtering for real ECG data

Two more parameters extracted from the WT were added. These parameters are the root-mean-square values of level L7 and level L8. The choice for these levels is based on their frequency content, which contains the range defined for ventricular late potentials. An increase from 63% to 74% positive detection has been observed (Mousa, Yilmaz, 2001-b).

The following tables summarize the parameters generated for the Sussex data base ECG signals using the Simson's method. Based on the method we proposed for the proper calculation of the vector magnitude using the WT method, we have recalculated the parameters for the detection of VLP.

Table 7.3 WT-based Simson's parameters for normal signals

	Normal ECG signals				
	QM using L7+L8				
	QRS	**RMS**	**LAS**	**RMS**	**Area**
	95	132	17	115	128
	108	69	20	109	152
	107	54	19	97	56
	80	50	21	67	26
	93	102	24	88	104
	120	31	30	80	21
	94	86	20	82	36
	101	73	20	108	85
	90	64	16	98	34
	94	75	18	69	41
	92	76	17	90	39
	85	166	12	84	113
	80	103	21	74	36
	123	40	35	115	47
	101	30	32	81	38
	80	50	21	67	26
	93	102	24	88	104
Mean	96	77	22	89	64
STD	12	35	6	16	40

Tables 7.3 and 7.4 show these parameters calculated for two different types of ECG signals. Table 7.3 gives those values for a normal signals and table 7.4 is for the abnormal ECG signals. The calculations in each table are based on WT levels 7 and 8 for the vector magnitude calculation as presented in chapter 3 of this thesis. The mean and standard deviation are presented on the bottom of the table.

Table 7.4 WT-based Simson's parameters for abnormal signals

	VT classified ECG signals				
	QM using L7+L8				
	QRS	**RMS**	**LAS**	**RMS**	**Area**
	85	40	24	94	17
	130	18	37	197	24
	146	14	37	110	26
	118	28	33	104	70
	104	65	20	105	47
	85	129	40	120	36
	183	23	37	197	8
	97	25	33	73	7
	165	9	37	117	34
	159	8	37	103	88
	99	67	30	101	100
	172	18	37	162	9
	96	136	4	116	181
	97	32	30	81	48
	115	21	36	117	84
	95	26	37	97	16
	165	9	37	117	34
	89	34	37	109	7
	85	40	24	94	17
	149	18	37	136	17
	102	90	15	84	62
Mean	121	41	32	116	45
STD	33	37	9	33	42

A summary of these results based on the obtained means and standard deviations is presented in Table 7.5 and Table 7.6 for normal and abnormal signals respectively.

Table 7.5 Mean and standard deviations of the WT parameters

Signal	Normal				
Parameter.	**QRS**	**RMS40**	**LAS**	**RMS**	**Area**
Mean	96	77	22	89	64
STD	12	35	6	16	40

Table 7.6 Mean and standard deviations for the abnormal signals.

Signal	VT				
Parameter.	**QRS**	**RMS40**	**LAS**	**RMS**	**Area**
Mean	121	41	32	116	45
STD	33	37	9	33	42

7.7 Hacettepe university hospital data analysis

The system introduced in chapter 5 was used to carry out the recordings at the intensive care unit of the cardiology department of the Hacettepe hospital, a snapshot of the system in operation is shown in Fig. 7.14.

Fig. 7.14 A snapshot of the system in operation

A number of signals were recorded at the intensive care unit at the Hacettepe University hospital. A list of some of the characteristics and medical records are listed in Table 7.7.

Due to the difficult conditions of those patients, only two minutes were recorded for each one. The sampling rate was set at 3000 samples per second and the system's ADC is fixed at 16-bits. The entire records of these signals along with other data used in this thesis are included in the accompanying CD.

Table 7.7 Hacettepe database

NO.	Gender	Age	Weight	Smoking	Illness	Other
1	M	73	75	No	Unstable angina pectoris	HC
2	F	72	80	No	Myocardial Infarction (inferior)	HT, D
3	M	75	70	No	Myocardial Infarction (postoperatively)	HT, D, HC
4	M	75	65	No	Myocardial Infarction (inferior)	HC
5	M	58	75	Yes	Coronary artery disease start implantation	HT
6	M	46	70	No	Myocardial Infarction (anterior)	No

HT: Hypertension, HC: Hypercholesterolemia, D: Diabetic

Presented here in Fig 7.15 is a sample of applying the proposed method to these data sets. The first signal comes from patient number six in Table 7.7 classified as anterior myocardial infarction (AMI) and the other signal is from a normal subject used for control.

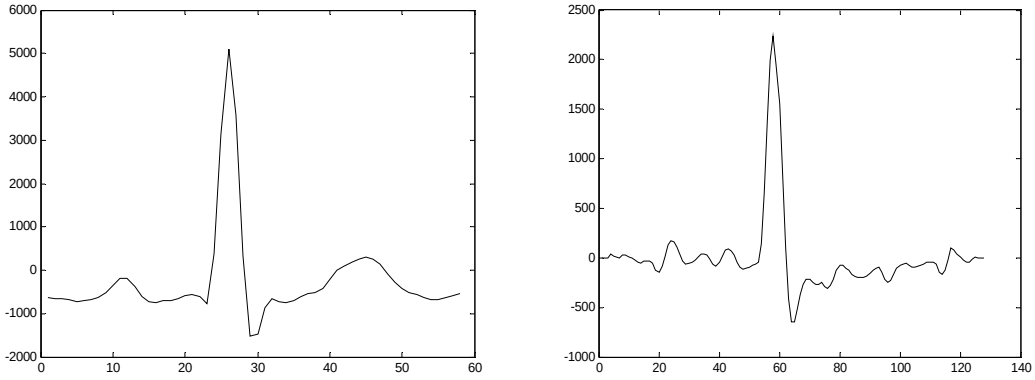

a. Normal b. Anterior MI

Original beats

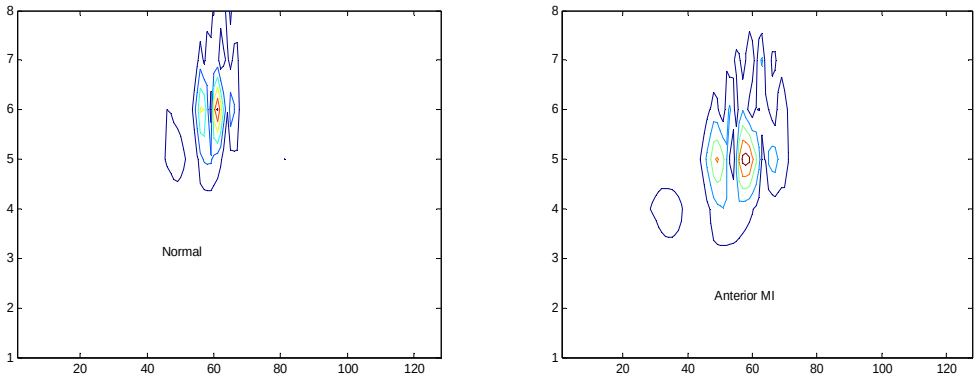

a. Normal b. Anterior MI

Contour plots of the WT

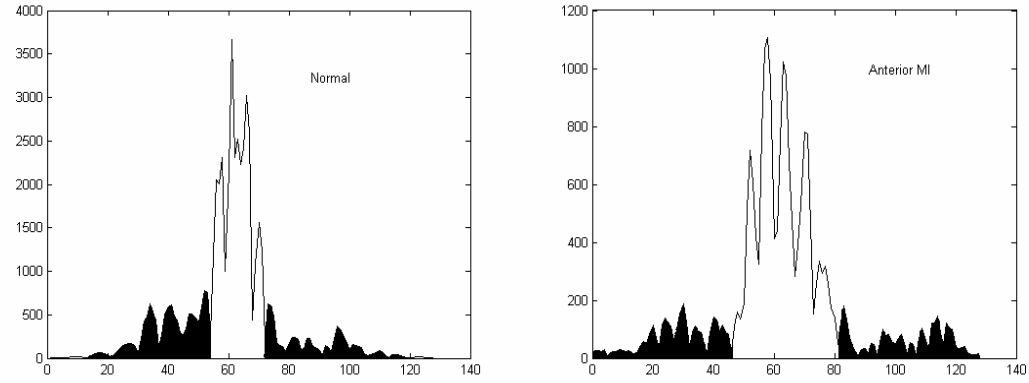

a. Normal b. Anterior MI

WT Filtered vector magnitudes

Fig. 7.15 Sample results from the Hacettepe database

7.8 Results of unified method

A number of networks were created to form the building blocks of the classification system as part of the unified method. A network from each of the WT and the complex cepstrum was chosen and were trained with only synthetic and normal real ECG signals without the introduction of any VLP positive signals to allow the network to find the required common features.

A sample of the training stage results is presented in Fig. 7.16 below.

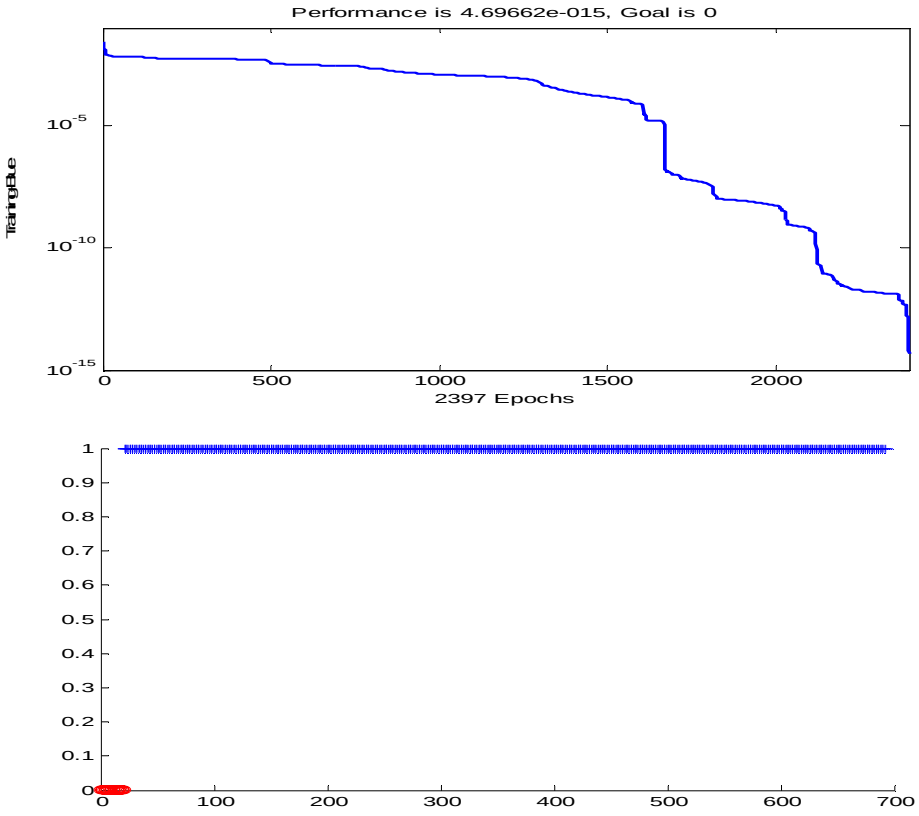

Fig. 7.16 A sample of the training results

First test

Results of applying the other types of signals to the neural networks are presented below in Fig. 7.17 with their corresponding statistics presented in Table 7.8.

Table 7.8 Classification of synthetic data

Original statistics				
-ve	+ve	Total	%-ve	%+ve
0	1100	1100	0	100

Statistics from CC				
-ve	+ve	Total	%-ve	%+ve
1	1099	1100	0.09	99.9

Statistics from WT				
-ve	+ve	Total	%-ve	%+ve
0	1100	1100	0	100

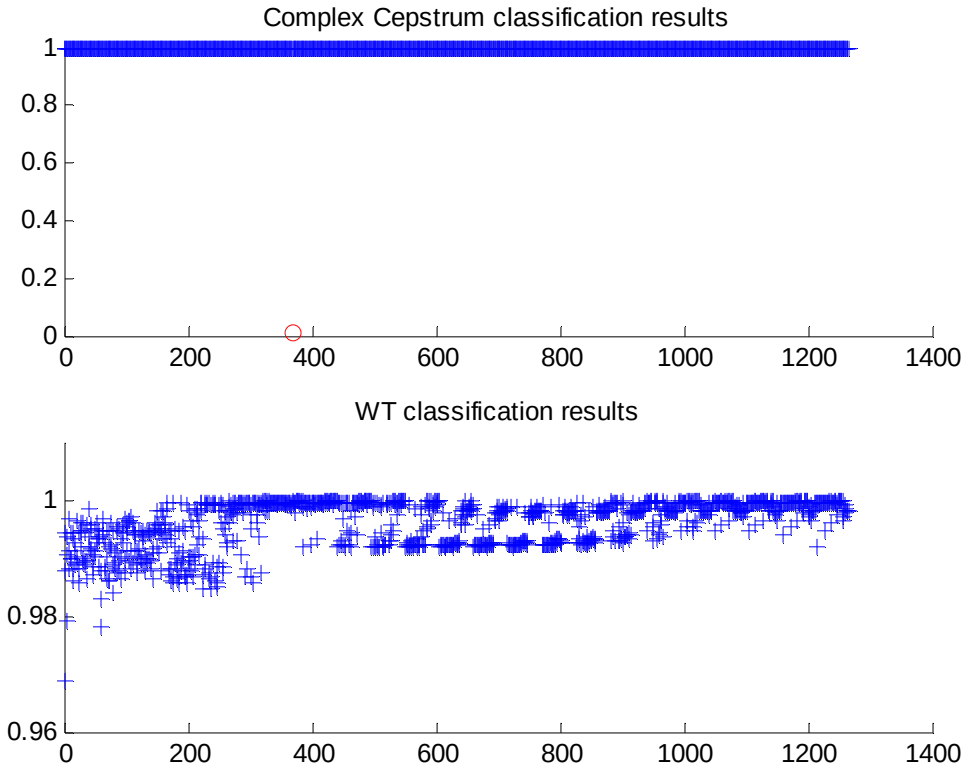

Fig. 7.17 Results of the classification of synthetic data

Second test

A number of VLP positive signals extracted from the Sussex database were applied to the network as a testing set with their results presented in Fig. 7.18 with their corresponding statistics presented in Table 7.9. The network was able to find common features relating synthetic signals to real VLP and classified all as DP positive.

Table 7.9 Classification of VLP positive data

Original statistics				
-ve	+ve	Total	%-ve	%+ve
0	6	6	0	100

Statistics from CC				
-ve	+ve	Total	%-ve	%+ve
6	0	6	100	0

Statistics from WT				
-ve	+ve	Total	%-ve	%+ve
0	6	6	0	100

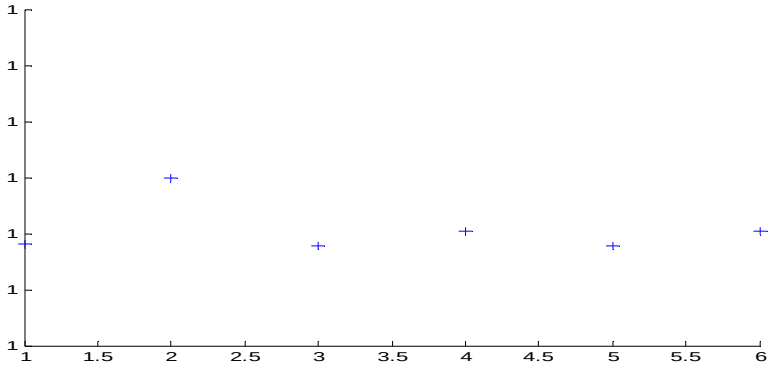

Fig. 7.18 Results of classification of VLP positive signals

Third test

Finally the unified method was used to classify real data sets that included signals classified by experts as normal and others as VT cases. The results are shown in Table 10 and their classification results presented in Fig. 7.19.

Table 7.10 Unified method classification results for real ECG data

Original statistics		
Normal	VT	Total
78	78	156

Statistics from CC		
DP-ve	DP+ve	Total
72	84	156

Statistics from WT		
DP-ve	DP+ve	Total
81	75	156

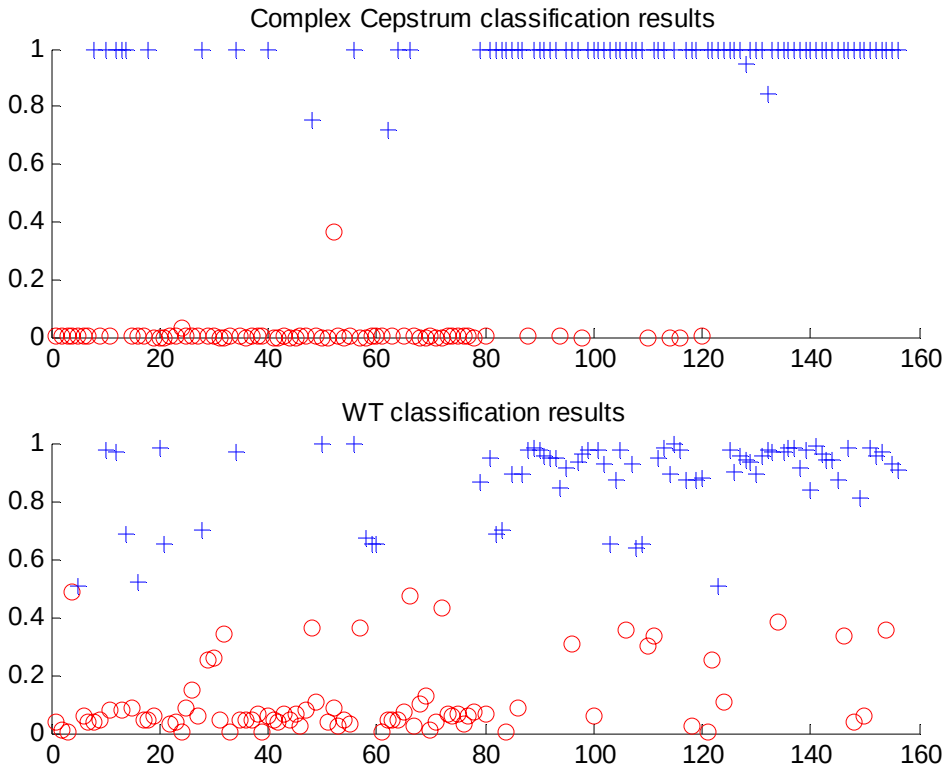

Fig. 7.19 Results of classification of real ECG signals

The application of the unified method gave excellent results in identifying the different types of signals including VLP positive ones. The WT classifier in the unified method was able to classify VLP positive cases based only on previous synthetic data knowledge while the complex cepstrum classier failed to capture commonalities between synthetic signals and VLPs.

The performances of different approaches are summarized in Table 7.11 below and it should be noted that if survival rates were increased from 5% to 20% about 40000 more lives could be saved each year in the USA according to the American Heart Association statistics.

Table 7.11 Results of all approaches for synthetic and real ECG signals

Synthetic:	**DP+ve**
Simson (VLP)	24% (264/1100)
Simson + WT	45% (495 /1100)
Unified method	99.5%(1100 /1100)

These results can be compared to the results of previous works in the field as can be seen in Table 7.12 below. The table shows 24% to 45% of VLP detection during a period of 10 years and a total of 1288 patients (E. Vester and B. Strauer, 1994).

Table 7.12 Results of different studies of the significance of late potentials following acute myocardial infarction

Authors	Numberof patients	VLP + (%)
Breithardt et al	132	59(45)
Denniss et al	306	80(26)
Kuchar et al	200	78(39)
Gomes et al	115	48(42)
Vezoni et al	220	62(28)
Gripps et al	159	38(24)
El-Sherif et al	156	39(25)
Total	1288	404(31)

CHAPTER 8

CONCLUSIONS

Standard methods are able to accurately detect signals falling at the end of the QRS and the three Simson parameters do show the presence of ventricular late potentials in general. However, they fail to detect delayed potentials outside this region when they actually exist.

Since VLP defines a limited class of potentials that can result from heart abnormalities that may occur anywhere in the cardiac cycle, it seems to be possible to give an alternative name as “delayed *potential (DP)*” to define a general space with VLP being a subspace of it. We conclude that these standard parameters are able to detect delayed signals only when they fall in the region of VLP. Furthermore, limiting the scope of analysis to a part of the signal only, the QRS will not give the complete picture regarding abnormalities occurring at other regions.

In this work we presented a broad definition of what may constitute VLPs namely delayed potentials (DP). In addition, a working model signal representing delayed potentials that represents and contains common features with VLPs. We also aimed at enlarging the window of ECG analysis outside the QRS complex to enable the detection of DP and other types of abnormalities.

The physical characteristics of the infarcts namely, size, position, orientation and type (**SPOT**) have a pronounced effect on the ability to detect their effect more readily.

Two basic needs were uncovered during this study, a need for good data and a need for good analysis methods. The need for good data necessitated the design and development of a data acquisition system with particular features

and characteristics. The designed system is a portable easy to use with special emphasis on patient safety. The system uses the USB port for communicating with laptop employed. It is a high-resolution with adjustable sampling rates of 3000 samples and more. It is also a multi-channel system with up to 12 leads multiplexed or 4 channels simultaneously.

The need for good analysis methods necessitated the development of the unified analysis approach employing different DSP techniques and tools. Use of more advanced digital signal processing tools is required in order to cover potentials existing in the entire cardiac cycle which included WT, complex cepstrum and artificial neural network applications.

The unified method includes an algorithm well suited for real time ECG preanalysis, classification and data size reduction based on correlation between different beats. It retains the clinically significant details of the individual ECG signal. It provides cardiologists and doctors with a summary of the signal characteristics to ease the analysis and bring their attention to the portions that may be of clinical value. This approach does not attempt to reduce the sampling rate as is the case with other compression algorithms.

There is no reason to assume that beats which are different from the template should be regarded as ectopic beats or be removed. On the contrary these beats may be the information carrying parts of the signal. Therefore, this method combines similar beats through correlation and does not eliminate any beats no matter how different they might be. Depending on the type of abnormality, beats that deviate from normal pattern may indeed carry the important information (clinically significant waveform features) and for this reason they are retained.

If a general opinion about status of the patient is sought, a low correlation value will suffice producing a template with minimum number of beats. If on the other hand the analysis dictates the discovery of finite details such as VLPs, the threshold value of correlation must be kept high which will in turn produce a template with a larger number of beats.

The WT provides good means of noise filtering and calculation of the vector magnitude without introducing cross-terms. These cross-terms arise when we square ECG leads containing different frequency components such as P, T, QRS and delayed potentials (DP). By choosing only appropriate levels to include in the calculation of the vector magnitude, we remove other undesirable components defined as cross-terms in our discussion. Based on the frequency content of the individual levels of the WT, the content of individual levels may be used to classify different abnormalities contained in ECG signals.

In conclusion the prevalence of VLP after acute myocardial infarction depends on the definition of what constitutes VLP, the site and type of myocardial infarction, time of recording and the analyzing technique.

It should be emphasized that the true test of any new method such as the one presented here is long-term application. Therefore, we strongly recommend that the proposed analysis scheme be employed under the cooperation of both the Electrical department and the cardiology department at the Hacettepe University hospital.

To finalize this work we present a list of the accomplished tasks during the entire study.

ACCOMPLISHMENTS

- ☑ A more general definition that takes into account the physical variation behind the causes of VLP namely the infarct expressed as **SPOT**
- ☑ Expanded analysis region to cover the entire cardiac cycle
- ☑ New method for V.M. calculation without cross-term components
- ☑ Noise reduction using WT denoising capabilities
- ☑ Portable high-resolution data acquisition system using USB port

    1. 3000 samples per second
    2. 16-bit resolution
    3. patient safety and isolation
    4. up to 12-channels

- ☑ New combined analysis method using time-domain, frequency-domain and the complex cepstrum based on the reported success of their individual performances.
- ☑ More parameters have been added from WT and the cepstrum
- ☑ Improved performance relative to current methods
- ☑ Our own data base
- ☑ Better alignment through the use of correlation and WT templates with only correlated beats averaged using the correlation template
- ☑ Information in ECG records are summarized in clusters for better classification
- ☑ Real time analysis are made possible through the use of dynamic averaging

In addition, the work was published in international conferences and journals:

- ☑ Seven conference papers
- ☑ Two Journal articles

REFERENCES

Breithardt G., Cain M. E., Elsheref N., Flowers N., Hombach V., Janse M., Simson M. B. and Stenbeck G.. 1991. “Standards for analysis of ventricular late potentials using high resolution or signal-averaged electrocardiography A statement by task force committee between the European society of cardiology, the American Heart Association and the American college of cardiology” European Heart Journal 12 pp 473-480

Burrus O. S., Gopinath R. A. and Guo H., 1998. “Intoduction to wavelets and wavelet transform; a primer”. Prentice Hall.

Cain M., Anderson J., Arnsdorf M., Mason J., Schienman M., Waldo A. 1996 “ Acc expert consensus document: signal averaging electrocardiography”. JACC Vol 27 No. 1 pp 238-249.

Friesen G. M., Jannett T. C., Jadallah M. A., Yates S. L., Quint S. R., Nagle H. T. 1990 “A comparison of the noise sensitivity of nine QRS detection algorithms”. IEEE trans. on Biomed. Eng, 37,No. 1. pp 85-98.

Fu L. 1994 “Neural networks in computers intelligence”. McGraw-Hill International Edition.

Gang L., Wenyu Y., Ling L., Qilian Y., Xuemin Y. 2000 “An artificial-intelligence approach to ECG analysis”. IEEE Eng. In Med. And Bio. pp 95-100.

Gramatikov B., 1993. “Digital filters for the detection of late potentials in high-resolution ECG”. Med.and Biomed. Eng. And Com. pp 415-420.

Haykin S. 1999. “Neural networks: a comprehensive foundation”. Prentice-Hall Inc.

Jane R., Rix H., Caminal P.. 1991 “Alignment methods for averaging high-resolution cardiac signals: a comparative study of performance”. IEEE Trans. Biomed Eng., vol 38,pp 571-579.

Laciar E., Jane R., Brooks D. H.. 2003 ”Improved alignment for noisy high-resolution ECG and Holter records using multiscale cross-correlation”. IEEE trans. on Biomed. Eng. Vol 50, No. 3, March. pp 344-354

Lander P., Deal R. B., Berberi E. J. 1988. ”The analysis of ventricular late potentials using orthogonal recordings”. IEEE trans. Biomed. Eng. Vol 35 No. 8 pp 629-639

Makuarvi M., Montonen J., Toivonen L., Leino M., Siltanen P., Katila T. 1994. "High-resolution and signal-averaged electrocardiography to separate post-myocardial infarction patients with and without ventricular tachycardia". European Heart Journal 15 pp 189-199

Mallat S. 1989 "A theory for multiresolution signal decomposition: the wavelet representation". *IEEE Trans Patt Anal Mach. Intell.* Vol 11.

Malmivuo J., Plonsey R., 1995. "Biomagnetism: principles and applications of bioelectric and biomagnetic fields". Oxford University Press.

Meste O., Rix H., 1994 "Ventricular late potentials characterization in time-frequency domain by means of a wavelet transform" IEEE trans. Biomed. Eng. Vol 41 No. 7 pp 625-634.

Mousa A., Yilmaz A. 2000-a "EKG sinyallerinde dalgacık analizi kullanılarak ventriküler geç potansiyellerin algılanması" *SIU 2000*, Belek, Turkey,.

Mousa A., Yilmaz A. 2000-b "Wavelet transform analysis of ventricular late potential in ECG signals using the TMS320C30." *BIOMED 2000* 7TH Int. symp. Ankara, Turkey,.

Mousa A., Yilmaz A. 2001-a "A method based on wavelet analysis for the detection of ventricular late potentials in ECG signals." IEEE 44th MWCAS 2001 Ohio, USA.

Mousa A., Yilmaz A. 2001-b "Neural network detection of ventricular late potentials in ECG signals using wavelet transform extracted parameters." 23rd Ann. Int. Conf. Of IEEE Eng. In Med. And Biology, Istanbul, Turkey,.

Mousa A., Yilmaz A. 2002 "Ortogonal EKG Kayıtlarından Elde Edilen Sinyal Vektör Büyüklüklerinin Dalgacık Dönüm Yöntemi Analizi " *SIU*, Pamukkale, Turkey.

Mousa A., Yilmaz A. 2004-a "Comparative analysis on wavelet transform based detection of finite duration low-amplitude signals related to ventricular late potentials". Physiological Measurements Journal. Vol 25 pp 1443-1457.

Mousa A., Yilmaz A. 2004-b "Detection of delayed potentials (DP) related to physical nature of myocardial infarction ". BIOMED 2004 International Biomedical Science Days. September 6-10 Ankara,Turkey.

Mousa A., Yilmaz A. 2004-c "Dynamic ECG template construction based on wavelet transform". BIOMED 2004 International Biomedical Science Days. September 6-10 Ankara,Turkey.

Murthy I., Rangaraj M., Udupa K., Goyal A. 1997 “Homomorphic analysis and modeling of ECG signals” IEEE trans. Biomed. Eng. Vol BME-26 No. 6 pp 330-344.

Murthy I., Rangaraj M., 1997 “New concepts for PVC detection” IEEE trans. Biomed. Eng. Vol BME-26 No. 7 pp 409-416.

Oppenheim V, Schafer R. W 1989 “Discrete-time signal processing”. Prent. Hall.

Pickering P. 1999. “A system designer’s guide to isolation devices”. Burr-Brown Corp. Tucson, Arizona

Raghuveer M., et al 1992 “Wavelet decomposition of event related potentials: Toward the definition of biologically natural components.” . IEEE Press.

Rajoub B., 2002 “An efficient coding algorithm for the compression of ECG signals using the wavelet transform” IEEE trans. Biomed. Eng. Vol 49 No. 4 pp 355-362.

Rioul O.,Vetterli M. 1991 “Wavelets and signal processing”. IEEE Sig. Proc. Mag. October: 14

Rompelman O., Ros H. H.. 1986 “Coherent averaging techniques: a tutorial review. Part 1: noise reduction and equivalent filter. Part2: rigger jitter, overlapping responses and nonperiodic stimulation:, IEEE J. Biomed. Eng., vol 8, pp 24-35.

Simson M. B. M.D. 1981. “Use of signals in the terminal QRS complex to identify patients with ventricular tachycardia after myocardial infarction”. Circulation vol 64 No 2

Thakor N. V., et al. 1993. “Multiresolution wavelet analysis of ECG during ischemia reperfusion in computer cardiology.” IEEE compu. Soc. Press.

Vester E. G. and Strauer B. E., 1994. “Ventricular late potentials: state of the art and future perspective”. European Heart Journal 15 34-48

Webster J. 1998. “Medical instrumentations: application and design”. 3rd edition New York Jhon Wiles & Sons.

Winter B., Webster J., 1983. “Reduction of interference due to common mode voltage in biopotential amplifiers”. ” IEEE trans. Biomed. Eng. Vol BME-30 No.1 pp 58-62.

Winter B., Webster J., 1983. “Driven-right-leg circuit design” IEEE trans. Biomed. Eng. Vol BME-30 No.1 pp 62-66.

Wu S., Qiao Y., Gao Z., lin F. 2001. “A novel method for beat-to-beat detection of ventricular late potentials”. IEEE Trans. Biomed. Eng. Vol 48 No. 8 pp 931-935.

Xue Q., Reddy B. 1997. “Late potential recognition by artificial neural networks”. IEEE trans. Biomed. Eng. Vol 44 No. 2 pp 132-143.

NHLBI: National Heart Lung and Blood institute, USA. www.nhlbi.nih.gov

AIHW: Australian Institute of Health and welfare, Australia. www.aihw.gov.au

NHS: National Health Survey (Australian Bureau of Stats) www.gov.au/Ausstats

ÖZGEÇMİŞ

MOUSA A. AYAD

Adres 1: Cankaya Üniversitesi

Telefon: (0312) 284-4500-170

Fax: (0312) 284-8043

Adres 2: Hacettepe Üniversitesi, Elektrik ve Elektronik Mühendisliği Bölümü, 06532 Beytepe, Ankara

Telefon: (0312) 2977000

Fax: (0312) 2992125

Elektronik Posta amousa@cankaya.edu.tr

Doğum Yeri ve Tarihi: Libya, 17-11-1954

Medeni Durumu **:** Evli

EĞİTİMİ

PhD (Doktora) - Eylül-1999 (başlama) Hacettepe Üniversitesi, Elektrik ve Elektronik Mühendisliği Bölümü, Ankara.

MSc (Master) - University of Wisconsin-Milwaukee, USA 1982

Elektronik Mühendisi - BS University of Wisconsin-Milwaukee, USA 1978

DENEYİMLERİ

İş Deneyimleri

* Şef Mühendis- Omar Mukhtar Üniversitesi : 1990-1993
* Ögretim Elemanı- Omar Mukhtar Üniversitesi : 1982-2000
* Araştırma Görevlisi - BS University of Wisconsin-Milwaukee, USA: 1980-1982
* Çankaya Üniversitesi.

İlgiliye,

Hacettepe Üniversitesi Araştırma Fonu tarafından desteklenen **0002602003** no'lu '.**VENTRİKÜLER GECİKMİŞ POTANSİYELLERİN (VGP) YÜKSEK ÇÖZÜNÜMLÜ KAYDI, İŞLENMESİ, SİNİR AĞLARI KULLANILARAK SINIFLANDIRILMASI, ARAŞTIRILMASI**' adlı projemizin son dönemine dönemine ait Sonuç Raporu ekte sunulmuştur.

Araştırma Konuları

Biyomedikal Sinyal İşleme, Dalgacık Dönüşümü, Mikroişlemciler, Sayısal Sistemler.

Aldığı Burslar

(1995-2001)- Omar Mukhtar Üniversitesi

.

Awards

- Best Poster Presentation Award : Biomed2000-Seventh International Symposium on Biomedical Science and Technology, September-2000.

Scholarships

- 1972-1977 Ministry Of Education Libya.
- 1989-1982 Garyounis University Libya.
- 1995-2001 Omar Mukhtar University Libya.

YAYINLAR

[1] Mousa A., Yilmaz A. "EKG sinyallerinde dalgacık analizi kullanılarak ventriküler geç potansiyellerin algılanması" *SIU 2000*, Belek, Turkey, 2000.

[2] Mousa A., Yilmaz A. "Wavelet transform analysis of ventricular late potential in ECG signals using the TMS320C30." *BIOMED 2000* 7TH Int. symp. Ankara, Turkey,2000.

[3] Mousa A., Yilmaz A. “A method based on wavelet analysis for the detection of ventricular late potentials in ECG signals.” IEEE 44th MWCAS 2001 Ohio, USA, 2001.

[4] Mousa A., Yilmaz A. “Neural network detection of ventricular late potentials in ECG signals using wavelet transform extracted parameters.” 23rd Ann. Int. Conf. Of IEEE Eng. In Med. And Biology, Istanbul, Turkey, 2001.

[5] Mousa A., Yilmaz A. “Ortogonal EKG Kayıtlarından Elde Edilen Sinyal Vektör Büyüklüklerinin Dalgacık Dönüm Yöntemi Analizi ” *SIU 2002*, Pamukkale, Turkey, 2002.

[6] Mousa A., Yilmaz A. “Detection of delayed potentials (DP) related to physical nature of myocardial infarction “. BIOMED 2004 International Biomedical Science Days. September 6-10 2004 Ankara,Turkey.

[7] Mousa A., Yilmaz A. “. Dynamic ECG template construction based on wavelet transform”. BIOMED 2004 International Biomedical Science Days. September 6-10 2004 Ankara,Turkey.

[8] Mousa A., Yilmaz A. “Comparative analysis on wavelet transform based detection of finite duration low-amplitude signals related to ventricular late potentials”. Physiological Measurements Journal. Vol 25 pp 1443-1457. 2004